# The Inflation Technique for Causal Inference with Latent Variables

Elie Wolfe,[1,*] Robert W. Spekkens,[1,†] and Tobias Fritz[1,2,‡]

[1] *Perimeter Institute for Theoretical Physics, Waterloo, Ontario, Canada, N2L 2Y5*
[2] *Max Planck Institute for Mathematics in the Sciences, Leipzig, Germany*

(Dated: October 5, 2016)

The problem of causal inference is to determine if a given probability distribution on observed variables is compatible with some causal structure. The difficult case is when the structure includes latent variables. We here introduce the *inflation technique* for tackling this problem. An inflation of a causal structure is a new causal structure that can contain multiple copies of each of the original variables, but where the ancestry of each copy mirrors that of the original. For every distribution compatible with the original causal structure we identify a corresponding family of distributions, over certain subsets of inflation variables, which is compatible with the inflation structure. It follows that compatibility constraints at the inflation level can be translated to compatibility constraints at the level of the original causal structure; even if the former are weak, such as observable statistical independences implied by disjoint causal ancestry, the translated constraints can be strong. In particular, we can derive inequalities whose violation by a distribution witnesses that distribution's incompatibility with the causal structure (of which Bell inequalities and Pearl's instrumental inequality are prominent examples). We describe an algorithm for deriving *all* of the inequalities for the original causal structure that follow from ancestral independences in the inflation. Applied to an inflation of the Triangle scenario with binary variables, it yields inequalities that are stronger in at least some aspects than those obtainable by existing methods. We also describe an algorithm that derives a weaker set of inequalities but is much more efficient. Finally, we discuss which inflations are such that the inequalities one obtains from them remain valid even for quantum (and post-quantum) generalizations of the notion of a causal model.

* ewolfe@perimeterinstitute.ca
† rspekkens@perimeterinstitute.ca
‡ fritz@mis.mpg.de

## CONTENTS



## I. INTRODUCTION

Given a joint probability distribution of some observed variables, the problem of **causal inference** is to determine which hypotheses about the causal mechanism can explain the given distribution. Here, a causal mechanism may comprise both causal relations among the observed variables, as well as causal relations among these and a number of unobserved variables. Causal inference problems arise in a wide variety of scientific disciplines, from sussing out biological pathways to enabling machine learning [1–4]. A closely related type of problem is to determine, for a given set of causal relations, the set of all distributions on observed variables that can be generated from them. A special case of both problems is the following decision problem: given a probability distribution and a hypothesis about the causal relations, determine whether the two are compatible—could the given distribution have been generated by the hypothesized causal relations? This is the problem that we focus on. We develop necessary conditions for a given distribution to be compatible with a given hypothesis about the causal relations.

In the simplest setting, the causal hypothesis consists of a directed acyclic graph (DAG) *all* of whose nodes correspond to observed variables. In this case, obtaining a verdict on the compatibility of a given distribution with the causal hypothesis is simple: the compatibility holds if and only if the distribution is Markov with respect to the DAG, which is to say that the distribution features all of the conditional independence relations that are implied by $d$-separation

relations among variables in the DAG. The DAGs that are compatible with the given distribution can be determined algorithmically [1].

A significantly more difficult case is when one considers a causal hypothesis which consists of a DAG whose nodes include **latent** (i.e., unobserved) variables, so that the set of observed variables is a strict subset of the nodes of the DAG. This case occurs, e.g., in situations where one needs to deal with the possible presence of unobserved confounders, and thus is particularly relevant for experimental design in statistics. It is useful to distinguish two varieties of this problem: (i) the causal hypothesis specifies that the latent variables are discrete and of a particular cardinality[1], and (ii) the nature of the latent variables is arbitrary.

Consider the first variety of causal inference problem, where the cardinalities of all the latent variables are finite. Then the mathematical problem which one must solve to infer the distributions that are compatible with the hypothesis is a quantifier elimination problem for some finite number of quantifiers, as follows. The probabilities making up the distribution of the observed variables can all be expressed as functions of the parameters specifying the conditional probabilities of each node given its parents, many of which involve latent variables. If one can eliminate these parameters, then one obtains constraints that refer exclusively to the probability distribution of the observed variables. This is a *nonlinear* quantifier elimination problem. The Tarski-Seidenberg theorem provides an *in principle* algorithm for an exact solution, but unfortunately the computational complexity of such quantifier elimination techniques is too large to be practical, except in particularly simple scenarios [5].[2]

The second variety of causal inference problem, where the latent variables are arbitrary, is even more difficult, but it is the one that has been the focus of most research and that motivates the present work. It is conceivable that inference problems of this variety can be expressed as quantifier elimination problems as well. This would be the case, for instance, if one could show that latent variables of a certain finite cardinality (as opposed to arbitrary latent variables) are sufficient to generate all the distributions compatible with a given DAG[3]. At present, however, the problem of finding an algorithm for deciding compatibility in this second case—let alone an efficient algorithm—remains wide open. Nonetheless, even if it *is* possible to achieve a reduction to the case of latent variables with finite cardinality, one would still be faced with a computationally impractical nonlinear quantifier elimination problem, as described above. As such, a heuristic technique for obtaining nontrivial constraints, such as the one presented in this work, is arguably more useful.

If one allows for latent variables, then the condition that all of the conditional independence relations among the observed variables should be explained by the structure of the DAG is still a necessary condition for compatibility of a DAG with a given distribution, but in general it is no longer a sufficient condition for compatibility, and this is what makes the problem difficult.

Historically, the insufficiency of the conditional independence relations for causal inference in the presence of latent variables was first noted by Bell in the context of the hidden variable problem in quantum physics [8]. Bell considered an experiment for which considerations from relativity theory implied a very particular causal structure, and he derived an inequality that any distribution compatible with this structure, and compatible with certain constraints imposed by quantum theory, must satisfy. Bell also showed that this inequality was violated by distributions generated from entangled quantum states with particular choices of incompatible measurements. Later work, by Clauser, Horne, Shimony and Holte (CHSH) showed how to derive inequalities directly from the causal structure [9]. The CHSH inequality was the first example of a compatibility condition that appealed to the strength of the correlations rather than simply the conditional independence relations inherent therein. Since then, many generalizations of the CHSH inequality have been derived for the same sort of causal structure [10]. The idea that such work is best understood as a contribution to the field of causal inference has only recently been put forward [11–14], as has the idea that techniques developed by researchers in the foundations of quantum theory may be usefully adapted to causal inference[4].

Subsequent to Bell's work, Pearl derived the **instrumental inequality** [22], which provides a necessary condition for the compatibility of a distribution with a causal structure known as the *instrumental scenario*. This causal structure is applicable, for instance, to certain kinds of noncompliance in drug trials. Later, Steudel and Ay [23] derived an inequality which must hold whenever a distribution on $n$ variables is compatible with a causal structure where no set of more than $c$ variables has a common ancestor, for arbitrary $n, c \in \mathbb{N}$. More recent work has focused specifically on the case of $n = 3$ and $c = 2$, a causal structure that has been called the Triangle scenario [12, 24] (Fig. 1).

Recently, Henson, Lal and Pusey [13] have investigated those DAGs for which merely confirming that a given distribution on observed variables satisfies the conditional independence relations implied by the DAG does not guarantee that this distribution is compatible with the DAG. They coined the term *interesting* for DAGs that have this property. They presented a catalogue of all potentially interesting DAGs having six or fewer nodes in [13, App. E],

[1] The cardinality of a variable is the number of possible values it can take.
[2] Techniques for finding approximate solutions to nonlinear quantifier elimination may help [6].
[3] Rosset and Gisin [7] have an unpublished proof purporting to upper bound the cardinality of the latent variables for the Triangle scenario (Fig. 1) using an observation that may apply to all DAGs. We do not pursue the question here.
[4] The current article being another example of the phenomenon [6, 14–21].

of which all but three were shown to be indeed interesting. The Bell scenario, the Instrumental scenario, and the Triangle scenario all appear in the catalogue, together with many others. Furthermore, the fraction of DAGs that are interesting increases as the total number of nodes increases. This highlights the need for moving beyond a case-by-case consideration of individual DAGs and for developing techniques for deriving constraints beyond conditional independence relations that can be applied to any interesting DAG. Shannon-type entropic inequalities are an example of such constraints [12, 16, 23–25]. They can be derived for a given DAG with relative ease, via exclusively linear quantifier elimination, since conditional independence relations are linear equations at the level of entropies. They also have the advantage that they apply regardless of the cardinality of the observed variables. Recent work has also looked at non-Shannon type inequalities, potentially further strengthening the entropic constraints [17, 26]. However, entropic techniques are still wanting, since the resulting inequalities are often rather weak. For example, they are not sensitive enough to witness some known incompatibilities, in particular for distributions that only arise in quantum but not classical models with a given causal structure [12, 17][5].

In order to improve this state of affairs, we here introduce a new technique for deriving necessary conditions for the compatibility of a distribution over observed variables with a given causal structure, which we term the *inflation technique*. Our technique is frequently capable of witnessing incompatibility when many other causal inference techniques fail. For example, in Example 2 of Sec. III B we prove that the tripartite "W-type" distribution is incompatible with the Triangle scenario, despite the incompatibility being invisible to other causal inference tools such as conditional independence relations, Shannon-type [16, 24, 25] or non-Shanon-type entropic inequalities [17], or covariance matrices [18].

The inflation technique works roughly as follows. For a given DAG under consideration, one can construct many new DAGs, termed *inflations* of this DAG. These duplicate one or more of the nodes of the original DAG, while mirroring the form of the subgraph describing each node's ancestry. Furthermore, the causal parameters that one adds to the inflation DAG are constrained to mirror those of the original DAG. We show that if the distributions over certain subsets of the observed variables are compatible with the original DAG, then the same distributions over certain copies of those subsets in the inflation DAG are compatible with the inflation DAG (Lemma 3). Similarly, we show that any necessary condition for compatibility of a distribution with the inflation DAG translates into a necessary condition for compatibility with the original DAG (Corollary 5). Thus standard techniques for deriving causal compatibility inequalities, applied to the inflation DAG, can be supplemented with the inflation technique to derive new causal compatibility inequalities for the original DAG.

Concretely, we consider causal compatibility inequalities for the inflation DAG that are obtained as follows. One begins by identifying inequalities that are derived from the marginal problem, that is, inequalities for a family of distributions, defined on various subsets of the variables, which hold if the family can be obtained as the marginals of a single joint distribution over all the variables. One then identifies instances within the inflation DAG of variables having disjoint ancestries, and infers the factorization of the distributions over these variables. These factorization conditions are substituted into the marginal problem inequalities to obtain causal compatibility inequalities for the inflation DAG. We show how to identify all factorization conditions from the structure of the inflation DAG, and also how to obtain *all* marginal problem inequalities by enumerating all facets of the associated **marginal polytope** (Sec. IV B). Translating the resulting causal compatibility inequalities on the inflation DAG back to the original DAG, we obtain causal compatibility conditions in the form of nonlinear *polynomial inequalities*. As a concrete example of our technique, we present all the causal compatibility inequalities that can be derived in this manner for the Triangle scenario (Sec. IV C). We also show how to efficiently obtain a partial set of marginal problem inequalities by enumerating transversals of a certain hypergraph (Sec. IV D).

Besides the entropic techniques discussed above, our method is the first systematic tool for causal inference with latent variables that goes beyond observed conditional independence relations while not assuming any bounds on the cardinality of each latent variable. While our method can be used to systematically generate necessary conditions for compatibility with a given causal structure, we do not know whether the set of inequalities thus generated are also sufficient.

While we present our technique primarily as a tool for standard causal inference, we also briefly discuss applications to *quantum* causal models and causal models within generalized probabilistic theories (Sec. V C). In particular, we discuss when our inequalities are also necessary conditions for a distribution over observed variables to be compatible with a given DAG within any generalized probabilistic theory.

---

[5] It should be noted that non-standard entropic inequalities can be obtained through a fine-graining of the causal scenario, namely by *conditioning* on the distinct finite possible outcomes of root variables ("settings"), and these types of inequalities *have* proven somewhat sensitive to quantum-classical separations [24, 27, 28]. Such inequalities are still limited, however, in that they are only applicable to those DAGs which feature observed root nodes. The potential utility of entropic analysis where fine-graining is generalized to *non*-root observed nodes is currently being explored by E.W. and Rafael Chaves. Jacques Pienaar has also alluded to similar considerations as a possible avenue for further research [26].

## II. BASIC DEFINITIONS OF CAUSAL MODELS AND COMPATIBILITY

A **causal model** consists of a pair of objects: a **causal structure** and a family of **causal parameters**. We define each in turn. First, recall that a directed acyclic graph (DAG) $G$ consists of a finite set of nodes $\mathsf{Nodes}(G)$ and a set of directed edges $\mathsf{Edges}(G)$, where a directed edge is an ordered pair of nodes, so that $\mathsf{Edges}(G) \subseteq \mathsf{Nodes}(G) \times \mathsf{Nodes}(G)$. This directed graph is assumed to be *acylic*, which means that there is no way to start and end at the same node by traversing edges forward. In the context of a causal model, each node $X \in \mathsf{Nodes}(G)$ carries a random variable that we denote by the same letter $X$. A directed edge $X \to Y$ corresponds to the possibility of a direct causal influence from the variable $X$ to the variable $Y$. In this way, the edges implement causal relations.

Our terminology for the causal relations between the nodes in a DAG is the standard one. The parents of a node $X$ in $G$ are defined as those nodes from which an outgoing edge terminates at $X$, i.e. $\mathsf{Pa}_G(X) = \{ Y \mid Y \to X \}$. (When the graph $G$ is clear from the context, we omit the subscript.) Similarly, the children of a node $X$ are defined as those nodes at which edges originating at $X$ terminate, i.e. $\mathsf{Ch}_G(X) = \{ Y \mid X \to Y \}$. If $\boldsymbol{U}$ is a set of nodes, then we put $\mathsf{Pa}_G(\boldsymbol{U}) := \bigcup_{X \in \boldsymbol{U}} \mathsf{Pa}_G(X)$ and $\mathsf{Ch}_G(\boldsymbol{U}) := \bigcup_{X \in \boldsymbol{U}} \mathsf{Ch}_G(X)$. The **ancestors** of a set of nodes $\boldsymbol{U}$, denoted $\mathsf{An}_G(\boldsymbol{U})$, are defined as those nodes which have a directed *path* to some node in $\boldsymbol{U}$, including the nodes in $\boldsymbol{U}$ themselves[6]. Equivalently, $\mathsf{An}(\boldsymbol{U}) := \bigcup_{n \in \mathbb{N}} \mathsf{Pa}^n(\boldsymbol{U})$, where $\mathsf{Pa}^n(\boldsymbol{U})$ is inductively defined via $\mathsf{Pa}^0(\boldsymbol{U}) := \boldsymbol{U}$ and $\mathsf{Pa}^{n+1}(\boldsymbol{U}) := \mathsf{Pa}(\mathsf{Pa}^n(\boldsymbol{U}))$.

A **causal structure** is a DAG $G$ that incorporates a distinction between two types of nodes: the set of observed nodes $\mathsf{ObservedNodes}(G)$, and the set of latent nodes $\mathsf{LatentNodes}(G)$[7]. Following [13], we will depict the observed nodes by triangles and the latent nodes by circles, as in Fig. 1. Henceforth, we will use the terms "DAG" and "causal structure" interchangeably, so that the specification of which variables are observed is considered to be part of the DAG. Frequently, we supplement the causal structure by a specification of the cardinalities of the observed variables. While these are finite in all our examples, the inflation technique applies just as well in the case of continuous variables.

The second component of a causal model is a family of **causal parameters**. The causal parameters specify, for each node $X$, the conditional probability distribution over the values of the random variable $X$, given the values of the variables in $\mathsf{Pa}(X)$. In the case of root nodes, we have $\mathsf{Pa}(X) = \emptyset$, and the conditional distribution is an unconditioned distribution. We write $P_{Y|X}$ for the conditional distribution of a variable $Y$ given a variable $X$, while the particular conditional probability of the variable $Y$ taking the value $y$ given that the variable $X$ takes the values $x$ is denoted[8] $P_{Y|X}(y|x)$. Therefore, a family of causal parameters has the form

$$\{P_{A|\mathsf{Pa}_G(A)} : A \in \mathsf{Nodes}(G)\}. \tag{1}$$

Finally, a **causal model** $M$ consists of a causal structure together with a family of causal parameters,

$$M = (G, \{P_{A|\mathsf{Pa}_G(A)} : A \in \mathsf{Nodes}(G)\}).$$

A causal model specifies a joint distribution of all variables in the DAG via

$$P_{\mathsf{Nodes}(G)} = \prod_{A \in \mathsf{Nodes}(G)} P_{A|\mathsf{Pa}_G(A)}, \tag{2}$$

where $\prod$ denotes the usual product of functions, so that e.g. $(P_{Y|X} \times P_Y)(x, y) := P_{Y|X}(y|x)P_X(x)$. A distribution $P_{\mathsf{Nodes}(G)}$ arises in this way if and only if it satisfies the Markov conditions associated to $G$.

The joint distribution over the observed variables is obtained from the joint distribution over all variables by marginalization over the latent variables,

$$P_{\mathsf{ObservedNodes}(G)} = \sum_{\{X : X \in \mathsf{LatentNodes}(G)\}} P_{\mathsf{Nodes}(G)}, \tag{3}$$

where $\sum_X$ denotes marginalization over the variable $X$, so that $(\sum_X P_{XY})(y) := \sum_x P_{XY}(xy)$.

A given distribution of observed variables is said to be **compatible** with a given causal structure if there is some choice of the causal parameters that yields the given distribution via Eqs. (2) and (3). Furthermore, a given set of marginal distributions on various subsets of observed variables is said to be compatible with a given causal structure if and only if there exists a joint distribution of observed variables that yields these marginals and is compatible with the causal structure.

---

[6] The inclusion of a node within the set of its ancestors is contrary to the colloquial use of the term "ancestors". One uses this definition so that any correlation between two variables can always be attributed to a common "ancestor". This includes, for instance, the case where one variable is a parent of the other.

[7] Pearl [1, Def. 2.3.2] uses the term *latent structure* when referring to a DAG supplemented by a specification of latent nodes, whereas here that specification is implicit in our term *causal structure*.

[8] Although our notation suggests that all variables are either discrete or described by densities, we do not make this assumption. All of our equations can be translated straightforwardly into proper measure-theoretic notation.

## III. THE INFLATION TECHNIQUE FOR CAUSAL INFERENCE

### A. Inflations of a causal model

We now introduce the notion of **an inflation of a causal model**. If a causal model lives on a DAG $G$, then an inflation of this model lives on an **inflation DAG** $G'$.

There are many possible choices of inflation DAGs $G'$ for a given $G$, forming a set $\mathsf{Inflations}(G)$. The particular choice of $G' \in \mathsf{Inflations}(G)$ then determines the inflation model completely: the family of causal parameters of the inflation model $M'$ is determined by a function $M' = \mathsf{Inflation}_{G\to G'}(M)$ that we define below. We begin by defining when a DAG $G'$ is an inflation of $G$, building on some preliminary definitions.

For a subset of nodes $\boldsymbol{V} \subseteq \mathsf{Nodes}(G)$, we denote the **induced subgraph** on $\boldsymbol{V}$ by $\mathsf{SubDAG}_G(\boldsymbol{V})$. It consists of the nodes $\boldsymbol{V}$ and those edges of $G$ which have both endpoints in $\boldsymbol{V}$. Of special importance to us is the **ancestral subgraph** $\mathsf{AnSubDAG}_G(\boldsymbol{V})$, which is the subgraph induced by the ancestry of $\boldsymbol{V}$, $\mathsf{AnSubDAG}_G(\boldsymbol{V}) \coloneqq \mathsf{SubDAG}_G(\mathsf{An}_G(\boldsymbol{V}))$.

In an inflation DAG $G'$, every node is also labelled by a node of $G$. That is, every node of the inflation DAG $G'$ is a copy of some node of the original DAG $G$, and the copies of a node $A$ of $G$ in $G'$ are denoted $A_1, \ldots, A_k$. The subscript that indexes the copies is termed the **copy-index**. When two objects (e.g. nodes, sets of nodes, DAGs, etc…) are the same up to copy-indices, then we use $\sim$ to indicate this, as in $A_i \sim A_j \sim A$. In particular, $\boldsymbol{U} \sim \boldsymbol{U}'$ for sets of nodes $\boldsymbol{U} \subseteq \mathsf{Nodes}(G)$ and $\boldsymbol{U}' \subseteq \mathsf{Nodes}(G')$ if and only if $\boldsymbol{U}'$ contains exactly one copy of every node in $\boldsymbol{U}$. Similarly, $\mathsf{SubDAG}_{G'}(\boldsymbol{U}') \sim \mathsf{SubDAG}_G(\boldsymbol{U})$ means that in addition to $\boldsymbol{U} \sim \boldsymbol{U}'$, an edge is present between two nodes in $\boldsymbol{U}'$ if and only if it is present between the two associated nodes in $\boldsymbol{U}$.

In order to be an inflation, $G'$ must locally mirror the causal structure of $G$:

**Definition 1.** *The DAG $G'$ is said to be an **inflation** of $G$, that is, $G' \in \mathsf{Inflations}(G)$, if and only if for every $A_i \in \mathsf{Nodes}(G')$, the ancestral subgraph of $A_i$ in $G'$ is equivalent, under removal of the copy-index, to the ancestral subgraph of $A$ in $G$,*

$$G' \in \mathsf{Inflations}(G) \quad \textit{iff} \quad \forall A_i \in \mathsf{Nodes}(G') : \ \mathsf{AnSubDAG}_{G'}(A_i) \sim \mathsf{AnSubDAG}_G(A). \tag{4}$$

To illustrate the notion of inflation, we consider the DAG of Fig. 1, which is called the *Triangle scenario* (for obvious reasons) and which has been studied by many authors [13 (Fig. E#8), 11 (Fig. 18b), 12 (Fig. 3), 24 (Fig. 6a), 29 (Fig. 1a), 30 (Fig. 8), 23 (Fig. 1b), 16 (Fig. 4b)]. Different inflations of the Triangle scenario are depicted in Figs. 2 to 6, which, for ease of reference, will be referred to as the *Web*, *Spiral*, *Capped*, and *Cut* inflations respectively.

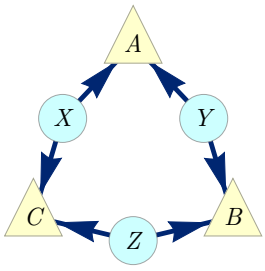


FIG. 1. The Triangle scenario.

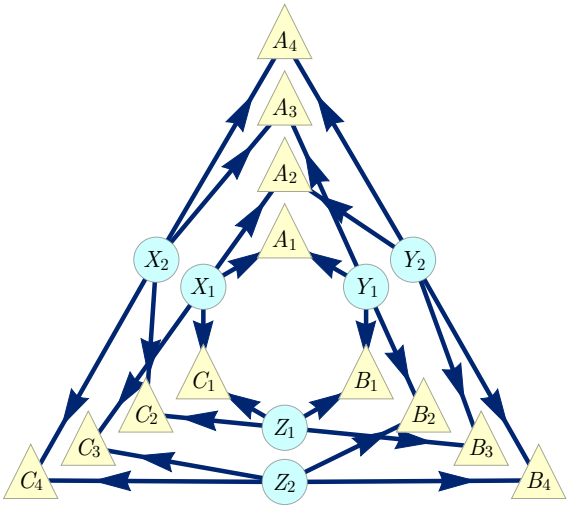


FIG. 2. The Web inflation of the Triangle scenario where each latent node has been duplicated and each observed node has been quadrupled. The four copies of each observed node correspond to the four possible choices of parentage given the pair of copies of each latent parent of the observed node.

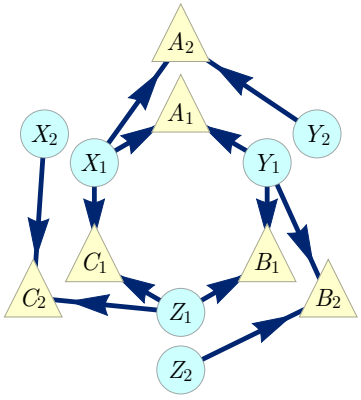


FIG. 3. The Spiral inflation of the Triangle scenario. Notably, this DAG is the ancestral subgraph of the set $\{A_1A_2B_1B_2C_1C_2\}$ in the Web inflation (Fig. 2).

We now define the function $\mathsf{Inflation}_{G\to G'}$, that is, we specify how causal parameters are defined for a given inflation DAG in terms of causal parameters on the original DAG.

**Definition 2.** *Consider causal models $M$ and $M'$ where $\mathsf{DAG}(M) = G$ and $\mathsf{DAG}(M') = G'$, where $G'$ is an inflation of $G$. Then $M'$ is said to be the $G \to G'$* **inflation of** *$M$, that is, $M' = \mathsf{Inflation}_{G\to G'}(M)$, if and only if for every node $A_i$ in $G'$, the manner in which $A_i$ depends causally on its parents within $G'$ is the same as the manner in which $A$ depends causally on its parents within $G$. Noting that $A_i \sim A$ and that $\mathsf{Pa}_{G'}(A_i) \sim \mathsf{Pa}_G(A)$ by Eq. (4), one can formalize this condition as:*

$$\forall A_i \in \mathsf{Nodes}(G') : \; P_{A_i|\mathsf{Pa}_{G'}(A_i)} = P_{A|\mathsf{Pa}_G(A)}. \tag{5}$$

For a given triple $G$, $G'$, and $M$, this definition specifies a unique inflation model $M'$, resulting in a well-defined function $\mathsf{Inflation}_{G\to G'}$.

To sum up, the inflation of a causal model is a new causal model where (i) each variable in the original DAG may have counterparts in the inflation DAG with ancestral subgraphs mirroring those of the originals, and (ii) the manner in which a variable depends causally on its parents in the inflation DAG is given by the manner in which its counterpart in the original DAG depends causally on its parents. The operation of modifying a DAG and equipping the modified version with conditional probability distributions that mirror those of the original also appears in the *do calculus* and *twin networks* of Pearl [1], and moreover bears some resemblance to the *adhesivity* technique used in deriving non-Shannon-type entropic inequalities (Appendix E).

We are now in a position to describe the key property of the inflation of a causal model, the one that makes it useful for causal inference. With notation as in Definition 2, let $P_{\boldsymbol{U}}$ and $P_{\boldsymbol{U}'}$ denote marginal distributions on some $\boldsymbol{U} \subseteq \mathsf{Nodes}(G)$ and $\boldsymbol{U}' \subseteq \mathsf{Nodes}(G')$, respectively. Then

$$\text{if} \quad \boldsymbol{U}' \sim \boldsymbol{U} \;\text{ and }\; \mathsf{AnSubDAG}_{G'}(\boldsymbol{U}') \sim \mathsf{AnSubDAG}_G(\boldsymbol{U}), \quad \text{then} \quad P_{\boldsymbol{U}'} = P_{\boldsymbol{U}}. \tag{6}$$

This follows from the fact that the distributions on $\boldsymbol{U}'$ and $\boldsymbol{U}$ depend only on their ancestral subgraphs and the parameters defined thereon, which by the definition of inflation are the same for $\boldsymbol{U}'$ and for $\boldsymbol{U}$. It is useful to have a name for those sets of observed nodes in $G'$ which satisfy the antecedent of Eq. (6), that is, for which one can find a copy-index-equivalent set in the original DAG $G$ with a copy-index-equivalent ancestral subgraph. We call such subsets of the observed nodes of $G'$ **injectable sets**,

$$\begin{aligned} &\boldsymbol{U}' \in \mathsf{InjectableSets}(G') \\ &\quad \text{iff} \quad \exists \boldsymbol{U} \subseteq \mathsf{ObservedNodes}(G) \;:\; \boldsymbol{U}' \sim \boldsymbol{U} \;\text{ and }\; \mathsf{AnSubDAG}_{G'}(\boldsymbol{U}') \sim \mathsf{AnSubDAG}_G(\boldsymbol{U}). \end{aligned} \tag{7}$$

Similarly, those sets of observed nodes in the original DAG $G$ which satisfy the antecedent of Eq. (6), that is, for which one can find a corresponding set in the inflation DAG $G'$ with a copy-index-equivalent ancestral subgraph, we

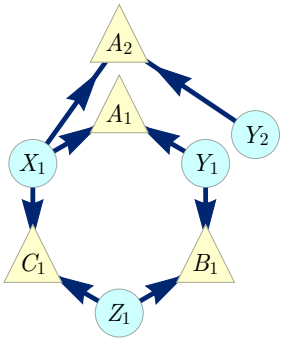


FIG. 4. The Capped inflation of the Triangle scenario; notably also the ancestral subgraph of the set $\{A_1A_2B_1C_1\}$ in the Spiral inflation (Fig. 3).

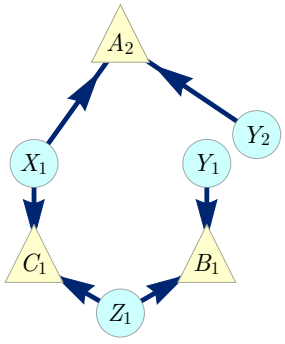


FIG. 5. The Cut inflation of the Triangle scenario; notably also the ancestral subgraph of the set $\{A_2B_1C_1\}$ in the Capped inflation (Fig. 4). Unlike the other examples, this inflation does not contain the Triangle scenario as a subgraph.

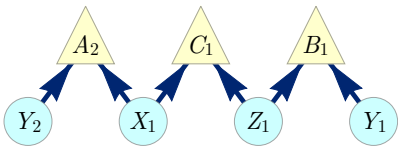


FIG. 6. A different depiction of the Cut inflation of Fig. 5.

describe as **images of the injectable sets** under the dropping of copy-indices,

$$\begin{aligned} &\boldsymbol{U} \in \mathsf{ImagesInjectableSets}(G) \\ &\quad \text{iff} \quad \exists \boldsymbol{U}' \subseteq \mathsf{ObservedNodes}(G') \;\; : \;\; \boldsymbol{U}' \sim \boldsymbol{U} \;\; \text{and} \;\; \mathsf{AnSubDAG}_{G'}(\boldsymbol{U}') \sim \mathsf{AnSubDAG}_{G}(\boldsymbol{U}). \end{aligned} \tag{8}$$

Clearly, $\boldsymbol{U} \in \mathsf{ImagesInjectableSets}(G)$ iff $\exists \boldsymbol{U}' \subseteq \mathsf{InjectableSets}(G')$ such that $\boldsymbol{U} \sim \boldsymbol{U}'$.

For example in the Spiral inflation of the Triangle scenario depicted in Fig. 3, the set $\{A_1B_1C_1\}$ is injectable because its ancestral subgraph is equivalent up to copy-indices to the ancestral subgraph of $\{ABC\}$ in the original DAG, and the set $\{A_2C_1\}$ is injectable because its ancestral subgraph is equivalent to that of $\{AC\}$ in the original DAG.

A set of nodes in the inflation DAG can only be injectable if it contains at most one copy of any node from the original DAG. More strongly, it can only be injectable if its ancestral subgraph contains at most one copy of any observed or latent node from the original DAG. Thus, in Fig. 3, $\{A_1A_2C_1\}$ is not injectable because it contains two copies of $A$, and $\{A_2B_1C_1\}$ is not injectable because its ancestral subgraph contains two copies of $Y$.

We can now express Eq. (6) in the language of injectable sets,

$$P_{\boldsymbol{U}'} = P_{\boldsymbol{U}} \quad \text{if} \quad \boldsymbol{U}' \sim \boldsymbol{U} \;\; \text{and} \;\; \boldsymbol{U}' \in \mathsf{InjectableSets}(G'). \tag{9}$$

In the example of Fig. 3, injectability of the sets $\{A_1B_1C_1\}$ and $\{A_2C_1\}$ thus implies that the marginals on each of these are equal to the marginals on their counterparts, $\{ABC\}$ and $\{AC\}$, in the original causal model, so that $P_{A_1B_1C_1} = P_{ABC}$ and $P_{A_2C_1} = P_{AC}$.

### B. Witnessing incompatibility

Finally, we can explain why inflation is relevant for deciding whether a distribution is compatible with a causal structure. For a family of marginal distributions $\{P_{\boldsymbol{U}} : \boldsymbol{U} \in \mathsf{ImagesInjectableSets}(G)\}$ to be compatible with $G$, there must be a causal model $M$ that yields a joint distribution with this family as its marginals. Looking at the inflation model $M' = \mathsf{Inflation}_{G \to G'}(M)$, Eq. (9) implies that $M'$ has the corresponding family of marginals given by $\{P_{\boldsymbol{U}'} : \boldsymbol{U}' \in \mathsf{InjectableSets}(G')\}$ with $P_{\boldsymbol{U}'} = P_{\boldsymbol{U}}$ for $\boldsymbol{U}' \sim \boldsymbol{U}$, and thus this family is compatible with $G'$.

The same considerations apply for any collection of injectable sets:

**Lemma 3.** *Let $G'$ be an inflation DAG of $G$. Let $S' \subseteq \mathsf{InjectableSets}(G')$ be a collection of injectable sets, and let $S \subseteq \mathsf{ImagesInjectableSets}(G)$ be the images of this collection under the dropping of copy-indices. If the family of marginal distributions $\{P_{\boldsymbol{U}} : \boldsymbol{U} \in S\}$ is compatible with $G$, then the corresponding family of marginal distributions $\{P_{\boldsymbol{U}'} : \boldsymbol{U}' \in S'\}$, defined via $P_{\boldsymbol{U}'} = P_{\boldsymbol{U}}$ for $\boldsymbol{U}' \sim \boldsymbol{U}$, is compatible with $G'$.*

We have thereby related a question about compatibility with the original causal structure to one about compatibility with the inflated causal structure. If one can show that the new compatibility question on $G'$ is answered in the negative, then one can infer that the original question is answered in the negative as well. Some simple examples serve to illustrate the idea.

**Example 1** **Incompatibility of perfect three-way correlation with the Triangle scenario**

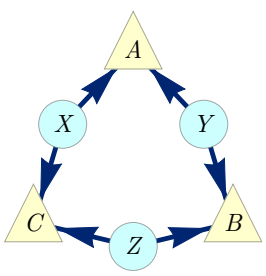


FIG. 7. The Triangle scenario. (Repeat of Fig. 1.)

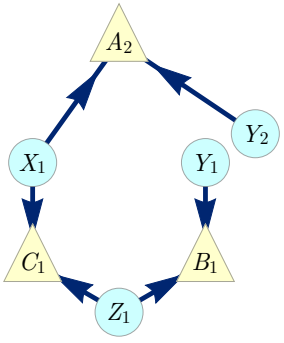


FIG. 8. The Cut inflation of the Triangle scenario. (Repeat of Fig. 5.)

Consider the following causal inference problem. We are given a joint distribution of three binary variables, $P_{ABC}$, where the marginal on each variable is uniform and the three are perfectly correlated,

$$P_{ABC} = \frac{[000] + [111]}{2}, \quad \text{i.e.,} \quad P_{ABC}(abc) = \begin{cases} \frac{1}{2} & \text{if } a = b = c, \\ 0 & \text{otherwise,} \end{cases} \tag{10}$$

and we would like to determine whether it is compatible with the Triangle scenario (Fig. 7). The notation $[abc]$ in Eq. (10) is shorthand for the deterministic distribution where $A$, $B$, and $C$ take the values $a, b$, and $c$ respectively; in terms of the Kronecker delta, $[abc] := \delta_{A,a}\delta_{B,b}\delta_{C,c}$.

Since there are no conditional independence relations among the observed variables in the Triangle scenario, there is no opportunity for ruling out the distribution on the grounds that it fails to satisfy the required conditional independences.

To solve the causal inference problem, we consider the Cut inflation (Fig. 8). The injectable sets include $\{A_2C_1\}$ and $\{B_1C_1\}$. Their images on the original DAG are $\{AC\}$ and $\{BC\}$, respectively.

We will show that the distribution of Eq. (10) is not compatible with the Triangle scenario by demonstrating that the contrary assumption of compatibility implies a contradiction. If the distribution of Eq. (10) were compatible with the Triangle scenario, then so too would be its marginals on $\{AC\}$ and $\{BC\}$, which are given by:

$$P_{AC} = P_{BC} = \frac{[00] + [11]}{2}.$$

By Lemma 3, this compatibility assumption would entail that the marginals

$$P_{A_2C_1} = P_{B_1C_1} = \frac{[00] + [11]}{2} \tag{11}$$

are compatible with the Cut inflation of the Triangle scenario. We now show that the latter compatibility cannot hold, thereby obtaining our contradiction. It suffices to note that (i) the only joint distribution that exhibits perfect correlation between $A_2$ and $C_1$ and between $B_1$ and $C_1$ also exhibits perfect correlation between $A_2$ and $B_1$, and (ii) $A_2$ and $B_1$ have no common ancestor in the Cut inflation DAG and hence must be marginally independent in any distribution that is compatible with it.

We have therefore certified that the distribution $P_{ABC}$ of Eq. (10) is not compatible with the Triangle scenario, recovering a result originally proven by Steudel and Ay [23].

**Example 2** **Incompatibility of the W-type distribution with the Triangle scenario**

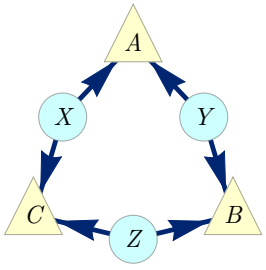


FIG. 9. The Triangle scenario. (Repeat of Fig. 1.)

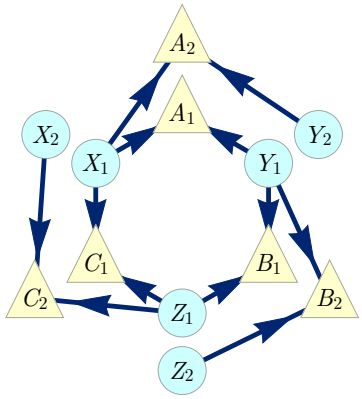


FIG. 10. The Spiral inflation of the Triangle scenario. (Repeat of Fig. 3.)

Consider another causal inference problem on the Triangle scenario, namely, that of determining whether the distribution

$$P_{ABC} = \frac{[100] + [010] + [001]}{3}, \quad \text{i.e.,} \quad P_{ABC}(abc) = \begin{cases} \frac{1}{3} & \text{if } a + b + c = 1, \\ 0 & \text{otherwise.} \end{cases} \tag{12}$$

is compatible with it. We call this the W-type distribution[9]. To settle this compatibility question, we consider the Spiral inflation of the Triangle scenario (Fig. 10). The injectable sets in this case include $\{A_1B_1C_1\}$, $\{A_2C_1\}$, $\{B_2A_1\}$, $\{C_2B_1\}$, $\{A_2\}$, $\{B_2\}$ and $\{C_2\}$.

Therefore, we turn our attention to determining whether the marginals of the W-type distribution on the images of these injectable sets are compatible with the Triangle scenario. These marginals are:

$$P_{ABC} = \frac{[100] + [010] + [001]}{3}, \tag{13}$$

$$P_{AC} = P_{BA} = P_{CB} = \frac{[10] + [01] + [00]}{3}, \tag{14}$$

$$P_A = P_B = P_C = \frac{2}{3}[0] + \frac{1}{3}[1]. \tag{15}$$

By Lemma 3, this compatibility holds only if the associated marginals for the injectable sets, namely,

$$P_{A_1B_1C_1} = \frac{[100] + [010] + [001]}{3}, \tag{16}$$

$$P_{A_2C_1} = P_{B_2A_1} = P_{C_2B_1} = \frac{[10] + [01] + [00]}{3}, \tag{17}$$

$$P_{A_2} = P_{B_2} = P_{C_2} = \frac{2}{3}[0] + \frac{1}{3}[1], \tag{18}$$

are compatible with the Spiral inflation (Fig. 10). Eq. (17) implies that $C_1 = 0$ whenever $A_2 = 1$. It similarly implies that $A_1 = 0$ whenever $B_2 = 1$, and that $B_1 = 0$ whenever $C_2 = 1$,

$$\begin{aligned} A_2 = 1 &\implies C_1 = 0, \\ B_2 = 1 &\implies A_1 = 0, \\ C_2 = 1 &\implies B_1 = 0. \end{aligned} \tag{19}$$

Our inflation DAG is such that $A_2$, $B_2$ and $C_2$ have no common ancestor and consequently are marginally independent in any distribution compatible with it. Together with the fact that each value of these variables has a nonzero probability of occurrence (by Eq. (18)), this implies that

$$\text{Sometimes} \quad A_2 = 1 \text{ and } B_2 = 1 \text{ and } C_2 = 1. \tag{20}$$

Finally, Eq. (19) together with Eq. (20) entails

$$\text{Sometimes} \quad A_1 = 0 \text{ and } B_1 = 0 \text{ and } C_1 = 0. \tag{21}$$

This, however, contradicts Eq. (16). Consequently, the family of marginals described in Eqs. (16-18) is *not* compatible with the DAG of Fig. 10. By Lemma 3, this implies that the family of marginals described in Eqs. (13-15)—and therefore the W-type distribution of which they are marginals—is not compatible with the Triangle scenario.

To our knowledge, this is a new result. In fact, the incompatibility of the W-type distribution with the Triangle scenario cannot be derived via any of the following existing causal inference techniques:

1. Checking conditional independence relations is not relevant here, as there are *no* conditional independence relations implied between any observed variables in the Triangle scenario.

2. The relevant Shannon-type entropic inequalities for the Triangle scenario have been classified, and they do not witness the incompatibility either [16, 24, 25].

3. Moreover, *no* entropic inequality can witness the W-type distribution as unrealizable. Weilenmann and Colbeck [17] have constructed an inner approximation to the entropic cone of the Triangle causal structure, and the W-distribution lies inside this. In other words, a distribution with the same entropic profile as the W-type distribution *can* arise from the Triangle scenario.

---

[9] The name stems from the fact that this distribution is reminiscent of the famous quantum state appearing in [31], called the *W state*.

4. The newly-developed method of covariance matrix causal inference due to Åberg *et al.* [18], which gives tighter constraints than entropic inequalities for the Triangle scenario, also cannot detect the incompatibility.

Therefore, in this case at least, the inflation technique appears to be more powerful.

We have arrived at our incompatibility verdict by combining inflation with reasoning reminiscent of Hardy's version of Bell's theorem [32, 33]. Sec. IV D will present a generalization of this kind of argument and its applications to causal inference.

**Example 3** **Incompatibility of PR-box correlations with the Bell scenario**

Bell's theorem [8–10, 34] concerns the question of whether the distribution obtained in an experiment involving a pair of systems that are measured at space-like separation is compatible with a causal structure of the form of Fig. 11. Here, the observed variables are $\{A, B, X, Y\}$, and $\Lambda$ is a latent variable acting as a common cause of $A$ and $B$. We shall term this causal structure the *Bell scenario*. While the causal inference formulation of Bell's theorem is not the traditional one, several recent articles have introduced and advocated this perspective [11 (Fig. 19), 13 (Fig. E#2), 14 (Fig. 1), 24 (Fig. 1), 35 (Fig. 2b), 36 (Fig. 2)].

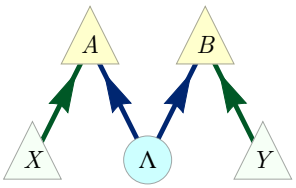


FIG. 11. The causal structure of the bipartite Bell scenario. The local outcomes $A$ and $B$ of Alice's and Bob's measurements is assumed to be a function of some latent common cause and their independent local experimental settings $X$ and $Y$.

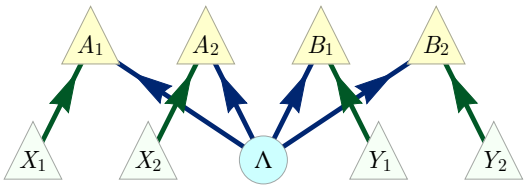


FIG. 12. An inflation DAG of the bipartite Bell scenario, where both local settings and outcome variables have been duplicated.

We consider the distribution $P_{ABXY} = P_{AB|XY} P_X P_Y$, where $P_X$ and $P_Y$ are arbitrary full-support distributions[10] over the binary variables $X$ and $Y$, and

$$P_{AB|XY} = \frac{[00|00] + [11|00] + [00|10] + [11|10] + [00|01] + [11|01] + [01|11] + [10|11]}{8},$$
$$\text{i.e.,}\quad P_{AB|XY}(ab|xy) = \begin{cases} \frac{1}{2} & \text{if } a \oplus b = x \cdot y, \\ 0 & \text{otherwise,} \end{cases} \tag{22}$$

a conditional distribution that was discovered by Tsirelson [37] and later independently by Popescu and Rohrlich [38, 39]. It has become known in the field of quantum foundations as the *PR-box* after the latter authors.[11]

The Bell scenario implies nontrivial conditional independences[12] among the observed variables, namely, $X \perp\!\!\!\perp Y$, $A \perp\!\!\!\perp Y|X$, and[13] $B \perp\!\!\!\perp X|Y$, as well as those that can be generated from these by the semi-graphoid axioms [11]. It is straightforward to check that these conditional independence relations are respected by the $P_{ABXY}$ resulting from Eq. (22). It is well-known that this distribution is nonetheless incompatible with the Bell scenario, for example since it violates the CHSH inequality. Here we prove this incompatibility via the inflation technique, using the inflation of the Bell scenario depicted in Fig. 12.

We begin by noting that $\{A_1B_1X_1Y_1\}$, $\{A_2B_1X_2Y_1\}$, $\{A_1B_2X_1Y_2\}$, $\{A_2B_2X_2Y_2\}$, $\{X_1\}$, $\{X_2\}$, $\{Y_1\}$, and $\{Y_2\}$ are all injectable sets. By Lemma 3, it follows that any causal model that recovers $P_{ABXY}$ inflates to a model that results in marginals

$$P_{A_1B_1X_1Y_1} = P_{A_2B_1X_2Y_1} = P_{A_1B_2X_1Y_2} = P_{A_2B_2X_2Y_2} = P_{ABXY}, \tag{23}$$
$$P_{X_1} = P_{X_2} = P_X, \qquad P_{Y_1} = P_{Y_2} = P_Y. \tag{24}$$

[10] In the literature on the Bell scenario, these variables are known as "settings". Generally, we may think of observed root variables as settings, coloring them light green in the DAG figures. They are natural candidates for variables to condition on.

[11] The PR-box is of interest because it represents a manner in which experimental observations could deviate from the predictions of quantum theory while still being consistent with relativity.

[12] Recall that variables $X$ and $Y$ are conditionally independent given $Z$ if $P_{XY|Z}(xy|z) = P_{X|Z}(x|z)P_{Y|Z}(y|z)$ for all $z$ with $P_Z(z) > 0$. Such a conditional independence is denoted by $X \perp\!\!\!\perp Y \mid Z$.

[13] In the context of a Bell experiment, where $\{X, A\}$ are space-like separated from $\{Y, B\}$, the conditional independences $A \perp\!\!\!\perp Y|X$ and $B \perp\!\!\!\perp X|Y$ encode the impossibility of sending signals faster than the speed of light.

Using the definition of conditional probability, we infer that

$$P_{A_1B_1|X_1Y_1} = P_{A_2B_1|X_2Y_1} = P_{A_1B_2|X_1Y_2} = P_{A_2B_2|X_2Y_2} = P_{AB|XY}. \tag{25}$$

Because $\{X_1\}$, $\{X_2\}$, $\{Y_1\}$, and $\{Y_2\}$ have no common ancestor in the inflation DAG, these variables must be marginally independent in any distribution compatible with the inflation DAG, so that $P_{X_1X_2Y_1Y_2} = P_{X_1}P_{X_2}P_{Y_1}P_{Y_2}$. Given the assumption that the distributions $P_X$ and $P_Y$ have full support, it follows from Eq. (24) that

$$\text{Sometimes} \quad X_1 = 0 \text{ and } X_2 = 1 \text{ and } Y_1 = 0 \text{ and } Y_2 = 1. \tag{26}$$

On the other hand, from Eq. (25) together with the definition of PR-box, Eq. (22), we conclude that

$$\begin{aligned} X_1 = 0,\, Y_1 = 0 &\implies A_1 = B_1, \\ X_1 = 0,\, Y_2 = 1 &\implies A_1 = B_2, \\ X_2 = 1,\, Y_1 = 0 &\implies A_2 = B_1, \\ X_2 = 1,\, Y_2 = 1 &\implies A_2 \neq B_2. \end{aligned} \tag{27}$$

Combining this with Eq. (26), we obtain

$$\text{Sometimes} \quad A_1 = B_1 \text{ and } A_1 = B_2 \text{ and } A_2 = B_1 \text{ and } A_2 \neq B_2. \tag{28}$$

No values of $A_1$, $A_2$, $B_1$, and $B_2$ can jointly satisfy these conditions. So we have reached a contradiction, showing that our original assumption of compatibility of $P_{ABXY}$ with the Bell scenario must have been false.

The structure of this proof parallels that of standard proofs of the incompatibility of the PR-box with the Bell scenario. Standard proofs focus on a set of variables $\{A_0A_1B_0B_1\}$ where $A_x$ is the value of $A$ when $X = x$ and $B_y$ is the value of $B$ when $Y = y$. Note that the distribution $\sum_\lambda P(A_0|\lambda)P(A_1|\lambda)P(B_0|\lambda)P(B_1|\lambda)P(\lambda)$ is a joint distribution of these four variables for which the marginals on pairs $\{A_0B_0\}$, $\{A_0B_1\}$, $\{A_1B_0\}$ and $\{A_1B_1\}$ are those that can arise in the Bell scenario. The existence of such a joint distribution rules out the possibility of having $A_1 = B_1$, $A_1 = B_2$, $A_2 = B_1$ but $A_2 \neq B_2$, and therefore shows that the PR-box distribution is incompatible with the Bell scenario [40, 41]. In light of our use of Eq. (26), the reasoning based on the inflation DAG of Fig. 12 is really the same argument in disguise.

Appendix G shows that the inflation of the Bell scenario of the form of Fig. 12 is sufficient to witness the incompatibility of any distribution that is incompatible with the Bell scenario.

**Example 4 Incompatibility of Pienaar correlations with a modification of the Triangle scenario**

Consider the DAG of Fig. 23. This is a modification of the Triangle scenario where one of the latent variables becomes observed and which we term the *Modifed Triangle Scenario*. Henson, Lal and Pusey showed that this DAG is a candidate for being 'interesting' in the sense that ...

In Pienaar [26], it was shown that the following distribution, which is easily verified to satisfy the CI relations among the observed variables in the Modified Triangle Scenario, namely, $Y \perp\!\!\!\perp C$ and $A \perp\!\!\!\perp B|Y$ [13], is nonetheless incompatible with it:

$$P^{\text{Pien}}_{ABCY} := \frac{[0000] + [0110] + [0001] + [1011]}{4}, \quad \text{i.e.,} \quad P^{\text{Pien}}_{YABC}(yabc) := \begin{cases} \frac{1}{4} & \text{if } y \cdot c = a \text{ and } (y \oplus 1) \cdot c = b, \\ 0 & \text{otherwise.} \end{cases} \tag{29}$$

Here, we will establish this incompatibility using the inflation technique. To do so, we use the inflation of the Modified Triangle scernario that is depicted in Fig. 24 and which we term the Parachute Inflation. The injectable sets include $\{A_1B_1C_1Y_1\}$ and $\{A_2B_1C_2Y_1\}$. They share the same image on the original DAG, namely, the set of all observed variables, $\{ABCY\}$. It follows that

$$P_{A_1B_1C_1Y_1} = P_{A_2B_1C_2Y_1} = P^{\text{Pien}}_{ABCY}. \tag{30}$$

If $P^{\text{Pien}}_{ABCY}$ is compatible with the Modified Triangle Scenario, then by Lemma 3, $P_{A_1B_1C_1Y_1}$ and $P_{A_2B_1C_2Y_1}$ are compatible with the Parachute inflation of the Modified Triangle Scenario. We can show that $P^{\text{Pien}}_{ABCY}$ is *incompatible* with the Modified Triangle Scenario, therefore, by assuming that $P_{A_1B_1C_1Y_1}$ and $P_{A_2B_1C_2Y_1}$ are compatible with the Parachute inflation of the Modified Triangle Scenario and deriving a contradiction.

Note first that we can rewrite Eq. 29 as

$$P_{ABCY} = \frac{1}{2}([00]_{BC} + [11]_{BC})[0]_A[0]_Y + \frac{1}{2}([00]_{AC} + [11]_{AC})[0]_B[1]_Y, \tag{31}$$

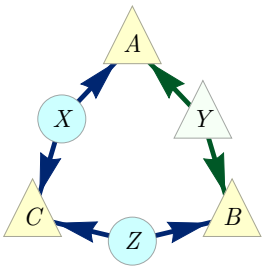


FIG. 13. DAG #15 in Ref. [13], which we term the Modified Triangle Scenario.

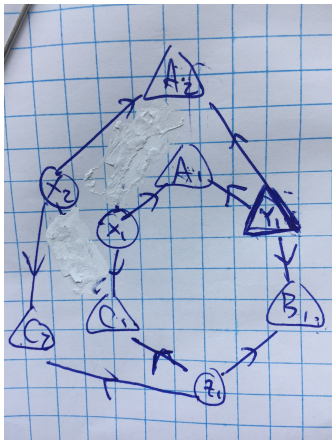

FIG. 14. The Parachute inflation of Fig. 23.

in which form it is evident that

$$P_{AC|Y=1} = \frac{1}{2}([00]_{AC} + [11]_{AC}), \tag{32}$$

$$P_{BC|Y=0} = \frac{1}{2}([00]_{BC} + [11]_{BC}),. \tag{33}$$

Given Eq. 30, we infer that

$$P_{A_1C_1|Y_1=1} = \frac{1}{2}([00]_{A_1C_1} + [11]_{A_1C_1}), \tag{34}$$

$$P_{A_2C_2|Y_1=1} = \frac{1}{2}([00]_{A_2C_2} + [11]_{A_2C_2}). \tag{35}$$

and that

$$P_{B_1C_1|Y_1=0} = \frac{1}{2}([00]_{B_1C_1} + [11]_{B_1C_1}), \tag{36}$$

$$P_{B_1C_2|Y_1=0} = \frac{1}{2}([00]_{B_1C_2} + [11]_{B_1C_2}). \tag{37}$$

Any distribution $P_{B_1C_1C_2Y_1}$ which has marginals $P_{B_1C_1Y_1}$ and $P_{B_1C_2Y_1}$ that reproduce the conditional distributions of Eq. (36) and Eq. (37) respectively, must be such that

$$P_{B_1C_1C_2|Y_1=0} = \frac{1}{2}([000]_{B_1C_1C_2} + [111]_{B_1C_1C_2}). \tag{38}$$

The reason is that if $B_1$ and $C_1$ are perfectly correlated, as in Eq. (36), and $B_1$ and $C_2$ are perfectly correlated, as in Eq. (37), then $C_1$ and $C_2$ must be perfectly correlated as well. Indeed, marginalizing Eq. (38) over $B_1$, we obtain

$$P_{C_1C_2|Y_1=0} = \frac{1}{2}([00]_{C_1C_2} + [11]_{C_1C_2}). \tag{39}$$

But the Parachute inflation of the Modified Triangle Scenario is such that $C_1C_2$ and $Y_1$ are ancestrally independent, so that

$$P_{C_1C_2|Y_1} = P_{C_1C_2}, \tag{40}$$

and therefore $P_{C_1C_2|Y_1=0} = P_{C_1C_2|Y_1=1}$, so that we can infer from Eq. (39) that

$$P_{C_1C_2|Y_1=1} = \frac{1}{2}([00]_{C_1C_2} + [11]_{C_1C_2}). \tag{41}$$

Finally, we note that any distribution $P_{A_1A_2C_1C_2Y_1}$ which has marginals $P_{A_1C_1Y_1}$, $P_{A_2C_2Y_1}$, and $P_{C_1C_2Y_1}$ that reproduce the conditional distributions of Eq. (34), Eq. (35) and Eq. (41) respectively must be such that

$$P_{A_1A_2C_1C_2|Y_1=1} = \frac{1}{2}([0000]_{A_1A_2C_1C_2} + [1111]_{A_1A_2C_1C_2}). \tag{42}$$

The reason is that if $A_1$ and $C_1$ are perfectly correlated, as in Eq. (34), and $A_2$ and $C_2$ are perfectly correlated, as in Eq. (35), and $C_1$ and $C_2$ are perfectly correlated, as in Eq. (41), then $A_1$ and $A_2$ must be perfectly correlated as well. Indeed, marginalizing Eq. (42) over $C_1C_2$, we obtain

$$P_{A_1A_2|Y_1=1} = \frac{1}{2}([00]_{A_1A_2} + [11]_{A_1A_2}). \tag{43}$$

Finally, we note that in the Parachute inflation of the Modified Triangle Scenario, $A_1$ is d-separated from $A_2$ given $Y_1$, which implies that $P_{A_1A_2|Y_1} = P_{A_1|Y_1}P_{A_2|Y_1}$. This is inconsistent with Eq. (43), so we have derived a contradiction.

### C. Deriving causal compatibility inequalities

The inflation technique can be used not only to witness the incompatibility of a given distribution with a given causal structure, but also to derive necessary conditions that a distribution must satisfy to be compatible with the given causal structure. When these conditions are expressed as inequalities, we will refer to them as *causal compatibility inequalities*. Formally, we have:

**Definition 4.** *Let $G$ be a causal structure and let $S$ be a family of subsets of the observed variables of $G$, $S \subseteq 2^{\mathsf{ObservedNodes}(G)}$. Let $I_S$ denote an inequality that operates on the corresponding family of distributions, $\{P_{\boldsymbol{U}} : \boldsymbol{U} \in S\}$. Then $I_S$ is a* **causal compatibility inequality for the causal structure** *$G$ whenever it is satisfied by every family of distributions $\{P_{\boldsymbol{U}} : \boldsymbol{U} \in S\}$ that is compatible with $G$.*

While violation of a causal compatibility inequality witnesses the incompatibility with the causal structure, satisfaction of the inequality does not guarantee compatibility. This is the sense in which it merely provides a *necessary* condition for compatibility.

The inflation technique is useful for deriving causal compatibility inequalities because of the following consequence of Lemma 3:

**Corollary 5.** *Suppose that $G'$ is an inflation of $G$. Let $S' \subseteq \mathsf{InjectableSets}(G')$ be a family of injectable sets and $S \subseteq \mathsf{ImagesInjectableSets}(G)$ the images of members of $S'$ under the dropping of copy-indices. Let $I_{S'}$ be a causal compatibility inequality for $G'$ operating on families $\{P_{\boldsymbol{U}'} : \boldsymbol{U}' \in S'\}$. Define an inequality $I_S$ as follows: in the functional form of $I_{S'}$, replace every occurrence of a term $P_{\boldsymbol{U}'}$ by $P_{\boldsymbol{U}}$ for the unique $\boldsymbol{U} \in S$ with $\boldsymbol{U} \sim \boldsymbol{U}'$. Then $I_S$ is a causal compatibility inequality for $G$ operating on families $\{P_{\boldsymbol{U}} : \boldsymbol{U} \in S\}$.*

The proof is as follows. Suppose that the family $\{P_{\boldsymbol{U}} : \boldsymbol{U} \in S\}$ is compatible with $G$. By Lemma 3, it follows that the family $\{P_{\boldsymbol{U}'} : \boldsymbol{U}' \in S'\}$ where $P_{\boldsymbol{U}'} := P_{\boldsymbol{U}}$ for $\boldsymbol{U}' \sim \boldsymbol{U}$ is compatible with $G'$. Since $I_{S'}$ is a causal compatibility inequality for $G'$, it follows that $\{P_{\boldsymbol{U}'} : \boldsymbol{U}' \in S'\}$ satisfies $I_{S'}$. But by the definition of $I_S$, its evaluation on $\{P_{\boldsymbol{U}} : \boldsymbol{U} \in S\}$ is equal to $I_{S'}$ evaluated on $\{P_{\boldsymbol{U}'} : \boldsymbol{U}' \in S'\}$. It therefore follows that $\{P_{\boldsymbol{U}} : \boldsymbol{U} \in S\}$ satisfies $I_S$. Since $\{P_{\boldsymbol{U}} : \boldsymbol{U} \in S\}$ was an arbitrary family compatible with $G$, we conclude that $I_S$ is a causal compatibility inequality for $G$.

We now present some simple examples of causal compatibility inequalities for the Triangle scenario that one can derive from the inflation technique via Corollary 5. Some terminology and notation will facilitate their description. We refer to a pair of nodes which do not share any common ancestor as being **ancestrally independent**. This is equivalent to being $d$-separated by the empty set [1–4]. Given that the conventional notation for $X$ and $Y$ being $d$-separated by $Z$ in the DAG $G$ is $X \perp_G Y|Z$, we denote $X$ and $Y$ being ancestrally independent within $G$ as $X \perp_G Y$.

Generalizing to sets, $\boldsymbol{U} \perp_G \boldsymbol{V}$ indicates that no node in $\boldsymbol{U}$ shares a common ancestor with any node in $\boldsymbol{V}$ within the DAG $G$,

$$\boldsymbol{U} \perp_G \boldsymbol{V} \quad \text{iff} \quad \mathsf{An}_G(\boldsymbol{U}) \cap \mathsf{An}_G(\boldsymbol{V}) = \emptyset. \tag{44}$$

Furthermore, the notation $\boldsymbol{U} \perp_G \boldsymbol{V} \perp_G \boldsymbol{W}$ should be understood as indicating that $\boldsymbol{U} \perp_G \boldsymbol{V}$ and $\boldsymbol{V} \perp_G \boldsymbol{W}$ and $\boldsymbol{U} \perp_G \boldsymbol{W}$.

**Example 5** **A causal compatibility inequality in terms of *correlators***

As in Example 1 of the previous section, consider the Cut inflation of the Triangle scenario (Fig. 8), where all observed variables are binary. For technical convenience, we assume that they take values in the set $\{-1, +1\}$, rather than taking values in $\{0, 1\}$ as was presumed in the last section.

The injectable sets that we make use of are $\{A_2C_1\}$, $\{B_1C_1\}$, $\{A_2\}$, and $\{B_1\}$. From Corollary 5, any causal compatibility inequality for the inflation DAG that operates on the marginal distributions of $\{A_2C_1\}$, $\{B_1C_1\}$, $\{A_2\}$, and $\{B_1\}$ will yield a causal compatibility inequality for the original DAG that can be evaluated on the marginal distributions on $\{AC\}$, $\{BC\}$, $\{A\}$, and $\{B\}$. We begin by noting that for *any* distribution on three binary variables $\{A_2B_1C_1\}$, that is, *regardless* of the causal structure in which they are embedded, the marginals on $\{A_2C_1\}$, $\{B_1C_1\}$ and $\{A_2B_1\}$ satisfy the following inequality for expectation values [42–46],

$$\langle A_2C_1\rangle + \langle B_2C_1\rangle - \langle A_2B_1\rangle \leq 1. \tag{45}$$

This is an example of a constraint on pairwise correlators that arises from the presumption that they are consistent with a joint distribution. (The problem of deriving such constraints is the *marginal constraint problem*, discussed in detail in Sec. IV.)

But in the Cut inflation of the Triangle scenario (Fig. 8) $A_2$ and $B_1$ have no common ancestor and consequently any distribution compatible with this DAG must make $A_2$ and $B_1$ marginally independent. In terms of correlators, this can be expressed as

$$A_2 \perp B_1 \implies \langle A_2B_1\rangle = \langle A_2\rangle\langle B_1\rangle. \tag{46}$$

Substituting this into Eq. (45), we have

$$\langle A_2C_1\rangle + \langle B_2C_1\rangle \leq 1 + \langle A_2\rangle\langle B_1\rangle. \tag{47}$$

This is an example of a simple but nontrivial causal compatibility inequality for the DAG of Fig. 8. Finally, by Corollary 5, we infer that

$$\langle AC\rangle + \langle BC\rangle \leq 1 + \langle A\rangle\langle B\rangle \tag{48}$$

is a causal compatibility inequality for the Triangle scenario. This inequality expresses the fact that as long as $A$ and $B$ are not completely biased, there is a tradeoff between the strength of $AC$ correlations and the strength of $BC$ correlations.

Given the symmetry of the Triangle scenario under permutations and sign flips of $A$, $B$ and $C$, it is clear that the image of inequality Eq. (48) under any such symmetry is also a valid causal compatibility inequality. Together, these inequalities constitute a type of monogamy[14] of correlations in the Triangle scenario with binary variables: if any two observed variables with unbiased marginals are perfectly correlated, then they are both uncorrelated with the third.

**Example 6** **A causal compatibility inequality in terms of *entropic quantities***

One way to derive constraints that are independent of the cardinality of the observed variables is to express these in terms of the mutual information between observed variables rather than in terms of correlators. The inflation technique can also be applied to achieve this. To see how this works in the case of the Triangle scenario, consider again the Cut inflation (Fig. 8).

One can follow the same logic as in the preceding example, but starting from a different constraint on marginals. For any distribution on three variables $\{A_2B_1C_1\}$ of arbitrary cardinality (again, regardless of the causal structure in which they are embedded), the marginals on $\{A_2C_1\}$, $\{B_1C_1\}$ and $\{A_2B_1\}$ satisfy the inequality [25, Eq. (29)]

$$I(A_2 : C_1) + I(C_1 : B_1) - I(A_2 : B_1) \leq H(C_1), \tag{49}$$

[14] We are here using the term "monogamy" in the same sort of manner in which it is used in the context of entanglement theory [47].

where $H(X)$ denotes the Shannon entropy of the distribution of $X$, and $I(X:Y)$ denotes the mutual information between $X$ and $Y$ with respect to the marginal on $X$ and $Y$. The fact that $A_2$ and $B_1$ have no common ancestor in the inflation DAG implies that in any distribution that is compatible with the inflation DAG, $A_2$ and $B_1$ are marginally independent. This is expressed entropically as the vanishing of their mutual information,

$$A_2 \perp B_1 \implies I(A_2 : B_1) = 0. \tag{50}$$

Substituting the latter equality into Eq. (49), we have

$$I(A_2 : C_1) + I(C_1 : B_1) \leq H(C_1). \tag{51}$$

This is another example of a nontrivial causal compatibility inequality for the DAG of Fig. 8. By Corollary 5, it follows that

$$I(A : C) + I(C : B) \leq H(C) \tag{52}$$

is also a causal compatibility inequality for the Triangle scenario. This inequality was originally derived in [12]. Our rederivation in terms of inflation coincides with the proof found by Henson *et al.* [13].

**Example 7** **A causal compatibility inequality in terms of *joint probabilities***

Consider the Spiral inflation of the Triangle scenario (Fig. 10) with the injectable sets $\{A_1B_1C_1\}$, $\{A_1B_2\}$, $\{B_1C_2\}$, $\{A_1, C_2\}$, $\{A_2\}$, $\{B_2\}$, and $\{C_2\}$. We derive a causal compatibility inequality under the assumption that the observed variables are binary, adopting the convention that they take values in $\{0, 1\}$.

We begin by noting that the following is a constraint that holds for any joint distribution of $\{A_1B_1C_1A_2B_2C_2\}$, regardless of the causal structure,

$$P_{A_2B_2C_2}(111) \leq P_{A_1B_2C_2}(111) + P_{B_1C_2A_2}(111) + P_{A_2C_1B_2}(111) + P_{A_1B_1C_1}(000). \tag{53}$$

To prove this claim, it suffices to check that the inequality holds for each of the $2^6$ deterministic assignments of outcomes to $\{A_1B_1C_1A_2B_2C_2\}$, from which the general case follows by linearity. A more intuitive proof will be provided in Sec. IV D.

Next, we note that certain sets of variables have no common ancestors with other sets of variables in the inflation DAG, which implies the marginal independence of these sets. Such independences are expressed in the language of joint distributions as factorization,

$$\begin{aligned} A_1B_2 \perp C_2 &\implies P_{A_1B_2C_2} = P_{A_1B_2}P_{C_2}, \\ B_1C_2 \perp A_2 &\implies P_{B_1C_2A_2} = P_{B_1C_2}P_{A_2}, \\ A_2C_1 \perp B_2 &\implies P_{A_2C_1B_2} = P_{A_2C_1}P_{B_2}, \\ A_2 \perp B_2 \perp C_2 &\implies P_{A_2B_2C_2} = P_{A_2}P_{B_2}P_{C_2}. \end{aligned} \tag{54}$$

Substituting these equations into Eq. (53), we obtain the polynomial inequality

$$P_{A_2}(1)P_{B_2}(1)P_{C_2}(1) \leq P_{A_1B_2}(11)P_{C_2}(1) + P_{B_1C_2}(11)P_{A_2}(1) + P_{A_2C_1}(11)P_{B_2}(1) + P_{A_1B_1C_1}(000). \tag{55}$$

This, therefore, is a causal compatibility inequality for the DAG of Fig. 10. Finally, by Corollary 5, we infer that

$$P_A(1)P_B(1)P_C(1) \leq P_{AB}(11)P_C(1) + P_{BC}(11)P_A(1) + P_{AC}(11)P_B(1) + P_{ABC}(000) \tag{56}$$

is a causal compatibility inequality for the Triangle scenario.

What is distinctive about this inequality is that—through the presence of the term $P_{ABC}(000)$—it takes into account genuine three-way correlations, while our earlier inequalities only depend on the two-variable marginals. This inequality is strong enough to demonstrate the incompatibility of the W-type distribution of Eq. (12) with the Triangle scenario: for this distribution: the right-hand side of the inequality vanishes while the left-hand side does not.

Of the known techniques for witnessing the incompatibility of a distribution with a DAG or deriving necessary conditions for compatibility, the most straightforward is to consider the constraints implied by ancestral independences among the observed variables of the DAG. The constraints derived in the last two sections have all made use of this basic technique, but at the level of the inflation DAG rather than the original DAG. The constraints that one thereby infers for the original DAG reflect facts about its causal structure that cannot be expressed in terms of ancestral independences among its observed variables. The inflation technique exposes these facts in the ancestral independences among observed variables of the inflation DAG.

In the rest of this article, we shall continue to rely only on the ancestral independences among observed variables within the inflation DAG to infer compatibility constraints on the original DAG. Nonetheless, it seems plausible that the inflation technique can also amplify the power of *other* techniques that do not merely consider ancestral independences among the observed variables. We consider some prospects in Sec. V.

## IV. SYSTEMATICALLY WITNESSING INCOMPATIBILITY AND DERIVING INEQUALITIES

This section considers the problem of how to generalize the above examples of causal inference via the inflation technique to a systematic procedure. We start by introducing the crucial concept of *pre-injectable set*, which figures implicitly in our earlier examples. By reformulating Example 1, we sketch our general method and explain why solving a *marginal problem* is an essential subroutine of our method. Subsequently, Sec. IV A explains how to systematically identify all of the pre-injectable sets for a given inflation DAG. Sec. IV B describes how to solve any sort of marginal problem. This may involve determining all the facets of the *marginal polytope*, which is computationally costly (Appendix A). It is therefore useful to also consider relaxations of the marginal problem that are more tractable by deriving valid linear inequalities which may or may not bound the marginal polytope tightly. We describe one such approach based on possibilistic Hardy-type paradoxes and the hypergraph transversal problem in Sec. IV D.

As far as causal compatibility inequalities are concerned, we limit ourselves to those expressed in terms of probabilities[15], as these are generally the most powerful. However, essentially the same techniques can be used to derive inequalities expressed in terms of entropies [25], as demonstrated in Example 6.

In the examples from the previous section, the initial inequality—a constraint upon marginals that is independent of the causal structure—involves sets of observed variables that are *not* all injectable sets. Each of these sets can, however, be partitioned into disjoint subsets each of which *is* injectable such that the partitioning represents ancestral independence in the inflation DAG. For instance, in Example 5, the set $\{A_2B_1\}$ is not injectable, but it can be partitioned into the singleton sets $\{A_2\}$ and $\{B_1\}$ which are ancestrally independent and each of which is injectable. It is useful to have a name for such sets of observed variables: we call them **pre-injectable**. So for any $\boldsymbol{U}'$ in the inflation DAG $G'$,

$$\begin{aligned}&\boldsymbol{U}' \in \mathsf{PreInjectableSets}(G')\\ &\qquad \text{iff} \quad \exists\{\boldsymbol{U}'_i \in \mathsf{InjectableSets}(G')\} \quad \text{s.t.} \quad \boldsymbol{U}' = \bigcup_i \boldsymbol{U}'_i \quad \text{and} \quad \forall i \neq j : \boldsymbol{U}'_i \perp_{G'} \boldsymbol{U}'_j.\end{aligned} \tag{57}$$

Every injectable set is trivially pre-injectable. A pre-injectable set will be termed *maximal* if it is not a proper subset of another pre-injectable set.

Because ancestral independence in the DAG implies statistical independence for any distribution compatible with the DAG, it follows that if $\boldsymbol{U}'$ is a pre-injectable set with ancestrally independent components $\boldsymbol{U}'_1, \ldots, \boldsymbol{U}'_n$, then we have the factorization

$$P_{\boldsymbol{U}'} = P_{\boldsymbol{U}'_1} \cdots P_{\boldsymbol{U}'_n} \tag{58}$$

for any distribution compatible with $G'$. The situation, therefore, is this: for any constraint that one can derive for the marginals on the pre-injectable sets based on the existence of a joint distribution—and hence without reference to the causal structure—one can infer a constraint that *does* refer to the causal structure by substituting within the derived constraint a factorization of the form of Eq. (58).

As a build-up to our exposition of a systematic application of the inflation technique, we now revisit Example 1. As before, to demonstrate the incompatibility of the W distribution of Eq. (10) with the Triangle scenario, we assume compatability and derive a contradiction. Given the W distribution, Lemma 3 implies that the marginal distributions on the injectable sets of the Cut inflation of the Triangle scenario are

$$P_{A_2C_1} = P_{B_1C_1} = \frac{1}{2}[00] + \frac{1}{2}[11], \tag{59}$$

and

$$P_{A_2} = P_{B_1} = \frac{1}{2}[0] + \frac{1}{2}[1]. \tag{60}$$

From the fact that $A_2$ and $B_1$ are ancestrally independent in the Cut inflation, we also infer that the distribution on the pre-injectable set $\{A_2B_1\}$ must be

$$P_{A_2B_1} = P_{A_2}P_{B_1} = \left(\frac{1}{2}[0] + \frac{1}{2}[1]\right) \times \left(\frac{1}{2}[0] + \frac{1}{2}[1]\right) = \frac{1}{4}[00] + \frac{1}{4}[01] + \frac{1}{4}[10] + \frac{1}{4}[11]. \tag{61}$$

---

[15] Or, for binary variables, equivalently in terms of correlators, as in the first example of Sec. III C.

But there is no three-variable distribution $P_{A_2B_1C_1}$ that would have as its two-variable marginals the distributions of Eqs. (59,61). For as we noted in our prior discussion of this example, the perfect correlation between $A_2$ and $C_1$ exhibited by $P_{A_2C_1}$ and the perfect correlation between $B_1$ and $C_1$ exhibited by $P_{B_1C_1}$ would entail perfect correlation between $A_2$ and $B_1$ as well, which is at odds with (61). We have therefore derived a contradiction and consequently can infer the incompatibility of the W distribution with the Triangle scenario.

Generalizing to an arbitrary DAG, therefore, the procedure is as follows:

1. Based on the inflation DAG under consideration, identify the pre-injectable sets and how they each partition into injectable sets.

2. From the given distribution on the original DAG, infer the family of marginal distributions on the pre-injectable sets of the inflation DAG as follows: the distribution on any injectable set is equal to the corresponding distribution on its image in the original DAG; the distribution on any pre-injectable set is the product of the distributions on the injectable sets into which it is partitioned.

3. Determine whether the family of distributions obtained in step 2 are the marginals of a single joint distribution. If not, then the original distribution is incompatible with the original DAG; otherwise, it may or may not be compatible.

The procedure for systematically deriving causal compatibility inequalities is analogous: instead of determining whether a given family of distributions can arise as marginals of a joint distribution, one rather determines all *constraints* that such a family must satisfy in order to arise from a joint distribution. These constraint translate into causal compatibility inequalities for the inflation DAG via the ancestral independences of Eq. (58), and then into causal compatibility inequalities for the original DAG via Corollary 5.

The pre-injectable sets play a crucial role in linking the original DAG with the inflation DAG. They are precisely those sets of variables whose joint distributions in the inflation model are fully specified by the causal model on the original DAG, as they can be computed using Eq. (58) and Lemma 3. So we begin with the problem of identifying the pre-injectable sets systematically.

### A. Identifying the pre-injectable sets

To identify the pre-injectable sets of an inflation DAG $G'$, we must first identify the injectable sets. This problem can be reduced to identifying the injectable pairs of nodes, because if all of the pairs in a set of nodes are injectable, then so too is the set itself. This can be proven as follows. Let $\varphi : G' \to G$ be the projection map from $G'$ to the original DAG $G$, corresponding to removing copy-indices. Then $\varphi$ has the characteristic feature that it preserves and reflects edges to edges: if $A \to B$ in $G'$, then also $\varphi(A) \to \varphi(B)$ in $G$, and vice versa; this follows from the assumption that $G'$ is an inflation of $G$. A set $\boldsymbol{U} \subseteq \mathsf{ObservedNodes}(G')$ is injectable if and only if the restriction of $\varphi$ to $\mathsf{An}(U)$ is an injective map. But now injectivity of a map means precisely that no two different elements of the domain get mapped to the same element of the codomain. So if $\boldsymbol{U}$ is injectable, then so is each of its two-element subsets; conversely, if $\boldsymbol{U}$ is not injectable, then $\varphi$ maps two nodes among the ancestors of $\boldsymbol{U}$ to the same node, which means that there are two nodes in the ancestry that differ only by copy-index. Each of these two nodes must be an ancestor of at least some node in $\boldsymbol{U}$; if one chooses two such descendants, then one gets a two-element subset of $\boldsymbol{U}$ such that $\varphi$ is not injective on the ancestry of that subset, and therefore this two-element set of observed nodes is not injectable.

To enumerate the injectable sets, it is therefore useful to encode certain features of the inflation DAG in an undirected graph which we call the **injection graph**. The nodes of the injection graph are the observed nodes of the inflation DAG, and a pair of nodes $A_i$ and $B_j$ share an edge if the pair $\{A_iB_j\}$ is injectable. For example, Fig. 15 shows the injection graph of the Spiral inflation of the Triangle scenario (Fig. 3). The property noted above states that the injectable sets are precisely the cliques[16] of the injection graph. While for many other applications only the maximal cliques are of interest, our application of the inflation technique requires knowledge of all nonempty cliques.

Given a list of the injectable sets, the pre-injectable sets can be read off from the **pre-injection graph**. The nodes of the pre-injection graph are taken to be the injectable sets in $G'$, and two nodes share an edge if the associated injectable sets are ancestrally independent. Fig. 16 depicts an example. The pre-injectable sets correspond to the cliques of the pre-injection graph: the union of all the injectable sets that make up the nodes of a clique is a pre-injectable set, while the individual nodes already give us the partition into injectable sets relevant for the factorization relation of Eq. (58).

[16] A *clique* is a set of nodes in an undirected graph any two of which share an edge.

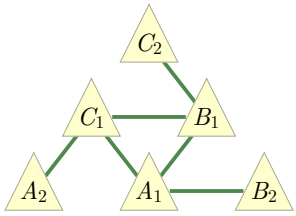


FIG. 15. The injection graph corresponding to the Spiral inflation of the Triangle scenario (Fig. 3), wherein a pair of nodes are adjacent iff they are pairwise injectable.

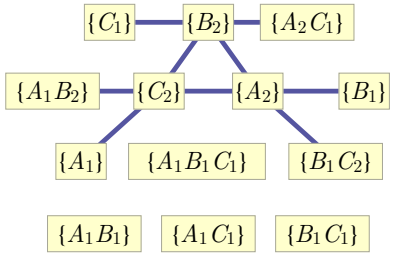


FIG. 16. The pre-injection graph corresponding to the Spiral inflation of the Triangle scenario (Fig. 3), wherein a pair of injectable sets are adjacent iff they are ancestrally independent.

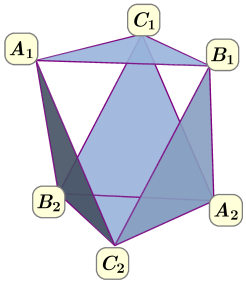


FIG. 17. The simplicial complex of pre-injectable sets for the Spiral inflation of the Triangle scenario (Fig. 3). The 5 faces correspond to the maximal pre-injectable sets, namely $\{A_1B_1C_1\}$, $\{A_1B_2C_2\}$, $\{A_2B_1C_2\}$, $\{A_2B_2C_1\}$ and $\{A_2B_2C_2\}$.

For our purposes, it is sufficient to enumerate the maximal pre-injectable sets, so that one only needs to consider the maximal cliques of the pre-injection graph.

From Figs. 15 and 16, we easily infer the injectable sets and the maximal pre-injectable sets, as well as the partition of the maximal pre-injectable sets into ancestrally independent subsets. For the Spiral example, this results in:

$$\underbrace{\begin{array}{c}\{A_1\},\ \{B_1\},\ \{C_1\},\\ \{A_2\},\ \{B_2\},\ \{C_2\},\\ \{A_1B_1\},\ \{A_1C_1\},\ \{B_1C_1\},\\ \{A_1B_2\}.\ \{A_2C_1\},\ \{B_1C_2\},\\ \{A_1B_1C_1\}\end{array}}_{\text{injectable sets}} \qquad \underbrace{\begin{array}{c}\{A_1B_1C_1\}\\ \{A_1B_2C_2\}\\ \{B_1C_2A_2\}\\ \{C_1A_2B_2\}\\ \{A_2B_2C_2\}\end{array}}_{\substack{\text{maximal}\\ \text{pre-injectable sets}}} \qquad \underbrace{\begin{array}{c}\{A_1B_2\}\perp\{C_2\}\\ \{B_1C_2\}\perp\{A_2\}\\ \{C_1A_2\}\perp\{B_2\}\\ \{A_2\}\perp\{B_2\}\perp\{C_2\}\end{array}}_{\substack{\text{relevant}\\ \text{ancestral independences}}} \tag{62}$$

Having identified the pre-injectable sets and how they partition into injectable sets, we now infer the factorization relations implied by ancestral independences, which is Eq. (54) in the Spiral example. Next, we discuss the other ingredient of our systematic procedure: the marginal problem.

### B. The marginal problem and its solution

The third step in our procedure is determining whether the given distributions on pre-injectable sets can arise as marginals of one joint distribution on all observed nodes of the inflation DAG. In general, the problem of determining whether a given family of distributions can arise as marginals of some joint distribution is known as the *marginal problem*[17]. In order to derive causal compatibility inequalities, one must solve the closely related problem of determining necessary and sufficient *constraints* that a family of marginal distributions must satisfy in order for the marginal problem to have a solution. For better clarity, we distinguish these two variants of the marginal problem as the **marginal satisfiability problem** and the **marginal constraint problem**. The generic **marginal problem** will be used as an umbrella term referring to both types.

To specify either sort of marginal problem, one must specify the full set of variables to be considered, denoted $\boldsymbol{X}$, together with a family of subsets of $\boldsymbol{X}$, denoted $(\boldsymbol{U}_1, \ldots, \boldsymbol{U}_n)$ and called **contexts**. The family of contexts can be visualized through the simplicial complex that it generates, as illustrated in Fig. 17. A **marginal scenario** consists of a specification of contexts together with a specification of the cardinality of each variable. Every joint distribution $P_{\boldsymbol{X}}$ defines a family of marginal distributions $(P_{\boldsymbol{U}_1}, \ldots, P_{\boldsymbol{U}_n})$ through marginalization, $P_{\boldsymbol{U}_i} := \sum_{\boldsymbol{X}\setminus\boldsymbol{U}_i} P_{\boldsymbol{X}}$. The marginal problem concerns the converse inference. In the marginal satisfiability problem, a concrete family of distributions $(P_{\boldsymbol{U}_1}, \ldots, P_{\boldsymbol{U}_n})$ is given, and one wants to decide whether there exists a joint distribution $\hat{P}_{\boldsymbol{X}}$ such that $P_{\boldsymbol{U}_i} = \sum_{\boldsymbol{X}\setminus\boldsymbol{U}_i} \hat{P}_{\boldsymbol{X}}$ for all $i$. In the marginal constraint problem, one seeks to find conditions on the family of

[17] For further references and an outline of the long history of the marginal problem, see [25]. An alternative account using the language of presheaves can also be found in [48].

distributions $(P_{\boldsymbol{U}_1}, \ldots, P_{\boldsymbol{U}_n})$, considered as parameters, for when a joint distribution $\hat{P}_{\boldsymbol{X}}$ exists which reproduces these as marginals, $P_{\boldsymbol{U}_i} = \sum_{\boldsymbol{X}\setminus\boldsymbol{U}_i} \hat{P}_{\boldsymbol{X}}$ for all $i$.

In order for $\hat{P}_{\boldsymbol{X}}$ to exist, distributions on different contexts must be consistent on the intersection of contexts, that is, marginalizing $P_{\boldsymbol{U}_i}$ to the variables in $\boldsymbol{U}_i \cap \boldsymbol{U}_j$ must result in the same distribution as marginalizing $P_{\boldsymbol{U}_j}$ to those variables. In many cases, this is not sufficient[18]; indeed, we have already seen examples of additional constraints, namely, the inequalities (45), (49) and (53) from Sec. III C. So what are the necessary and sufficient conditions? To answer this question, it helps to realize two things:

- The set of possibilities for the distribution $P_{\boldsymbol{X}}$ is the convex hull of the deterministic assignments of values to $\boldsymbol{X}$ (the deterministic distributions), and
- The map $P_{\boldsymbol{X}} \mapsto (P_{\boldsymbol{U}_1}, \ldots, P_{\boldsymbol{U}_n})$, describing marginalization to each of the contexts in $(\boldsymbol{U}_1, \ldots, \boldsymbol{U}_n)$, is linear.

Hence the image of the set of possibilities for the distribution $P_{\boldsymbol{X}}$ under the map $P_{\boldsymbol{X}} \mapsto (P_{\boldsymbol{U}_1}, \ldots, P_{\boldsymbol{U}_n})$ is exactly the convex hull of the deterministic assignments of values to $(\boldsymbol{U}_1, \ldots, \boldsymbol{U}_n)$ which are consistent where these contexts overlap. Since there are only finitely many such deterministic assignments, this convex hull is a polytope; it is called the **marginal polytope** [50]. Together with the above equations on coinciding submarginals, the facet inequalities of this polytope solve the marginal constraint problem. The marginal satisfiability problem asks about membership in the polytope; by the above, this becomes a linear program with the joint probabilities $P_{\boldsymbol{X}}$ as the unknowns.

To express this more concretely, we write the marginal satisfiability problem in the form of a generic linear program.

Let the **joint distribution vector** $\boldsymbol{x}$ be the vector associated with the joint probability distribution $P_{\boldsymbol{X}}$, that is, the vector whose components are the probabilities $P_{\boldsymbol{X}}(x)$. Let the **marginal distribution vector** $\boldsymbol{b}$ be the vector that is the concatenation over $i$ of the vectors associated with the distributions $P_{\boldsymbol{U}_i}$. Finally, let the **marginal description matrix** $\boldsymbol{M}$ be the matrix representation of the linear map corresponding to marginalization on each of the contexts, that is, $P_{\boldsymbol{X}} \to (P_{\boldsymbol{U}_1}, \ldots, P_{\boldsymbol{U}_n})$ where $P_{\boldsymbol{U}_i} = \sum_{\boldsymbol{X}\setminus\boldsymbol{U}_i} P_{\boldsymbol{X}}$. The components of $\boldsymbol{M}$ all take the value zero or one.

In this notation, the marginal satisfiability problem consists of determining whether, for a given vector $\boldsymbol{b}$, the following constraints are feasible:

$$\exists\, \boldsymbol{x} : \boldsymbol{x} \geq \boldsymbol{0},\ \boldsymbol{M}\boldsymbol{x} = \boldsymbol{b}, \tag{63}$$

where the component-wise inequality $\boldsymbol{x} \geq \boldsymbol{0}$ enforces the constraint that $P_{\boldsymbol{X}}$ is a probability distribution. This is clearly a linear program.

In the example of Fig. 17 with binary variables, $\boldsymbol{M}$ is a $48 \times 64$ matrix, so that $\boldsymbol{M}\boldsymbol{x} = \boldsymbol{b}$ represents 48 equations and $\boldsymbol{x} \geq \boldsymbol{0}$ represents 64 inequalities; explicit representations of $\boldsymbol{M}$, $\boldsymbol{x}$, and $\boldsymbol{b}$ for this example can be found in Appendix B. A single linear program can then assess whether there is a solution in $\boldsymbol{x}$ for a given marginal distribution vector $\boldsymbol{b}$. If this is not the case, then the marginal satisfiability problem has a negative answer.

Since linear programming is quite easy, probing specific distributions for compatibility for a given inflation DAG is computationally inexpensive. For instance, using the Web inflation of the Triangle scenario (Fig. 2), which contains a large number of observed variables, our numerical computations have reproduced the result of [12, Theorem 2.16], that a certain distribution considered therein is incompatible with the Triangle scenario[19].

In the case of the marginal constraint problem, the vector $\boldsymbol{b}$ is not given, but one rather wants to find conditions on $\boldsymbol{b}$ that hold if and only if Eq. (63) has a solution. As per the above, this is a problem of **facet enumeration**[20] for the marginal polytope. Equivalently, it is the problem of **linear quantifier elimination**[21] for the system of Eq. (63): one tries to find a system of linear equations and inequalities in $\boldsymbol{b}$ such that some $\boldsymbol{b}$ satisfies the system if and only if Eq. (63) has a solution. There is a unique minimal system achieving this, and it consists of the constraints of consistency on the intersections of contexts (mentioned above), together with the facet inequalities of the marginal polytope. Taken together, these form a system of linear equations and inequalities that is equivalent to Eq. (63), but does not contain any quantifiers. In our application, the equations expressing consistency on the intersections of contexts are guaranteed to hold automatically, so that only the facet inequalities are of interest to us.

In terms of Eq. (63), a valid inequality for the marginal distribution vector $\boldsymbol{b}$—such as a facet inequality of the marginal polytope—can always be expressed as $\boldsymbol{y}^T\boldsymbol{b} \geq 0$ for some vector $\boldsymbol{y}$. Validity of an inequality $\boldsymbol{y}^T\boldsymbol{b} \geq 0$ means precisely that $\boldsymbol{y}^T\boldsymbol{M} \geq \boldsymbol{0}$, since the columns of $\boldsymbol{M}$ are the vertices of the marginal polytope. The marginal satisfiability

[18] Depending on how the contexts intersect with one another, this *may* be sufficient. A precise characterization for when this occurs has been found by Vorob'ev [49], see also ? , Thm. 2] for an application of of this characterization enabling computationally significant shortcuts in solving the marginal constraint problem.

[19] This distribution *is*, however, quantum-compatible with the Triangle scenario (Sec. V C).

[20] In Appendix A, we provide an overview of techniques for facet enumeration.

[21] Linear quantifier elimination has already been used in causal inference for deriving entropic causal compatibility inequalities [16, 24]. In that task, however, the unknowns being eliminated are entropies on sets of variables of which one or more is latent. By contrast, the unknowns being eliminated above are all probabilities on sets of variables all of which are observed—but on the inflation DAG rather than the original DAG.

problem for a given vector $\boldsymbol{b}_0$ has no solution if and only if there is a vector $\boldsymbol{y}$ that yields a valid inequality but for which $\boldsymbol{y}^T\boldsymbol{b}_0 < 0$. Necessity follows by noting that if Eq. (63) does have a solution $\boldsymbol{x}$ for a given vector $\boldsymbol{b}_0$, then the fact that $\boldsymbol{y}^T\boldsymbol{M} \geq \boldsymbol{0}$ and the fact that $\boldsymbol{x} \geq \boldsymbol{0}$ implies that $\boldsymbol{y}^T\boldsymbol{b}_0 = \boldsymbol{y}^T\boldsymbol{M}\boldsymbol{x} \geq 0$. Sufficiency follows from Farkas' lemma. Most linear programming tools are capable of returning a *Farkas infeasibility certificate* [51] whenever a linear program has no solution. In our case, if the marginal problem is infeasible for a vector $\boldsymbol{b}_0$, then the certificate is a vector $\boldsymbol{y}$ that yields a valid inequality but for which $\boldsymbol{y}^T\boldsymbol{b}_0 < 0$.[22].

Upon substituting the factorization relations of Eq. (58) and deleting copy indices, any valid inequality for the marginal problem turns into a causal compatibility inequality. This applies both to facet inequalities of the marginal polytope, and to Farkas infeasibility certificates. In the latter case, one obtains an explicit causal compatibility inequality which witnesses the given distribution as incompatible with the given DAG. In other words, if a given distribution is witnessed as incompatible with a DAG using the technique we have described, then with little additional numerical effort, one can also obtain a causal compatibility inequality that exhibits the incompatibility. This may have applications to problems where the facet enumeration is computationally intractable.

Summarizing, we have shown how to leverage the marginal satisfiability problem to witness causal incompatibility of particular distributions, and how to leverage the marginal constraint problem to derive causal compatibility inequalities.

### C. A list of causal compatibility inequalities for the Triangle scenario

As an example of the above method, we present all of the causal compatibility inequalities that one can derive for the Triangle scenario with binary observed variables using ancestral independences in the Spiral inflation (Fig. 3). To present these in an efficient manner, we leverage symmetries of the set of inequalities. Clearly, a permutation of the observed variables is a symmetry whenever it extends to a graph automorphism, which is a permutation of all nodes that takes edges to edges. Furthermore, any permutation among the values assigned to an individual observed variable (i.e., the sample space of that variable) is a symmetry of the set of inequalities, as is any composition of such permutations. In the case of the Triangle DAG, all 6 permutations of the three observed variables are symmetries, and there are $2^3$ permutations of the triple of the values of these three variables (the products of local permutations) that are symmetries. A given inequality, therefore, can lead to at most 48 distinct inequalities under the action of the symmetry operations. We have found numerically that there are four classes of irredundant inequalities that are inequivalent relative to these symmetry operations.[23] We here present a single representative inequality from each of these classes; the multiplicity of inequalities contained in each symmetry class is marked in parentheses to the right of each representative. The full set can be obtained by closing under the symmetry operations. We have here chosen to express these inequalities in terms of correlators (where the two possible values of each variables to be $\{-1, +1\}$), rather than in terms of joint probabilities, because such a presentation is more compact.

$$0 \leq 1 - \langle AC\rangle - \langle BC\rangle + \langle A\rangle\langle B\rangle \qquad (\times 12) \qquad (64)$$

$$0 \leq 3 - \langle A\rangle - \langle B\rangle - \langle C\rangle + 2\langle AB\rangle + 2\langle AC\rangle + 2\langle BC\rangle + \langle ABC\rangle + \langle A\rangle\langle B\rangle + \langle A\rangle\langle C\rangle + \langle B\rangle\langle C\rangle - \langle A\rangle\langle BC\rangle - \langle B\rangle\langle AC\rangle - \langle C\rangle\langle AB\rangle + \langle A\rangle\langle B\rangle\langle C\rangle \qquad (\times 8) \qquad (65)$$

$$0 \leq 4 + 2\langle C\rangle - 2\langle AB\rangle - 3\langle AC\rangle - 2\langle BC\rangle - \langle ABC\rangle + 2\langle A\rangle\langle B\rangle + \langle A\rangle\langle C\rangle - \langle A\rangle\langle BC\rangle - \langle C\rangle\langle AB\rangle + \langle A\rangle\langle B\rangle\langle C\rangle \qquad (\times 24) \qquad (66)$$

$$0 \leq 4 - 2\langle AB\rangle - 2\langle AC\rangle - 2\langle BC\rangle - \langle ABC\rangle + 2\langle A\rangle\langle B\rangle + 2\langle A\rangle\langle C\rangle + 2\langle B\rangle\langle C\rangle - \langle A\rangle\langle BC\rangle - \langle B\rangle\langle AC\rangle - \langle C\rangle\langle AB\rangle \qquad (\times 8) \qquad (67)$$

A machine-readable and closed-under-symmetries version of this list of inequalities may be found in Appendix F.

### D. Causal compatibility inequalities via Hardy-type inferences from logical tautologies

Enumerating all the facets of the marginal polytope is computationally feasible only for small examples. But our method transforms *every* inequality that bounds the marginal polytope into a causal compatibility inequality. We now present a general approach for deriving a special type of such inequalities very quickly.

---

[22] Farkas infeasibility certificates are available, for example, in *Mosek*, *Gurobi*, and *CPLEX*, as well as by accessing dual variables in *cvxr*/*cvxopt*.

[23] An inequality is irredundant if at least one distribution violates it without violating any of the other inequalities.

In the literature on Bell inequalities, it has been noticed that incompatibility with the Bell DAG can sometimes be witnessed by merely looking at which joint outcomes have zero probability and which ones have nonzero probability. In other words, instead of considering the *probability* of an outcome, the inconsistency of some marginal distributions can be evident from considering only the *possibility* or *impossibility* of each outcome. This insight is originally due to Hardy [32], and versions of Bell's theorem that are based on the violation of such **possibilistic constraints** are known as **Hardy-type paradoxes** [40, 52–55]; a partial classification of these can be found in [33]. The method that we describe in the second half of this section can be used to compute a complete classification of possibilistic constraints for *any* marginal problem.

Possibilistic constraints follow from a consideration of *logical relations* that can hold among deterministic assignments to the observed variables. Such logical constraints can also be leveraged to derive probabilistic constraints instead of possibilistic ones, as shown in [43, 56]. This results in a partial solution to any given (probabilistic) marginal problem. Essentially, we solve a possibilistic marginal problem [33], then upgrade the possibilistic constraints into probabilistic inequalities, resulting in a set of probabilistic inequalities whose satisfaction is a necessary but insufficient condition for satisfying the corresponding probabilistic marginal problem. We now demonstrate how to systematically derive all inequalities of this type.

We have already provided a simple example of a Hardy-type argument in Example 2, in the logic used to demonstrate that the family of distributions of Eqs. (16-18) cannot arise as the marginals of a single joint distribution. For our present purposes, it is useful to recast that argument into a new but manifestly equivalent form. First, for the family of distributions in question, we have

$$\begin{aligned} A_2 = 1 \implies C_1 = 0, \\ B_2 = 1 \implies A_1 = 0, \\ C_2 = 1 \implies B_1 = 0, \\ \text{Never} \quad A_1 = 0 \text{ and } B_1 = 0 \text{ and } C_1 = 0. \end{aligned} \tag{68}$$

From the last constraint one infers that at least one of $A_1$, $B_1$ and $C_1$ must be 1, which from the three other constraints implies that at least one of $A_2$, $B_2$ and $C_2$ must be 0, so that it is not the case that all of $A_2$, $B_2$ and $C_2$ are 1. Thus Eq. (68) implies

$$\text{Never} \quad A_2 = 1 \text{ and } B_2 = 1 \text{ and } C_2 = 1. \tag{69}$$

However, the Spiral inflation (Fig. 10) is such that $A_2$, $B_2$, and $C_2$ have no common ancestor and consequently the distribution on the pre-injectable set $\{A_2B_2C_2\}$ is the product of the distributions on $A_2$, $B_2$ and $C_2$. Since each of the latter has full support (Eq. (18)), it follows that the distribution on $\{A_2B_2C_2\}$ also has full support, which contradicts Eq. (69).

We are here interested in recasting the argument in a manner amenable to systematic generalization. This is done as follows. We work in a marginal scenario where the contexts are $\{A_2B_2C_2\}$, $\{A_2C_1\}$, $\{B_2A_1\}$, $\{C_2B_1\}$, and $\{A_1B_1C_1\}$, and all variables are binary. The first step of the argument is to note that[24]

$$\begin{aligned} &\neg[A_2{=}1, C_1{=}1] \bigwedge \neg[B_2{=}1, A_1{=}1] \bigwedge \neg[C_2{=}1, B_1{=}1] \bigwedge \neg[A_1{=}0, B_1{=}0, C_1{=}0] \\ &\qquad \implies \neg[A_2{=}1, B_2{=}1, C_2{=}1]. \end{aligned} \tag{70}$$

is a logical tautology for binary variables. It can be understood as a constraint on marginal *deterministic assignments*, which can be thought of as a logical counterpart of a linear inequality bounding the marginal polytope. The second and final step of the argument notes that the given marginal distributions are such that the antecedent is always true, while the consequent is sometimes false.

To see how to translate this into a constraint on marginal *distributions*, we rewrite Eq. (70) in its contrapositive form,

$$[\mathbf{A_2{=}1}, \mathbf{B_2{=}1}, \mathbf{C_2{=}1}] \implies [\mathbf{A_2{=}1}, C_1{=}1] \vee [\mathbf{B_2{=}1}, A_1{=}1] \vee [\mathbf{C_2{=}1}, B_1{=}1] \vee [A_1{=}0, B_1{=}0, C_1{=}0]. \tag{71}$$

Next, we note that if a logical tautology can be expressed as

$$E_0 \implies E_1 \vee \ldots \vee E_n, \tag{72}$$

[24] Here, $\wedge$, $\vee$ and $\neg$ denote conjunction, disjunction and negation respectively.

then by applying the union bound—which asserts that the probability of at least one of a set of events occuring is no greater than the sum of the probabilities of each event occuring—one obtains

$$P(E_0) \leq \sum_{j=1}^{n} P(E_j). \tag{73}$$

Applying this to Eq. (71) in particular yields

$$P_{A_2B_2C_2}(\mathbf{111}) \leq P_{A_1B_2}(11) + P_{B_1C_2}(11) + P_{A_2C_1}(11) + P_{A_1B_1C_1}(000), \tag{74}$$

which is a constraint on the marginal *distributions*.

This inequality allows one to demonstrate the incompatibility of the family of distributions of Eqs. (16-18) with the Spiral inflation just as easily as one can with the tautology of Eq. (70). The fact that $A_2$, $B_2$ and $C_2$ are ancestrally independent in the Spiral inflation implies that $P_{A_2B_2C_2} = P_{A_2}P_{B_2}P_{C_2}$. It then suffices to note that for the given family of distributions, the probability on the left-hand side of Eq. (74) is nonzero (which corresponds to the consequent of Eq. (70) being sometimes false) while every probability on the right-hand side is zero (which corresponds to the antecedent of Eq. (70) being always true). But, of course, the inequality can witness many other incompatibilities in addition to this one.

As another example, consider the marginal problem where the variables are $A$, $B$ and $C$, with each being binary, and the contexts are the pairs $\{AB\}$, $\{AC\}$, and $\{BC\}$. The following tautology provides a constraint on marginal deterministic assignments:[25]

$$[\mathbf{A{=}0}, \mathbf{C{=}0}] \implies [\mathbf{A{=}0}, B{=}0] \vee [B{=}1, \mathbf{C{=}0}]. \tag{75}$$

Applying the union bound, one obtains a constraint on marginal distributions,[26]

$$P_{AC}(\mathbf{00}) \leq P_{AB}(\mathbf{0}0) + P_{BC}(\mathbf{1}0).$$

In this section, we seek to determine, for any marginal scenario, the set of *all* inequalities that can be derived in this manner. We do so by **enumerating** the full set of tautologies of the form of Eqs. (70,75). This boils down to solving the possibilistic version of the marginal constraint problem.

We outline the general procedure using the marginal scenario of Fig. 17, where the full set of variables is $\{A_1A_2B_1B_2C_1C_2\}$ and the contexts are the maximal pre-injectable sets of the Sprial inflation (specified in Eq. (62)), namely, $\{A_1B_1C_1\}$, $\{A_1B_2C_2\}$, $\{A_2B_1C_2\}$, $\{A_2B_2C_1\}$ and $\{A_2B_2C_2\}$. As before, we will express the constraints on marginal deterministic assignments as logical implications with a valuation (assignment of outcomes) on one of the contexts as the **antecedent** and a disjunction over valuations on contexts as the **consequent**. In the following, we explain how to generate *all* such implications which are tight in the sense that the consequent is minimal, i.e., involves as few terms as possible in the disjunction.

First, we fix the antecedent by choosing some context and a joint valuation of its variables. In order to generate all constraints on marginal deterministic assignments, one will have to perform this procedure for *every* context as the antecedent and every choice of valuation thereon. For the sake of concreteness, we take the above example with $[\mathbf{A_2{=}1}, \mathbf{B_2{=}1}, \mathbf{C_2{=}1}]$ as the antecedent. Each logical implication we consider is required to have the property that any variable that appears in both the antecendent and the consequent must be given the same value in both.

To formally determine all valid consequents, it is useful to introduce two hypergraphs associated to the problem. Recall the definition of the incidence matrix of a hypergraph: if vertex $i$ is contained in edge $j$ of the hypergraph, the component in the $i$th row and $j$th colum of the matrix is 1; otherwise it is 0.

The first hypergraph we consider is the one whose incidence matrix is the marginal description matrix $\boldsymbol{M}$ for the marginal problem being considered (this matrix was introduced near Eq. (63)). Each vertex in this hypergraph corresponds to a valuation on some particular context. Each hyperedge corresponds to a possible joint valuation of *all* the variables. A hyperedge contains a vertex if the valuation represented by the hyperedge is an extension of the valuation represented by the vertex. For example, the hyperedge $[A_1{=}0, \mathbf{A_2{=}1}, B_1{=}0, \mathbf{B_2{=}1}, C_1{=}1, \mathbf{C_2{=}1}]$ contains the vertex $[A_1{=}0, \mathbf{B_2{=}1}, \mathbf{C_2{=}1}]$. In our example following Fig. 17, this initial hypergraph has $5 \cdot 2^3 = 40$ vertices and $2^6 = 64$ hyperedges.

The second hypergraph is a subhypergraph of the first one. We delete from the first hypergraph all vertices and hyperedges which contradict the outcomes supposed by the antecedent. In our example, because the vertex

---

[25] This is a tautology since $E \wedge F \implies E \wedge F \wedge (G \vee \neg G) = (E \wedge F \wedge G) \vee (E \wedge F \wedge \neg G) \implies (E \wedge G) \vee (F \wedge \neg G)$.

[26] This inequality is equivalent to Eq. (45).

$[\mathbf{A_2{=}1}, \mathbf{B_2{=}0}, C_1{=}1]$ contradicts the antecedent $[\mathbf{A_2{=}1}, \mathbf{B_2{=}1}, \mathbf{C_2{=}0}]$, we delete it. We also delete the vertex corresponding to the antecedent itself. In our example, this second hypergraph has $2^3 + 3 \cdot 2^1 = 14$ vertices and $2^3 = 8$ hyperedges.

All valid (minimal) consequents are (minimal) **transversals** of this latter hypergraph. A transversal is a set of vertices which has the property that it intersects every hyperedge in at least one vertex. In order to get implications which are as tight as possible, it is sufficient to enumerate only the minimal transversals. Doing so is a well-studied problem in computer science with various natural reformulations and for which manifold algorithms have been developed [57].

In our example, it is not hard to check that the consequent of

$$\begin{aligned}[\mathbf{A_2{=}1}, \mathbf{B_2{=}1}, \mathbf{C_2{=}1}] \quad \Longrightarrow \quad & [A_1{=}1, \mathbf{B_2{=}1}, \mathbf{C_2{=}1}] \vee [\mathbf{A_2{=}1}, B_1{=}1, \mathbf{C_2{=}1}] \\ & \vee [\mathbf{A_2{=}1}, \mathbf{B_2{=}1}, C_1{=}1] \vee [A_1{=}0, B_1{=}0, C_1{=}0]\end{aligned} \tag{76}$$

is such a minimal transversal: every assignment of values to all variables which extends the assignment on the left-hand side satisfies at least one of the terms on the right, but this ceases to hold as soon as one removes any one term on the right.

We convert these implications into inequalities in the usual way via the union bound (i.e., replacing "⇒" by "≤" at the level of probabilities and the disjunctions by sums). For example Eq. (76) translates into the constraint on marginal distributions

$$P_{A_2B_2C_2}(\mathbf{111}) \leq P_{A_1B_2C_2}(\mathbf{111}) + P_{A_2B_1C_2}(\mathbf{111}) + P_{A_2B_2C_1}(\mathbf{111}) + P_{A_1B_1C_1}(000). \tag{77}$$

This inequality is a strengthening of Eq. (74). Eq. (77) was used earlier in this article as the starting point of our third example of how to derive a causal compatibility inequality for the Triangle scenario, Eq. (53). Because Eq. (76) is the progenitor of this inequality, it can be thought of as the progenitor of the causal compatibility inequality that one derives from it, namely, Eq. (56).

Inequalities that one derives from hypergraph transversals are generally weaker than those that result from a complete solution of the marginal problem. Nevertheless, many Bell inequalities are of this form, the CHSH inequality among them [56]. So it seems that this method is still sufficiently powerful to generate plenty of interesting inequalities. At the same time, the method should be significantly easier to implement in practice than the full-fledged facet enumeration, even if one does it for every possible antecedent. Interestingly, all of the irredundant polynomial inequalities represented in Eqs. (64-67) are *all* derivable by means of hypergraph transversals!

In conclusion, facet enumeration is the preferred method for deriving inequalities for the marginal problem when it is computationally tractable. When it is not, enumerating hypergraph transversals presents a good alternative.

## V. FURTHER PROSPECTS FOR THE INFLATION TECHNIQUE

Lemma 3 and Corollary 5 state that any causal inference technique on an inflation DAG $G'$ can be transferred to the original DAG $G$. In the previous section, we have found that even extremely weak techniques on $G'$—namely the existence of a joint distribution plus ancestral independences—can lead to significant and new results for causal inference on $G$. In the following two subsections, we consider two additional possibilities for constraints that might be exploited in this way to enhance the power of inflation further.

### A. Using *d*-separation relations on the inflation DAG

In Sec. IV, we considered causal inference by studying the existence of a joint distribution on observed nodes of the inflation DAG, and then making use of the ancestral independences to factorize the joint distributions on the pre-injectable sets into those on the injectable sets.

It is natural to wonder whether one can sometimes make use of facts about the causal structure that go beyond ancestral independences. It is standard practice, when deriving compatibility conditions for a DAG, to make use of arbitrary $d$-separation relations among variables: if, in a given DAG, $\boldsymbol{X}$ and $\boldsymbol{Y}$ are $d$-separated[27] by $\boldsymbol{Z}$, then a distribution is compatible with that DAG only if it satisfies the conditional independence relation $\boldsymbol{X} \perp\!\!\!\perp \boldsymbol{Y}|\boldsymbol{Z}$. For $\boldsymbol{Z} = \emptyset$, this specializes to ancestral independence of $\boldsymbol{X}$ and $\boldsymbol{Y}$. Thus it is natural to ask: can the inflation technique also

[27] The notion of $d$-separation is treated at length in [1, 3, 11, 13], so we elect not to review it here.

sensibly make use of other $d$-separation relations among sets of observed variables? Yes, many $d$-separation relations can be incorporated into the marginal problem by simply generalizing the notion of pre-injectable sets, although some $d$-separation relations can only be accounted for via nonlinear quantifier elimination.

Every conditional independence relation $\boldsymbol{X} \perp\!\!\!\perp \boldsymbol{Y}|\boldsymbol{Z}$ can be expressed as a polynomial equation in terms of probabilities: while it is most commonly written as $P_{\boldsymbol{XY}|\boldsymbol{Z}}(\boldsymbol{xy}|\boldsymbol{z}) = P_{\boldsymbol{X}|\boldsymbol{Z}}(\boldsymbol{x}|\boldsymbol{z})P_{\boldsymbol{Y}|\boldsymbol{Z}}(\boldsymbol{y}|\boldsymbol{z})$ for all $\boldsymbol{x}$, $\boldsymbol{y}$, and $\boldsymbol{z}$, it can also be written in terms of unconditional probabilities, where it takes the form

$$\forall \boldsymbol{xyz} : P_{\boldsymbol{XYZ}}(\boldsymbol{xyz})P_{\boldsymbol{Z}}(\boldsymbol{z}) = P_{\boldsymbol{XZ}}(\boldsymbol{xz})P_{\boldsymbol{YZ}}(\boldsymbol{yz}).$$

Such a nonlinear constraint can generically be incorporated as a further restriction on the joint distributions compatible with the inflation DAG, supplementing the basic constraints of nonnegativity of probabilities for the joint distribution of the observed variables and the constraints implied by ancestral independences.

Consider, however, an inflation DAG $G'$ wherein $\boldsymbol{X'}$ and $\boldsymbol{Y'}$ are $d$-separated by $\boldsymbol{Z'}$ and moreoever where the sets $\{\boldsymbol{X'Z'}\}$ and $\{\boldsymbol{Y'Z'}\}$ are both injectable. In such an instance, the distribution on $\{\boldsymbol{X'Y'Z'}\}$ can be inferred exclusively from distributions on injectable sets,

$$P_{\boldsymbol{X'Y'Z'}}(\boldsymbol{xyz}) = \begin{cases} \frac{P_{\boldsymbol{XZ}}(\boldsymbol{xz})P_{\boldsymbol{YZ}}(\boldsymbol{yz})}{P_{\boldsymbol{Z}}(\boldsymbol{z})} & \text{if } P_{\boldsymbol{Z}}(\boldsymbol{z})>0 \\ 0 & \text{if } P_{\boldsymbol{Z}}(\boldsymbol{z})=0 \end{cases}. \tag{78}$$

It is therefore straightforward to obtain causal compatibility criteria incorporating the conditional independence implied by the $d$-separation as follows: Treat $\{\boldsymbol{X'Y'Z'}\}$ as a **super-pre-injectable** set, in the sense that it counts as a member of the family of *knowable* marginal distributions in $G'$. Inequalities which reference $P_{\boldsymbol{X'Y'Z'}}$ can be obtained through linear programming by demanding the consistency of all the knowable marginal distributions in $G'$. Such linear constraints become polynomial by making the substitution per Eq. (78), and can then be translated into constraints for the original DAG $G$ per Corollary 5.

The notion of super-pre-injectability is recursive: The set $\{\boldsymbol{X'Y'Z'}\}$ is super-pre-injectable if $\boldsymbol{X'}$ and $\boldsymbol{Y'}$ are $d$-separated by $\boldsymbol{Z'}$ and both $\{\boldsymbol{X'Z'}\}$ and $\{\boldsymbol{Y'Z'}\}$ are super-pre-injectable. It should be clear the pre-injectability defined in Eq. (57) is a special case of super-pre-injectability. It is likely that one could obtain stronger polynomial inequalities – equivalently, stronger witnessing power when testing a specific distribution – by considering maximal super-pre-injectable sets instead of maximal pre-injectable sets. For brevity, the authors do not include explicit examples here. An illustration highlighting the contrast between pre-injectable sets and super-pre-injectable sets is given in Fig. 19. The two $d$-separation criteria implying $X_1Y_1 \perp\!\!\!\perp X_3X_6Y_3Y_6Z_2|Z_1$ and $X_3Y_3 \perp\!\!\!\perp X_6Y_6|Z_2$ can be leveraged to define a marginal distribution over a super-pre-injectable set:

$$P_{X_1X_3X_6Y_1Y_3Y_6Z_1Z_2}(xx'x''yy'y''zz') = \begin{cases} \frac{P_{X_1Y_1Z_1}(xyz)P_{X_3Y_3Z_1}(x'y'z)P_{X_6Y_6Z_2}(x''y''z')}{P_{Z_1}(z)P_{Z_2}(z')} & \text{if } P_{Z_1}(z)>0 \wedge P_{Z_2}(z')>0 \\ 0 & \text{if } P_{Z_1}(z)=0 \vee P_{Z_2}(z')=0 \end{cases}. \tag{79}$$

On the other hand, even super-pre-injectability is unable to incorporate the constraint $X_1X_2Y_1Y_2 \perp\!\!\!\perp X_5X_6Y_5Y_6|Z_1Z_2$ resulting from the corresponding $d$-separation in Fig. 19.

Not all $d$-separation criteria in the inflation DAG can be incorporated linearly, however. For example, in the Spiral inflation of the Triangle scenario (Fig. 3), $A_1$ and $C_2$ are $d$-separated by $\{A_2B_2\}$, in addition to being ancestrally

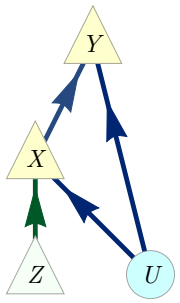


FIG. 18. The instrumental scenario of Pearl [22].

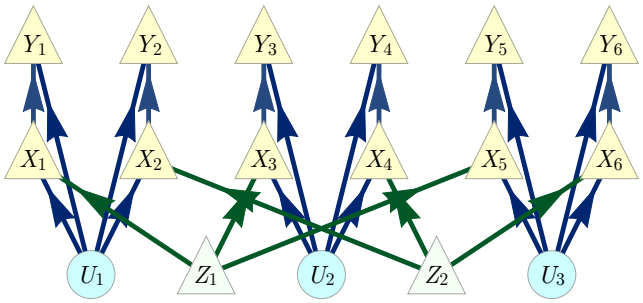


FIG. 19. An inflation DAG of the instrumental scenario illustrating super-pre-injectable sets. The massive set $\{X_1X_3X_6Y_1Y_3Y_6Z_1Z_2\}$ is super-pre-injectable, whereas the largest pre-injectable sets contain only six variables, such as $\{X_1X_4Y_1Y_4Z_1Z_2\}$.

independent. Hence one can try to incorporate the constraint that

$$\forall a_1a_2b_2c_2 : P_{A_1A_2B_2C_2}(a_1a_2b_2c_2)P_{A_2B_2}(a_2b_2) = P_{A_1A_2B_2}(a_1a_2b_2)P_{A_2B_2C_2}(a_2b_2c_2) \tag{80}$$

Every probability that appears in such an equation, though not defined on an injectable set, can still be expressed as a marginal of the joint distribution of all observed variables. For instance, we can express $P_{A_2B_2}$ as

$$\forall a_2b_2 : \; P_{A_2B_2}(a_2b_2) = \sum\nolimits_{a_1b_1c_1c_2} P_{A_1A_2B_1B_2C_1C_2}(a_1a_2b_1b_2c_1c_2). \tag{81}$$

Upon substituting such relations into Eq. (80), one obtains a system of polynomial equations and inequalities in terms of the joint probabilities. We can then proceed with quantifier elimination as we did before, eliminating the unknowns $P_{A_1A_2B_1B_2C_1C_2}(a_1a_2b_1b_2c_1c_2)$ from this system. The additional difficulty now is that some of the equations are nonlinear. This idea even applies to some ancestral independences between sets that are not pre-injectable: for example, $A_1A_2B_2 \perp\!\!\!\perp C_2$ is also guaranteed in the Spiral inflation of the Triangle scenario (Fig. 3), and results in a polynomial equation closely related to Eq. (80).

Many modern computer algebra systems have functions capable of tackling nonlinear quantifier elimination symbolically[28]. Currently, however, it is generally not practical to perform nonlinear quantifier elimination on large polynomial systems with many unknowns to be eliminated. It may help to exploit results on the concrete algebraic-geometric structure of these particular systems [58].

If one is seeking merely to assess the compatibility of a *given* distribution with the causal structure, then one can avoid the quantifier elimination problem and simply try and solve an existence problem: after substituting the values that the given distribution prescribes for the outcomes on pre-injectable sets into the polynomial system in terms of the unknown global joint probabilities, one must only determine whether that system has a solution. Most computer algebra systems can resolve such *satisfiability* questions quite easily[29].

It is also possible to use a mixed strategy of linear and nonlinear quantifier elimination, such as Chaves [6] advocates. The explicit results of [6] are directly causal implications of the *original* DAG, achieved by applying a mixed quantifier elimination strategy. Perhaps further causal compatibility inequalities will be derivable by applying such a mixed quantifier elimination strategy to inflation DAGs.

### B. Using copy-index equivalence on the inflation DAG

By the definition of an inflation model (Definition 2), if two variables in the inflation DAG $G'$ are copy-index-equivalent, $A_i \sim A_j$, then each depends on its parents in the same fashion as $A$ depends on its parents in the original DAG $G$. By transitivity, also $A_i$ and $A_j$ have the same dependence on their parents. Formally, from $A_i \sim A$ and $A_j \sim A$ and the definition of inflation, we infer that $P_{A_i|\mathsf{Pa}_{G'}(A_i)} = P_{A|\mathsf{Pa}_G(A)}$ and $P_{A_j|\mathsf{Pa}_{G'}(A_j)} = P_{A|\mathsf{Pa}_G(A)}$, which implies

$$P_{A_i|\mathsf{Pa}_{G'}(A_i)} = P_{A_j|\mathsf{Pa}_{G'}(A_j)}. \tag{82}$$

The ancestral subgraphs of $A_i$ and $A_j$ are also equivalent, and consequently equations like Eq. (82) also hold for all of the ancestors of $A_i$ and $A_j$. We conclude that the marginal distributions of $A_i$ and $A_j$ must also be equal, $P_{A_i} = P_{A_j}$. More generally, it may be possible to find pairs of contexts in $G'$ of any size such that constraints of the form of Eq. (82) imply that the marginal distributions on these two contexts must be equal.

For example, consider the pair of contexts $\{A_1A_2B_1\}$ and $\{A_1A_2B_2\}$ for the marginal scenario defined by the Spiral inflation (Fig. 3). Neither of these two contexts is an injectable set. Nonetheless, because of Eq. (82), we can conclude that their marginal distributions coincide in any inflation model,

$$\forall aa'b : \; P_{A_1A_2B_1}(aa'b) = P_{A_1A_2B_2}(aa'b). \tag{83}$$

We can also conclude that in the inflation model these marginal distributions satisfy $P_{A_1A_2B_1} = P_{A_2A_1B_2}$—where now the order of $A_1$ and $A_2$ is opposite on the two sides of the equation—or equivalently,

$$\forall aa'b : \; P_{A_1A_2B_1}(aa'b) = P_{A_1A_2B_2}(a'ab). \tag{84}$$

---

[28] For example *Mathematica*$^{TM}$'s `Resolve` command, *Redlog*'s `rlposqe`, or *Maple*$^{TM}$'s `RepresentingQuantifierFreeFormula`.

[29] For example *Mathematica*$^{TM}$'s `Reduce`ExistsRealQ` function. Specialized satisfiability software such as SMT-LIB's `check-sat` [59] are particularly apt for this purpose.

These constraints entail that $P_{A_1A_2B_2}$ must be symmetric under exchange of $A_1$ and $A_2$, which in itself is another equation of the type above.

Parameters such as $P_{A_1A_2B_1}(a_1a_2b)$, $P_{A_1A_2B_2}(a_1a_2b)$ and $P_{A_1A_2}(a_1a_2)$ can each be expressed as sums of the unknowns $P_{A_1A_2B_1B_2C_1C_2}(a_1a_2b_1b_2c_1c_2)$, so that relations such as Eqs. (83,84) each constitute an additional equation that can be added to the system of equations and inequalities that constitute the starting point of the satisfiability problem (if one is seeking to test the compatibility of a given distribution with the inflation DAG) or the quantifier elimination problem (if one is seeking to derive causal compatibility inequalities for the inflation DAG). If any such additional constraints yield stronger constraints at the level of the inflation DAG, then they may translate into stronger constraints at the level of the original DAG.

The general problem of finding pairs of marginal contexts in the inflation DAG for which relations of copy-index-equivalence imply equality of the marginal distributions, and the conditions under which such equalities may yield tighter inequalities, are discussed in Appendix C.

### C. Causal inference in quantum theory and in generalized probabilistic theories

Recent work has sought to explore quantum generalizations of the notion of a causal model, termed *quantum causal models* [13, 14, 29, 60, 61]. We here use the quantum generalization that is implied by the approach of [13].

The causal structures are still represented by DAGs, with a distinction between observed and latent nodes. However, the latent nodes are now associated with sets of quantum channels and the observed nodes are now associated with sets of quantum measurements. Observed nodes are still labelled by random variables, which represent the outcome of the associated measurement. One also makes a distinction between edges in the DAG that carry classical information and edges that carry quantum information.[30] An observed node can have incoming edges of either type: those that come from other observed nodes carry classical information, while those that come from latent nodes carry quantum information. Each quantum measurement in the set that is associated to an observed node acts on the collection of quantum systems received by this node (i.e., on the tensor product of the Hilbert spaces associated to the incoming edges). The classical variables that are received by the node act collectively as a control variable, determining which measurement in the set is implemented. Finally, the random variable that is associated to the node encodes the outcome of the measurement. All of the outgoing edges of an observed node are classical and simply broadcast the outcome of the measurement to the children nodes. A latent node can also have incoming edges that carry classical variables as well as incoming edges that carry quantum systems. Each quantum channel in the set that is associated to a latent node takes the collection of quantum systems associated to the incoming edges as its quantum input and the collection of quantum systems associated to the outgoing edges as its quantum output (the input and output spaces need not have the same dimension). The classical variables that are received by the node act collectively as a control variable, determining which channel in the set is implemented.

A quantum causal model is still ultimately in the service of explaining joint distributions over observed classical variables. The joint distribution of these variables is the only experimental data with which one can confront a given quantum causal model. The basic problem of causal inference for quantum causal models, therefore, concerns the compatibility of a joint distribution of observed classical variables with a given DAG, where the model supplementing the DAG is allowed to be quantum, in the sense defined above. If this happens, we say that the distribution is *quantumly compatible* with the DAG.

One motivation for studying quantum causal models is that they offer a new perspective on an old problem in the field of quantum foundations: that of establishing precisely which of the principles of classical physics must be abandoned in quantum physics. It was noticed by Fritz [12] and Wood and Spekkens [11] that Bell's theorem [34] states that there are distributions on observed nodes of the Bell DAG that are quantumly compatible but not classically compatible with the DAG. Moreover, it was shown in [11] that these distributions cannot be explained by *any* causal structure while complying with the additional principle that conditional independences should not be fine-tuned, i.e., while demanding that any observed conditional independence should be accounted for by the DAG. These results suggest that quantum theory is perhaps best understood as revising our notions of the nature of unobserved entities, and of how one represents causal dependences thereon and incomplete knowledge thereof, while nonetheless *preserving* the spirit of causality and the principle of no fine-tuning [60, 62, 63].

Another motivation for studying quantum causal models is a practical one. Violations of Bell inequalities have been shown to constitute resources for information processing [64–66]. Hence it seems plausible that if one can find DAGs that are different from the Bell scenario but for which their exist distributions that are quantumly compatible with the

[30] In many cases this notion of quantum causal model can also be formulated in a manner that does not require a distinction between two kinds of edges [14].

DAG but not classically compatible, then this quantum-classical separation may also find applications to information processing. For example, it has been shown that in addition to the Bell scenario, such a quantum-classical separation also exists in the bilocality scenario [30] and the Triangle scenario [12], and it is likely that many more DAGs with this property will be found. The hope is that on any DAG supporting a quantum-classical separation, some of the separating distributions may constitute a resource for information processing.

So for both foundational and practical reasons, there is good reason to find examples of DAGs that exhibit a quantum-classical separation. However, this is by no means an easy task. The set of distributions that are quantumly compatible with a given DAG is quite hard to separate from the set of distributions that are classically compatible with that DAG [12, 13]. For example, both the classical and quantum sets respect the conditional independence relations among observed nodes that are implied by the $d$-separation relations of the DAG [13], and entropic inequalities are only of very limited use [12, 67]. We hope that the inflation technique will provide better tools for finding such separations.

In addition to quantum generalizations of causal models, one can define generalizations for other operational theories that are neither classical nor quantum [13, 14]. Such generalizations are formalized using the framework of *generalized probabilistic theories* (GPTs) [68, 69], which is sufficiently general to describe any operational theory that makes statistical predictions about the outcomes of experiments and passes some basic sanity checks. Some constraints on compatibility can be proven to be *theory-independent* in that they apply not only to classical and quantum causal models, but to any kind of generalized probabilistic causal model [13]. For example, the classically-valid conditional independence relations implied between observed variables in a DAG are all also valid in the GPT framework. Another example is the entropic monogamy inequality Eq. (52), which was proven in [13] to be GPT valid as well. These kinds of constraints are of interest because they clarify what any conceivable theory of physics must satisfy on a given causal structure.

The essential element in deriving such constraints is to only make reference to the observed nodes, as done in [13]. In fact, we now understand the argument of [13] to be an instance of the inflation technique. Nonetheless, we have seen that the inflation technique often yields inequalities that hold for the *classical* notion of compatibility, while having quantum and GPT violations, such as the Bell inequalities of Example 3 of Sec. III B and Appendix G. In fact, inflation can be used to derive inequalities with quantum violations for the Triangle scenario as well [70].

So what distinguishes applications of the inflation technique that yield inequalities for GPT compatibility from those that yield inequalities for classical compatibility? The distinction rests on a structural feature of the inflation DAG:

**Definition 6.** *In $G' \in \mathsf{Inflations}(G)$, an **inflationary fan-out** is a latent node that has two or more children that are copy-index equivalent.*

The Web and Spiral inflations of the Triangle scenario, depicted in Fig. 2 and Fig. 3 respectively, contain one or more inflationary fan-outs, as does the inflation of the Bell DAG that is depicted in Fig. 12. On the other hand, the simplest inflation of the Triangle scenario that we consider in this article, the Cut inflation depicted in Fig. 5, does not contain any inflationary fan-outs.

Our main observation is that if one uses an inflation DAG without an inflationary fan-out, then the resulting inequalities derived by the inflation technique will all be GPT valid. In other words, one can only hope to detect a GPT-classical separation if one uses an inflation DAG that *has* at least one inflationary fan-out. We now explain the intuition for why this is the case. In the classical causal model obtained by inflation, the copy-index-equivalent children of an inflationary fan-out causally depend on their parent node in precisely the same way as their counterparts in the original DAG do. For example, this dependence may be such that these two children are exact *copies* of the inflationary fan-out node. So when one tries to write down a quantum or GPT version of our notion of inflation, one quickly runs into trouble: in quantum theory, the *no-broadcasting theorem* shows that such duplication is impossible in a strong sense [71], and an analogous theorem holds for GPTs [72]. This is why in the presence of an inflationary fan-out, one cannot expect our inequalities to hold in the quantum or GPT case, which is consistent with the fact that they often do have quantum and GPT violations.

On the other hand, for any inflation DAG that does not contain an inflationary fan-out, the notion of an inflation model generalizes to the quantum case, as follows. By the definition of inflation, any node in $G'$ has an equivalent set of incoming edges to its counterpart in $G$, while by the assumption that the inflation DAG does not contain any inflationary fan-outs, any node in $G'$ has either the equivalent set of outgoing edges as its counterpart in $G$, or some pruning of this set. In the former case, one associates to this node the same set of quantum channels (if it is a latent node) or measurements (if it is an observed node) that are associated to its counterpart. In the latter case, one simply applies the partial trace operation on the pruned edges (if it is a latent node) or a marginalization on the pruned edges (if it is an observed node). That these prescriptions make sense depends crucially on the assumption that $G'$ is an inflation of $G$, so that the ancestries of any node in $G'$ mirrors the ancestry of the corresponding node in $G$ perfectly. Hence for inflation DAGs $G'$ without inflationary fan-outs, we have quantum analogues of Lemma 3 and Corollary 5. The problem of quantum causal inference on $G$ therefore translates into the corresponding problem on $G'$, and any constraint that we can derive on $G'$ translates back to $G$. In particular, our Examples 1, 5 and 6 also hold for quantum

causal inference: perfect correlation is not only classically incompatible with the Triangle scenario, it is quantumly incompatible as well, and the inequalities Eqs. (48,52) have no quantum violations.

All of these assertions about inflation DAGs that do not contain any inflationary fan-outs apply not only to quantum causal models, but to GPT causal models as well, using the definition of the latter provided in [13].

In the remainder of this section, we discuss the relation between the quantum and the GPT case. Since quantum theory is a particular generalized probabilistic theory, quantum compatibility trivially implies GPT compatibility. Through the work of Tsirelson [37] and Popescu and Rohrlich [38], it is known that the converse is not true: the Bell scenario manifests a GPT-quantum separation. The identification of distributions witnessing this difference, and the derivation of quantum causal compatibility inequalities with GPT violations, has been a focus of much foundational research in recent years. Traditionally, the foundational question has always been: why does quantum theory predict correlations that are *stronger* than one would expect classically? But now there is a new question being asked: why does quantum theory only allow correlations that are *weaker* than those predicted by other GPTs? There has been some interesting progress in identifying physical principles that can pick out the precise correlations that are exhibited by quantum theory [73–81]. Further opportunities for identifying such principles would be useful. This motivates the problem of classifying DAGs into those which have a quantum-classical separation, those which have a GPT-quantum separation and those which have both. Similarly, one can try to classify causal compatibility *inequalities* into those which are GPT-valid, those which are GPT-violable but quantumly valid, and those which are quantum-violable but classically valid.

The problem of deriving inequalities that are GPT-violable but quantumly valid is particularly interesting. Chaves *et al.* [29] have derived some entropic inequalities that can do so. At present, however, we do not see a way of applying the inflation technique to this problem.

## VI. CONCLUSIONS

We have described the *inflation technique* for causal inference in the presence of latent variables.

We have shown how many existing techniques for witnessing incompatibility and for deriving causal compatibility inequalities can be enhanced by the inflation technique, independently of whether these pertain to entropic quantities, correlators or probabilities. The computational difficulty of achieving this enhancement depends on the seed technique. We summarize the computational difficulty of the approaches that we have considered in Table I. A similar table could be drawn for the satisfiability problem, with relative difficulties preserved, but where none of the variants of the problem are computationally hard.

TABLE I. A comparison of different approaches for deriving constraints on compatibility at the level of the inflation DAG, which then translate into constraints on compatibility at the level of the original DAG.

| Input from causal structure | General problem → Standard algorithm(s) | Difficulty |
|---|---|---|
| Only ancestral independences among the observed variables | Facet enumeration of marginal polytope (Sec. IV B) → see Appendix A | Hard |
| | Finding possibilistic constraints by identifying hypergraph transversals (Sec. IV D) → see Eiter *et al.* [57] | Very easy |
| All $d$-separation conditions on the observed variables (Sec. V A) | Real quantifier elimination → Cylindrical algebraic decomposition [6] | Very hard |
| Ancestral independences among the observed variables + copy-index equivalences (Appendix C) | Linear quantifier elimination → Fourier-Motzkin elimination [82–86], Equality set projection [87, 88] | Hard |

Especially in Sec. IV, we have focused on one particular seed technique: the existence of a joint distribution on all observed nodes together with ancestral independences. We have shown how a complete or partial solution of the marginal problem for the pre-injectable sets of the inflation DAG can be leveraged to obtain criteria for causal compatibility, both at the level of witnessing particular distributions as incompatible and deriving causal compatibility inequalities. These inequalities are polynomial in the joint probabilities of the observed variables. They are capable of exhibiting the incompatibility of the W-type distribution with the Triangle scenario, while entropic techniques cannot, so that our polynomial inequalities are stronger than entropic inequalities in at least some cases (see Example 2 of Sec. III B). As far as we can tell, our inequalities are not related to the nonlinear causal compatibility inequalities which have been derived specifically to constrain classical networks [19–21], nor to the nonlinear inequalities which account for interventions to a given causal structure [36, 89].

We have shown that *some* of the causal compatibility inequalities we derive by the inflation technique are necessary conditions not only for compatibility with a classical causal model, but also for compatibility with a causal model in *any* generalized probabilistic theory, which includes quantum causal models as a special case. It would be enlightening to understand the general extent to which our polynomial inequalities for a given DAG can be violated by a distribution arising in a quantum causal model for that DAG. A variety of techniques exist for estimating the amount by which a Bell inequality [90, 91] is violated in quantum theory, but even finding a quantum violation of one of our *polynomial* inequalities for causal structures other than the Bell scenario presents a new task for which we currently lack a systematic approach. Nevertheless, we know that there exists a difference between classical and quantum also beyond Bell scenarios [12, Theorem 2.16], and we hope that our polynomial inequalities will perform better in probing this separation than entropic inequalities do [13, 29].

We have shown that the inflation technique can also be used to derive causal compatibility inequalities that hold for arbitrary generalized probabilistic theories, a significant generalization of the results of [13]. Such inequalities are also very significant insofar as they constitute a restriction on the sorts of statistical correlations that could arise in a given causal scenario even if quantum theory is superceded by some alternative physical theory. As long as the successor theory falls within the framework of generalized probabilistic theories, the restriction will hold.

Finally, an interesting open question is whether it might be possible to modify our methods somehow to derive causal compatibility inequalities that hold for quantum theory and are violated by some GPT. If it *is* possible, then this technique might provide an alternative approach to understanding the Tsirelson bound [10].

A single causal structure has an unlimited number of potential inflations. Selecting a good inflation from which strong polynomial inequalities can be derived is an interesting challenge. To this end, it would be desirable to understand how particular features of the original causal structure are exposed when different nodes in the DAG are duplicated. By isolating which features are exposed in each inflation, we could conceivably quantify the utility for causal inference of each inflation. In so doing, we might find that inflation DAGs beyond a certain level of variable duplication need not be considered. The multiplicity beyond which further inflation is irrelevant may be related to the maximum degree of those polynomials which tightly characterize a causal scenario. Presently, however, it is not clear how to upper bound either number, or whether finite upper bounds can even be expected.

Causal compatibility inequalities are, by definition, merely *necessary* conditions for compatibility. Depending on what kind of causal inference methods one uses at the level of an inflation DAG $G'$, one may or may not obtain sufficient conditions. An interesting question is: if one only uses the existence of a joint distribution and ancestral independences at the level of $G'$, then does one obtain sufficient conditions as $G'$ varies? In other words: if a given distribution is such that for every inflation DAG $G'$, the marginal problem of Sec. IV is solvable, then is the distribution compatible with the original DAG? This occurs for the Bell scenario, where it is enough to consider only one particular inflation (Appendix G). Some evidence against sufficiency in the general case is that we have not seen a way to use the inflation technique to rederive Pearl's instrumental inequality.

## ACKNOWLEDGMENTS

E.W. would like to thank Rafael Chaves and T.C. Fraser for suggestions which have improved this manuscript. T.F. would like to thank Nihat Ay and Guido Montúfar for discussion and references. This research was supported in part by Perimeter Institute for Theoretical Physics. Research at Perimeter Institute is supported by the Government of Canada through the Department of Innovation, Science and Economic Development Canada and by the Province of Ontario through the Ministry of Research, Innovation and Science.

## Appendix A: Algorithms for solving the marginal constraint problem

By solving the marginal constraint problem, what we mean is to determine all the facets of the marginal polytope for a given marginal scenario. Since the vertices of this polytope are precisely the deterministic assignments of values to all variables, which are easy to enumerate, solving the marginal problem is an instance of a **facet enumeration problem**: given the vertices of a convex polytope, determine its facets. This is a well-studied problem in combinatorial optimization for which a variety of algorithms are available [92].

A generic facet enumeration problem takes a matrix $\boldsymbol{V} \in \mathbb{R}^{d\times n}$, which lists the vertices as its columns, and asks for an inequality description of the set of vectors $\boldsymbol{b} \in \mathbb{R}^d$ that can be written as a convex combination of the vertices using weights $\boldsymbol{x} \in \mathbb{R}^n$ that are nonnegative and normalized,

$$\left\{ \boldsymbol{b} \in \mathbb{R}^d \;\middle|\; \exists \boldsymbol{x} \in \mathbb{R}^n : \; \boldsymbol{b} = \boldsymbol{V}\boldsymbol{x}, \;\; \boldsymbol{x} \geq \boldsymbol{0}, \;\; \sum_i x_i = 1 \right\}. \tag{A.1}$$

To solve the marginal problem one uses the marginal description matrix introduced in Sec. IV B as the input to the facet enumeration algorithm, i.e. $\boldsymbol{V} = \boldsymbol{M}$, see Eq. (63).

The oldest-known method for facet enumeration relies on **linear quantifier elimination** in the form of Fourier-Motzkin (FM) elimination [82, 83]. This refers to the fact that one starts with the system $\boldsymbol{b} = \boldsymbol{V}\boldsymbol{x}$, $\boldsymbol{x} \geq \boldsymbol{0}$ and $\sum_i x_i = 1$, which is the half-space representation of a convex polytope (a simplex), and then one needs to project onto $\boldsymbol{b}$-space by *eliminating* the variables $\boldsymbol{x}$ to which the existential *quantifier* $\exists \boldsymbol{x}$ refers. The Fourier-Motzkin algorithm is a particular method for performing this quantifier elimination one variable at a time; when applied to Eq. (A.1), it is equivalent to the *double description method* [83, 93]. Linear quantifier elimination routines are available in many software tools[31]. The authors found it convenient to custom-code a linear quantifier elimination routine in *Mathematica*™.

Other algorithms for facet enumeration that are not based on linear quantifier elimination include the following. *Lexicographic reverse search* (LRS) [95] explores the entire polytope by repeatedly pivoting from one facet to an adjacent one, and is implemented in `lrs`. Equality Set Projection (ESP) [87, 88] is also based on pivoting from facet to facet, though its implementation is less stable[32]. These algorithms could be interesting to use in practice, since each pivoting step churns out a new facet; by contrast, Fourier-Motzkin type algorithms only generate the entire list of facets at once, after all the quantifiers have been eliminated one by one.

It may also be possible to exploit special features of marginal polytopes in order to facilitate their facet enumeration, such as their high degree of symmetry: permuting the outcomes of each variable maps the polytope to itself, which already generates a sizeable symmetry group, and oftentimes there are additional symmetries given by permuting some of the variables. This simplifies the problem of facet enumeration [96, 97], and it may be interesting to apply dedicated software[33] to the facet enumeration problem of marginal polytopes [98–100].

---

[31] For example *MATLAB*™'s `MPT2`/`MPT3`, *Maxima*'s `fourier_elim`, *lrs*'s `fourier`, or *Maple*™'s (v17+) `LinearSolve` and `Projection`. The efficiency of most of these software tools, however, drops off markedly when the dimension of the final projection is much smaller than the initial space of the inequalities. Fast facet enumeration aided by Chernikov rules [84, 94] is implemented in *cdd*, *PORTA*, *qskeleton* , and *skeleton*. In the authors experience *skeleton* seemed to be the most efficient. Additionally, the package *polymake* offers multiple algorithms as options for computing convex hulls.

[32] ESP [86–88] is supported by `MPT2` but not `MPT3`, and by the (undocumented) option of projection in the *polytope* (v0.1.2 2016-07-13) python module.

[33] Such as *PANDA*, *Polyhedral*, or *SymPol*. The authors found *SymPol* to be rather effective for some small test problems, using the options "`./sympol -a --cdd`".

### Appendix B: Explicit marginal description matrix of the Spiral inflation with binary observed variables

Recall that the five maximal pre-injectable sets of the Spiral inflation DAG are $\{A_1B_1C_1\}$, $\{A_1B_2C_2\}$, $\{A_2B_1C_2\}$, $\{A_2B_2C_1\}$ and $\{A_2B_2C_2\}$, as illustrated in Fig. 17. Taking the variables to be binary, each pre-injectable set corresponds to $2^3 = 8$ equations pertinent to the marginal problem. The five *sets* of equations which relate the marginal probabilities to a posited joint distribution are given by

$$\begin{aligned}
&\forall a_1b_1c_1: \; P_{A_1B_1C_1}(a_1b_1c_1) = \sum\nolimits_{a_2b_2b_2} P_{A_1A_2B_1B_2C_1C_2}(a_1a_2b_1b_2c_1c_2),\\
&\forall a_1b_2c_2: \; P_{A_1B_2C_2}(a_1b_2c_2) = \sum\nolimits_{a_2b_1c_1} P_{A_1A_2B_1B_2C_1C_2}(a_1a_2b_1b_2c_1c_2),\\
&\forall a_2b_1c_2: \; P_{A_2B_1C_2}(a_2b_1c_2) = \sum\nolimits_{a_1b_2c_1} P_{A_1A_2B_1B_2C_1C_2}(a_1a_2b_1b_2c_1c_2),\\
&\forall a_2b_2c_1: \; P_{A_2B_2C_1}(a_2b_2c_1) = \sum\nolimits_{a_1b_1c_2} P_{A_1A_2B_1B_2C_1C_2}(a_1a_2b_1b_2c_1c_2),\\
&\forall a_2b_2c_2: \; P_{A_2B_2C_2}(a_2b_2c_2) = \sum\nolimits_{a_1b_1c_1} P_{A_1A_2B_1B_2C_1C_2}(a_1a_2b_1b_2c_1c_2).
\end{aligned} \tag{B.1}$$

As we noted in the main text, such conditions can be expressed in terms of a single matrix equality, $\boldsymbol{M}\boldsymbol{x} = \boldsymbol{b}$ where $\boldsymbol{x}$ is the **joint distribution vector**, $\boldsymbol{b}$ is the **marginal distribution vector** and $\boldsymbol{M}$ is the **marginal description**

**matrix**. In the Sprial example, we have:

the joint distribution vector $\boldsymbol{x}$ of length 64 is

$$\begin{pmatrix}
P_{A_1A_2B_1B_2C_1C_2}(000000)\\
P_{A_1A_2B_1B_2C_1C_2}(000001)\\
P_{A_1A_2B_1B_2C_1C_2}(000010)\\
P_{A_1A_2B_1B_2C_1C_2}(000011)\\
P_{A_1A_2B_1B_2C_1C_2}(000100)\\
P_{A_1A_2B_1B_2C_1C_2}(000101)\\
P_{A_1A_2B_1B_2C_1C_2}(000110)\\
P_{A_1A_2B_1B_2C_1C_2}(000111)\\
P_{A_1A_2B_1B_2C_1C_2}(001000)\\
P_{A_1A_2B_1B_2C_1C_2}(001001)\\
P_{A_1A_2B_1B_2C_1C_2}(001010)\\
P_{A_1A_2B_1B_2C_1C_2}(001011)\\
P_{A_1A_2B_1B_2C_1C_2}(001100)\\
P_{A_1A_2B_1B_2C_1C_2}(001101)\\
P_{A_1A_2B_1B_2C_1C_2}(001110)\\
P_{A_1A_2B_1B_2C_1C_2}(001111)\\
P_{A_1A_2B_1B_2C_1C_2}(010000)\\
P_{A_1A_2B_1B_2C_1C_2}(010001)\\
P_{A_1A_2B_1B_2C_1C_2}(010010)\\
P_{A_1A_2B_1B_2C_1C_2}(010011)\\
P_{A_1A_2B_1B_2C_1C_2}(010100)\\
P_{A_1A_2B_1B_2C_1C_2}(010101)\\
P_{A_1A_2B_1B_2C_1C_2}(010110)\\
P_{A_1A_2B_1B_2C_1C_2}(010111)\\
P_{A_1A_2B_1B_2C_1C_2}(011000)\\
P_{A_1A_2B_1B_2C_1C_2}(011001)\\
P_{A_1A_2B_1B_2C_1C_2}(011010)\\
P_{A_1A_2B_1B_2C_1C_2}(011011)\\
P_{A_1A_2B_1B_2C_1C_2}(011100)\\
P_{A_1A_2B_1B_2C_1C_2}(011101)\\
P_{A_1A_2B_1B_2C_1C_2}(011110)\\
P_{A_1A_2B_1B_2C_1C_2}(011111)\\
P_{A_1A_2B_1B_2C_1C_2}(100000)\\
P_{A_1A_2B_1B_2C_1C_2}(100001)\\
P_{A_1A_2B_1B_2C_1C_2}(100010)\\
P_{A_1A_2B_1B_2C_1C_2}(100011)\\
P_{A_1A_2B_1B_2C_1C_2}(100100)\\
P_{A_1A_2B_1B_2C_1C_2}(100101)\\
P_{A_1A_2B_1B_2C_1C_2}(100110)\\
P_{A_1A_2B_1B_2C_1C_2}(100111)\\
P_{A_1A_2B_1B_2C_1C_2}(101000)\\
P_{A_1A_2B_1B_2C_1C_2}(101001)\\
P_{A_1A_2B_1B_2C_1C_2}(101010)\\
P_{A_1A_2B_1B_2C_1C_2}(101011)\\
P_{A_1A_2B_1B_2C_1C_2}(101100)\\
P_{A_1A_2B_1B_2C_1C_2}(101101)\\
P_{A_1A_2B_1B_2C_1C_2}(101110)\\
P_{A_1A_2B_1B_2C_1C_2}(101111)\\
P_{A_1A_2B_1B_2C_1C_2}(110000)\\
P_{A_1A_2B_1B_2C_1C_2}(110001)\\
P_{A_1A_2B_1B_2C_1C_2}(110010)\\
P_{A_1A_2B_1B_2C_1C_2}(110011)\\
P_{A_1A_2B_1B_2C_1C_2}(110100)\\
P_{A_1A_2B_1B_2C_1C_2}(110101)\\
P_{A_1A_2B_1B_2C_1C_2}(110110)\\
P_{A_1A_2B_1B_2C_1C_2}(110111)\\
P_{A_1A_2B_1B_2C_1C_2}(111000)\\
P_{A_1A_2B_1B_2C_1C_2}(111001)\\
P_{A_1A_2B_1B_2C_1C_2}(111010)\\
P_{A_1A_2B_1B_2C_1C_2}(111011)\\
P_{A_1A_2B_1B_2C_1C_2}(111100)\\
P_{A_1A_2B_1B_2C_1C_2}(111101)\\
P_{A_1A_2B_1B_2C_1C_2}(111110)\\
P_{A_1A_2B_1B_2C_1C_2}(111111)
\end{pmatrix},$$

and the marginal distribution vector $\boldsymbol{b}$ of length 40 is

$$\begin{pmatrix}
P_{A_1B_1C_1}(0,0,0)\\
P_{A_1B_1C_1}(0,0,1)\\
P_{A_1B_1C_1}(0,1,0)\\
P_{A_1B_1C_1}(0,1,1)\\
P_{A_1B_1C_1}(1,0,0)\\
P_{A_1B_1C_1}(1,0,1)\\
P_{A_1B_1C_1}(1,1,0)\\
P_{A_1B_1C_1}(1,1,1)\\
P_{A_1B_2C_2}(0,0,0)\\
P_{A_1B_2C_2}(0,0,1)\\
P_{A_1B_2C_2}(0,1,0)\\
P_{A_1B_2C_2}(0,1,1)\\
P_{A_1B_2C_2}(1,0,0)\\
P_{A_1B_2C_2}(1,0,1)\\
P_{A_1B_2C_2}(1,1,0)\\
P_{A_1B_2C_2}(1,1,1)\\
P_{A_2B_1C_2}(0,0,0)\\
P_{A_2B_1C_2}(0,0,1)\\
P_{A_2B_1C_2}(0,1,0)\\
P_{A_2B_1C_2}(0,1,1)\\
P_{A_2B_1C_2}(1,0,0)\\
P_{A_2B_1C_2}(1,0,1)\\
P_{A_2B_1C_2}(1,1,0)\\
P_{A_2B_1C_2}(1,1,1)\\
P_{A_2B_2C_1}(0,0,0)\\
P_{A_2B_2C_1}(0,0,1)\\
P_{A_2B_2C_1}(0,1,0)\\
P_{A_2B_2C_1}(0,1,1)\\
P_{A_2B_2C_1}(1,0,0)\\
P_{A_2B_2C_1}(1,0,1)\\
P_{A_2B_2C_1}(1,1,0)\\
P_{A_2B_2C_1}(1,1,1)\\
P_{A_2B_2C_2}(0,0,0)\\
P_{A_2B_2C_2}(0,0,1)\\
P_{A_2B_2C_2}(0,1,0)\\
P_{A_2B_2C_2}(0,1,1)\\
P_{A_2B_2C_2}(1,0,0)\\
P_{A_2B_2C_2}(1,0,1)\\
P_{A_2B_2C_2}(1,1,0)\\
P_{A_2B_2C_2}(1,1,1)
\end{pmatrix},$$

i.e.

$$\begin{pmatrix}
P_{A_1A_2B_1B_2C_1C_2}(0,_,0,_,0,_)\\
P_{A_1A_2B_1B_2C_1C_2}(0,_,0,_,1,_)\\
P_{A_1A_2B_1B_2C_1C_2}(0,_,1,_,0,_)\\
P_{A_1A_2B_1B_2C_1C_2}(0,_,1,_,1,_)\\
P_{A_1A_2B_1B_2C_1C_2}(1,_,0,_,0,_)\\
P_{A_1A_2B_1B_2C_1C_2}(1,_,0,_,1,_)\\
P_{A_1A_2B_1B_2C_1C_2}(1,_,1,_,0,_)\\
P_{A_1A_2B_1B_2C_1C_2}(1,_,1,_,1,_)\\
P_{A_1A_2B_1B_2C_1C_2}(0,_,_,0,_,0)\\
P_{A_1A_2B_1B_2C_1C_2}(0,_,_,0,_,1)\\
P_{A_1A_2B_1B_2C_1C_2}(0,_,_,1,_,0)\\
P_{A_1A_2B_1B_2C_1C_2}(0,_,_,1,_,1)\\
P_{A_1A_2B_1B_2C_1C_2}(1,_,_,0,_,0)\\
P_{A_1A_2B_1B_2C_1C_2}(1,_,_,0,_,1)\\
P_{A_1A_2B_1B_2C_1C_2}(1,_,_,1,_,0)\\
P_{A_1A_2B_1B_2C_1C_2}(1,_,_,1,_,1)\\
P_{A_1A_2B_1B_2C_1C_2}(_,0,0,_,_,0)\\
P_{A_1A_2B_1B_2C_1C_2}(_,0,0,_,_,1)\\
P_{A_1A_2B_1B_2C_1C_2}(_,0,1,_,_,0)\\
P_{A_1A_2B_1B_2C_1C_2}(_,0,1,_,_,1)\\
P_{A_1A_2B_1B_2C_1C_2}(_,1,0,_,_,0)\\
P_{A_1A_2B_1B_2C_1C_2}(_,1,0,_,_,1)\\
P_{A_1A_2B_1B_2C_1C_2}(_,1,1,_,_,0)\\
P_{A_1A_2B_1B_2C_1C_2}(_,1,1,_,_,1)\\
P_{A_1A_2B_1B_2C_1C_2}(_,0,_,0,0,_)\\
P_{A_1A_2B_1B_2C_1C_2}(_,0,_,0,1,_)\\
P_{A_1A_2B_1B_2C_1C_2}(_,0,_,1,0,_)\\
P_{A_1A_2B_1B_2C_1C_2}(_,0,_,1,1,_)\\
P_{A_1A_2B_1B_2C_1C_2}(_,1,_,0,0,_)\\
P_{A_1A_2B_1B_2C_1C_2}(_,1,_,0,1,_)\\
P_{A_1A_2B_1B_2C_1C_2}(_,1,_,1,0,_)\\
P_{A_1A_2B_1B_2C_1C_2}(_,1,_,1,1,_)\\
P_{A_1A_2B_1B_2C_1C_2}(_,0,_,0,_,0)\\
P_{A_1A_2B_1B_2C_1C_2}(_,0,_,0,_,1)\\
P_{A_1A_2B_1B_2C_1C_2}(_,0,_,1,_,0)\\
P_{A_1A_2B_1B_2C_1C_2}(_,0,_,1,_,1)\\
P_{A_1A_2B_1B_2C_1C_2}(_,1,_,0,_,0)\\
P_{A_1A_2B_1B_2C_1C_2}(_,1,_,0,_,1)\\
P_{A_1A_2B_1B_2C_1C_2}(_,1,_,1,_,0)\\
P_{A_1A_2B_1B_2C_1C_2}(_,1,_,1,_,1)
\end{pmatrix}, \quad \text{(B.2)}$$

and the marginal description matrix $\boldsymbol{M}$ is

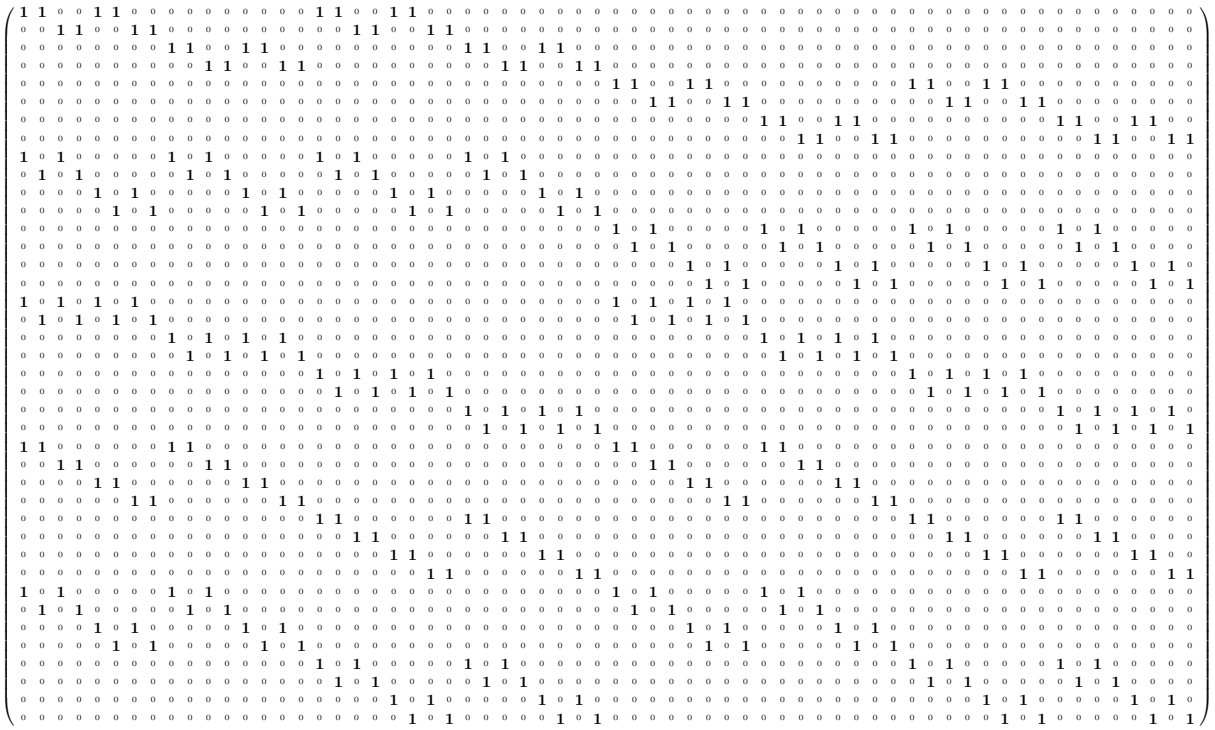

(B.3)

### Appendix C: Constraints on marginal distributions from copy-index equivalence relations

In Eq. (82), we noted that every copy of a variable in an inflation model has the same probabilistic dependence on its parents as every other copy. It followed that for certain pairs of marginal contexts, the marginal distributions in any inflation model are necessarily equal. We now describe how to identify such pairs of contexts.

Given $\boldsymbol{U}, \boldsymbol{V} \subseteq \mathsf{Nodes}(G')$ in an inflation DAG $G'$, let us say that a map $\varphi : \boldsymbol{U} \to \boldsymbol{V}$ is a **copy isomorphism** if it is a graph isomorphism[34] between $\mathsf{SubDAG}(\boldsymbol{U})$ and $\mathsf{SubDAG}(\boldsymbol{V})$ such that $\varphi(X) \sim X$ for all $X \in \boldsymbol{U}$, meaning that $\varphi$ maps every node $X \in \boldsymbol{U}$ to a node $\varphi(X) \in \boldsymbol{V}$ that is equivalent to $X$ under dropping the copy-index.

Furthermore, we say that a copy isomorphism $\varphi : \boldsymbol{U} \to \boldsymbol{V}$ is an **inflationary isomorphism** whenever it can be extended to a copy isomorphism on the ancestral subgraphs, $\Phi : \mathsf{An}(\boldsymbol{U}) \to \mathsf{An}(\boldsymbol{V})$. A copy isomorphism $\Phi : \mathsf{An}(\boldsymbol{U}) \to \mathsf{An}(\boldsymbol{V})$ defines an inflationary isomorphism $\varphi : \boldsymbol{U} \to \boldsymbol{V}$ if and only if $\Phi(\boldsymbol{U}) = \boldsymbol{V}$. So in practice, one can either start with $\varphi : \boldsymbol{U} \to \boldsymbol{V}$ and try to extend it to $\Phi : \mathsf{An}(\boldsymbol{U}) \to \mathsf{An}(\boldsymbol{V})$, or start with such a $\Phi$ and see whether it maps $\boldsymbol{U}$ to $\boldsymbol{V}$ and thereby restricts to a $\varphi$.

For given $\boldsymbol{U}$ and $\boldsymbol{V}$, a sufficient condition for equality of their marginal distributions in an inflation model is that there exists an inflationary isomorphism between them. Because $\boldsymbol{U}$ and $\boldsymbol{V}$ might themselves contain several variables that are copy-index equivalent (recall the examples of Sec. V B), equating the distribution $P_{\boldsymbol{U}}$ with the distribution $P_{\boldsymbol{V}}$ in an unambiguous fashion requires one to specify a correspondence between the variables that make up $\boldsymbol{U}$ and those that make up $\boldsymbol{V}$. This is exactly the data provided by the inflationary isomorphism $\varphi$. This result is summarized in the following lemma.

**Lemma 7.** *Let $G'$ be an inflation of $G$, and let $\boldsymbol{U}, \boldsymbol{V} \subseteq \mathsf{Nodes}(G')$. Then every inflationary isomorphism $\varphi : \boldsymbol{U} \to \boldsymbol{V}$ induces an equality $P_{\boldsymbol{U}} = P_{\boldsymbol{V}}$ for inflation models, where the variables in $\boldsymbol{U}$ are identified with those in $\boldsymbol{V}$ according to $\varphi$.*

This applies in particular when $\boldsymbol{V} = \boldsymbol{U}$, in which case the statement is that the distribution $P_{\boldsymbol{U}}$ is invariant under permuting the variables according to $\varphi$.

Lemma 7 is best illustrated by returning to our example from Sec. V B which considered the Spiral inflation of Fig. 3 and the pair of contexts $\boldsymbol{U} = \{A_1A_2B_1\}$ and $\boldsymbol{V} = \{A_1A_2B_2\}$. The map

$$\varphi \; : \; A_1 \mapsto A_1, \qquad A_2 \mapsto A_2, \qquad B_1 \mapsto B_2 \tag{C.1}$$

is a copy isomorphism between $\boldsymbol{U}$ and $\boldsymbol{V}$ because it trivially implements a graph isomorphism (both subgraphs are edgeless), and it maps each variable in $\boldsymbol{U}$ to a variable in $\boldsymbol{V}$ that is copy-index equivalent. There is a unique choice to extend $\varphi$ to a copy isomorphism $\Phi : \mathsf{An}(\boldsymbol{U}) \to \mathsf{An}(\boldsymbol{V})$, namely, by extending Eq. (C.1) to the ancestors via

$$\Phi \; : \; X_1 \mapsto X_1, \qquad Y_1 \mapsto Y_1, \qquad Y_2 \mapsto Y_2, \qquad Z_1 \mapsto Z_2, \tag{C.2}$$

which is again a copy isomorphism. Therefore $\varphi$ is indeed an inflationary isomorphism. From Lemma 7, we then conclude that any inflation model satisfies $P_{A_1A_2B_1} = P_{A_1A_2B_2}$.

Similarly, the map

$$\varphi' \; : \; A_1 \mapsto A_2, \qquad A_2 \mapsto A_1, \qquad B_1 \mapsto B_2 \tag{C.3}$$

is easily verified to be a copy isomorphism between $\mathsf{SubDAG}(\boldsymbol{U})$ and $\mathsf{SubDAG}(\boldsymbol{V})$, and there is again a unique choice to extend $\varphi'$ to a copy isomorphism $\Phi' : \mathsf{AnSubDAG}(\boldsymbol{U}) \to \mathsf{AnSubDAG}(\boldsymbol{V})$, by extending Eq. (C.3) with

$$\Phi' \; : \; X_1 \mapsto X_1, \qquad Y_1 \mapsto Y_2, \qquad Y_2 \mapsto Y_1, \qquad Z_1 \mapsto Z_2, \tag{C.4}$$

so that $\varphi'$ is verified to be an inflationary isomorphism. From Lemma 7, we then conclude that any inflation model also satisfies $P_{A_1A_2B_1} = P_{A_2A_1B_2}$. (And this in turn implies that for the context $\{A_1A_2\}$, the marginal distribution satisfies $P_{A_1A_2} = P_{A_2A_1}$.)

In order to avoid any possibility of confusion, we emphasize that it is not a plain copy isomorphism between the subgraphs of $\boldsymbol{U}$ and $\boldsymbol{V}$ themselves which results in coinciding marginal distributions, nor a copy isomorphism between the ancestral subgraphs of $\boldsymbol{U}$ and $\boldsymbol{V}$. It is rather an inflationary isomorphism between the subgraphs, i.e., a copy isomorphism between the ancestral subgraphs that restricts to a copy isomorphism between the subgraphs. To see why a copy isomorphism between ancestral subgraphs *by itself* may not be sufficient for deriving equality of marginal

[34] A graph isomorphism is a bijective map between the nodes of one graph and the nodes of another, such that both the map and its inverse take edges to edges.

distributions, we offer the following example. Take as the original DAG the instrumental scenario of Pearl [22], and consider the inflation depicted in Fig. 21. Consider the pair of contexts $\boldsymbol{U} = \{X_1Y_2Z_1\}$ and $\boldsymbol{V} = \{X_1Y_2Z_2\}$ on the inflation DAG. Since $\mathsf{SubDAG}(\boldsymbol{U})$ and $\mathsf{SubDAG}(\boldsymbol{V})$ are not isomorphic, there is no copy isomorphism between the two. On the other hand, the ancestral subgraphs are both given by the DAG of Fig. 22, so that the identity map is a copy isomorphism between $\mathsf{AnSubDAG}(X_1Y_2Z_1)$ and $\mathsf{AnSubDAG}(X_1Y_2Z_2)$.

One can try to make use of Lemma 7 when deriving polynomial inequalities with inflation via solving the marginal problem, by imposing the resulting equation $P_{\boldsymbol{U}} = P_{\boldsymbol{V}}$ as an additional constraint for every inflationary isomorphism $\varphi : \boldsymbol{U} \to \boldsymbol{V}$ between sets of observed nodes. This is advantageous to speed up to the linear quantifier elimination, since one can solve each of the resulting equations for one of the unknown joint probabilities and thereby eliminate that probability directly without Fourier-Motzkin elimination. Moreover, one could hope that these additional equations also result in tighter constraints on the marginal problem, which would in turn yielder tighter causal compatibility inequalities. Our computations have so far not revealed any example of such a tightening.

In some cases, this lack of impact can be explained as follows. Suppose that $\varphi : \boldsymbol{U} \to \boldsymbol{V}$ is an inflationary isomorphism which is not just the restriction of a copy isomorphism between the ancestral subgraphs, but even the restriction of a copy automorphism $\Phi' : G' \to G'$ of the entire inflation DAG onto itself; in particular, this assumption implies that $\Phi'$ also restricts to a copy isomorphism $\Phi : \mathsf{An}(\boldsymbol{U}) \to \mathsf{An}(\boldsymbol{V})$ between the ancestral subgraphs. In this case, the irrelevance of the additional constraint $P_{\boldsymbol{U}} = P_{\boldsymbol{V}}$ to the marginal problem for inflation models can be explained by the following argument.

Suppose that some joint distribution $P_{\mathsf{ObservedNodes}(G')}$ solves the unconstrained marginal problem, i.e., without requiring $P_{\boldsymbol{U}} = P_{\boldsymbol{V}}$. Now apply $\Phi'$ to the variables in $P_{\mathsf{ObservedNodes}(G')}$, switching the variables around, to generate a new distribution $P'_{\mathsf{ObservedNodes}(G')} := P_{\Phi'(\mathsf{ObservedNodes}(G'))}$. Because the set of marginal distributions that arise from inflation models is invariant under this switching of variables, we conclude that $P'$ is also a solution to the unconstrained marginal problem. Taking the uniform mixture of $P$ and $P'$ is therefore still a solution of the unconstrained marginal problem. But this uniform mixture also satisfies the supplementary constraint $P_{\boldsymbol{U}} = P_{\boldsymbol{V}}$. Hence the supplementary constraint is satisfiable whenever the unconstrained marginal problem is solvable, which makes adding the constraint irrelevant.

This argument does not apply when the inflationary isomorphism $\varphi : \boldsymbol{U} \to \boldsymbol{V}$ cannot be extended to a copy automorphism of the entire inflation DAG. It also does not apply if one uses $d$-separation conditions beyond ancestral independence on the inflation DAG as additional constraints (Sec. V A), because in this case the set of compatible distributions is not necessarily convex. In either of these cases, it is unclear whether or not constraints arising from copy-index equivalence could yield tighter inequalities.

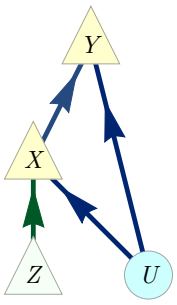


FIG. 20. The instrumental scenario of Pearl [22].

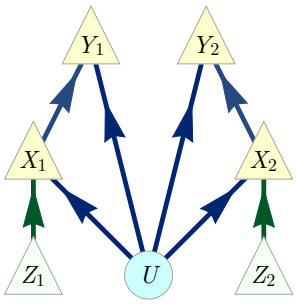


FIG. 21. An inflation DAG of the instrumental scenario which illustrates why coinciding ancestral subgraphs doesn't necessarily imply coinciding marginal distributions.

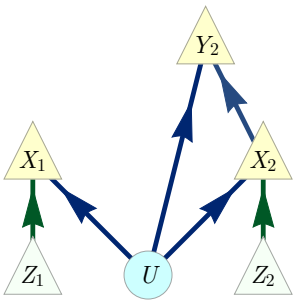


FIG. 22. The ancestral subgraph of Fig. 21 for either $\{X_1Y_2Z_1\}$ or $\{X_1Y_2Z_2\}$.

### Appendix D: Using the inflation technique to certify a DAG as "interesting"

By considering all possible $d$-separation conditions implied by a given DAG, one can infer the set of all conditional independence (CI) relations that must hold in any joint distribution over the observed variables that is compatible with the given DAG. In the presence of latent nodes, satisfying the CI relations among observed variables is generally not sufficient for compatibility with the DAG. Henson *et al.* [13] were concerned with identifying the **interesting** DAGs, by which they mean precisely those DAGs that exhibit a discrepancy between the set of observed distributions genuinely compatible with it and the set of observed distributions that merely satisfy its observed CI relations.

Henson *et al.* [13] derived necessary criteria on the structure of a DAG in order for it to be interesting, and they conjectured that their criteria may also be sufficient. As evidence in favour of this conjecture, they enumerated all possible DAGs with no more than six nodes satisfying their criteria, resulting in only 21 equivalence classes of potentially interesting DAGs. Of those 21, they further proved that 18 were unambiguously interesting by writing down explicit distributions which are incompatible despite satisfying the observed CI relations. Incompatibility was certified by means of entropic inequalities.

That left three classes of DAGs as *potentially* interesting. For each of these, Henson *et al.* [13] derived all Shannon-type entropic inequalities in two different ways, once by accounting for non-observed CI relations (that is, CI relations that do not refer exclusively to observed variables) and once without. The existence of *novel* Shannon-type inequalities upon accounting for non-observed CI relations is evidence for the DAG being interesting. The only loophole is that perhaps those novel Shannon-type inequalities are actually non-novel non-Shannon-type inequalities implied by the observed CI relations alone [13].

One way to close this loophole would be to show that the novel Shannon-type inequalities imply constraints beyond some inner approximation to the genuine entropy cone absent non-observed CI relations, perhaps along the lines of [17]. Another is to use causal compatibility inequalities beyond entropic inequalities to identify some CI-respecting but incompatible distributions. Pienaar [26] accomplished precisely this, and should be credited with the original insight to explicitly consider the different values that an observed root variable may take. In the following, we demonstrate how the inflation technique can be used for this purpose. So far, we have only considered one of the three enigmatic causal structures, namely, the one depicted in Fig. 23, which differs from the Triangle scenario by virtue of the variable $Y$ being observed rather than latent.

We consider the inflation DAG of Fig. 24, which is analogous to the Cut inflation of the Triangle scenario. Using Hardy-type tautologies, as described in Sec. IV D, we obtain causal compatibility inequalities for the inflation DAG, which in turn, via Corollary 5, yield the following causal compatibility inequalities for the DAG of Fig. 23:

$$P_Y(0)P_{YAC}(000) \leq P_{YA}(00)P_{YB}(00) + P_Y(0)P_{YBC}(010), \tag{D.1}$$

$$P_Y(0)P_{YAC}(100) \leq P_{YA}(10)P_{YB}(00) + P_Y(1)P_{YBC}(010). \tag{D.2}$$

For example, the second inequality is derived as follows. A Hardy-type tautology on the variables of the inflation DAG implies the following constraint on marginals:

$$P_{Y_1Y_2A_2C_1}(0100) \leq P_{Y_1Y_2A_2B_1}(0100) + P_{Y_1Y_2B_1C_1}(0110). \tag{D.3}$$

Applying factorization as per the ancestral independence relations of the inflation DAG, we obtain

$$P_{Y_1}(0)P_{Y_2C_1A_2}(100) \leq P_{Y_2A_2}(10)P_{Y_1B_1}(00) + P_{Y_2}(1)P_{Y_1B_1C_1}(010), \tag{D.4}$$

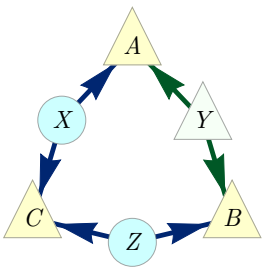


FIG. 23. DAG #15 in Ref. [13].

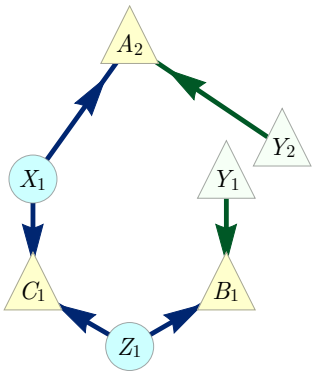


FIG. 24. A useful inflation of Fig. 23.

and finally translating this into a causal compatibility inequality on the original DAG using Corollary 5, we obtain Eq. (D.2).

In Pienaar [26], it was shown that the following distribution, which is easily verified to satisfy the CI relations among the observed variables in the DAG of Fig. 23, namely, $Y \perp\!\!\!\perp C$ and $A \perp\!\!\!\perp B|Y$ [13], is nonetheless incompatible with the DAG of Fig. 23:

$$P^{\text{Pien}}_{YABC} := \frac{[0000] + [0011] + [1000] + [1101]}{4}, \quad \text{i.e.,} \quad P^{\text{Pien}}_{YABC}(yabc) := \begin{cases} \frac{1}{4} & \text{if } y \cdot c = a \text{ and } (y \oplus 1) \cdot c = b, \\ 0 & \text{otherwise.} \end{cases} \tag{D.5}$$

It is easily verified that this distribution violates the causal compatibility inequality of Eq. (D.2). It is in this sense that the inflation technique can show that the DAG of Fig. 23 is interesting.

There is an alternative way to see that this distribution is not compatible with the DAG of Fig. 23 using our results from the main text. We consider the marginal on $ABC$ of $P^{\text{Pien}}_{YABC}$, which is

$$P^{\text{Pien}}_{ABC} := \frac{1}{2}[000] + \frac{1}{4}[011] + \frac{1}{4}[101]. \tag{D.6}$$

First, we note that any marginal distribution on $ABC$ that is compatible with the DAG of Fig. 23 is necessarily also compatible the Triangle scenario. Second, we note that $P^{\text{Pien}}_{ABC}$ is incompatible with the Triangle scenario. This follows from the fact that it violates one of the inequalities we derived in Sec. IV C. The relevant inequality is in the symmetry class of Eq. (65), and we express it here in terms of joint probabilities:

$$P_A(1)P_B(1)P_C(0) \leq P_{AB}(11)P_C(0) + P_{BC}(10)P_A(1) + P_{AC}(10)P_B(1) + P_{ABC}(001). \tag{D.7}$$

Clearly, this can be obtained from the inequality of Eq. (56) (the one that rejected the W-distribution of Eq. (12)) by the symmetry operation which flips the value assigned to $C$.

Just as the incompatibility of the W-distribution with the Triangle scenario was not detectable by entropic inequalities, as we noted in our discussion of Example 2 from Sec. III B, the same is true for the incompatibility of the distribution $P^{\text{Pien}}_{YABC}$ with the DAG of Fig. 23. $P^{\text{Pien}}_{YABC}$ not only satisfies all Shannon-type entropic inequalities pertinent to the DAG of Fig. 23, but lies within an inner approximation to the genuine entropy cone for that scenario[35]. In other words, there exists a distribution with the same joint and marginal entropies as $P^{\text{Pien}}_{YABC}$ which *is* compatible with the DAG of Fig. 23.

Finally, it may be worth noting that the inflation DAG depicted in Fig. 24 is precisely the "bilocality scenario" investigated by Branciard *et al.* [30]. Therefore, the inflation technique permits us to translate every causal compatibility inequality for the bilocality scenario into a causal compatibility inequality for the DAG of Fig. 23.

[35] This is due to Weilenmann and Colbeck (personal communication).

### Appendix E: The copy lemma and non-Shannon type entropic inequalities

As it turns out, the inflation technique is also useful outside of the problem of causal inference. As we argue in the following, inflation is secretly what underlies the **Copy Lemma** in the derivation of non-Shannon type entropic inequalities [101, Chapter 15]. The following formulation of the Copy Lemma is the one of Kaced [102].

**Lemma 8.** *Let $A$, $B$ and $C$ be random variables with distribution $P_{ABC}$. Then there exists a fourth random variable $A'$ and joint distribution $P_{AA'BC}$ such that:*

1. $P_{AB} = P_{A'B}$,
2. $A' \perp\!\!\!\perp AC \mid B$.

The proof via inflation is as follows.

*Proof.* Every joint distribution $P_{ABC}$ is compatible with a DAG of the form of Fig. 25. This follows from the fact that one may take $X$ to be any **sufficient statistic** for the joint variable $(A, C)$ given $B$, such as $X := (A, B, C)$. Next, we consider the inflation of Fig. 25 depicted in Fig. 26. The maximal injectable sets are $\{A_1B_1C_1\}$ and $\{A_2B_1\}$. By Lemma 3, because $P_{ABC}$ is assumed to be compatible with Fig. 25, it follows that the family of marginals $\{P_{A_1B_1C_1}, P_{A_2B_1}\}$, where $P_{A_1B_1C_1} := P_{ABC}$ and $P_{A_2B_1} := P_{AB}$, is compatible with the inflation of Fig. 26. The resulting joint distribution $P_{A_1A_2B_1C_1}$ has marginals $P_{A_1B_1} = P_{A_2B_1} = P_{AB}$ and satisfies the conditional independence relation $A_2 \perp\!\!\!\perp A_1C_1 \mid B_1$, since $A_2$ is $d$-separated from $A_1C_1$ by $B_1$ in Fig. 26. □

While it is also not hard to write down the distribution constructed in the proof explicitly as $P_{A_1A_2B_1C_1} := P_{A_1B_1C_1}P_{A_2B_1}P_{B_1}^{-1}$ [101, Lemma 15.8], the fact that one can rederive it using the inflation technique is significant. For one, all the non-Shannon type inequalities derived by Dougherty *et al.* [103] are obtained by applying some Shannon-type inequality to the distribution that is implied to exist by the Copy Lemma. Our result shows, therefore, that one can understand these non-Shannon type inequalities for a DAG as arising from Shannon-type inequalities applied to an inflation DAG. Indeed, it may be that the inflation technique may be a more general-purpose tool for deriving non-Shannon-type entropic inequalities. A natural direction for future research is to explore whether more sophisticated applications of the inflation technique might result in *new* examples of such inequalities.

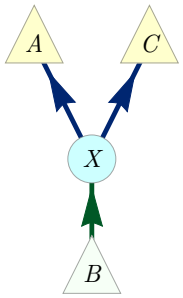


FIG. 25. A causal structure that is compatible with any distribution $P_{ABC}$.

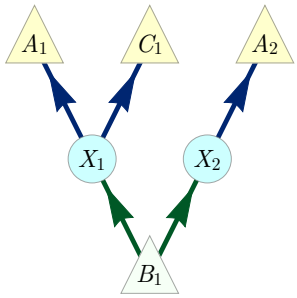


FIG. 26. An inflation of Fig. 25.

### Appendix F: Causal compatibility inequalities for the Triangle scenario in machine-readable format

Table II lists all the numerically irredundant polynomial inequalities resulting from consistent marginals of the Spiral inflation of Fig. 3. Stronger inequalities can be derived be considering larger inflations, such as the Wed inflation of Fig. 2. As noted previously, these inequalities are also implied by the hypergraph transversals technique per Sec. IV D. Each row in the table specifies the coefficient of the corresponding correlator monomial.

TABLE II. A machine-readable and closed-under-symmetries version of the table in Sec. IV C.

| constant | $\langle A\rangle$ | $\langle B\rangle$ | $\langle C\rangle$ | $\langle AB\rangle$ | $\langle AC\rangle$ | $\langle BC\rangle$ | $\langle ABC\rangle$ | $\langle A\rangle\langle B\rangle$ | $\langle A\rangle\langle C\rangle$ | $\langle B\rangle\langle C\rangle$ | $\langle A\rangle\langle BC\rangle$ | $\langle AC\rangle\langle B\rangle$ | $\langle AB\rangle\langle C\rangle$ | $\langle A\rangle\langle B\rangle\langle C\rangle$ |
|---|---|---|---|---|---|---|---|---|---|---|---|---|---|---|
| 1 | 0 | 0 | 0 | -1 | -1 | 0 | 0 | 0 | 0 | 1 | 0 | 0 | 0 | 0 |
| 1 | 0 | 0 | 0 | -1 | 1 | 0 | 0 | 0 | 0 | -1 | 0 | 0 | 0 | 0 |
| 1 | 0 | 0 | 0 | 1 | -1 | 0 | 0 | 0 | 0 | -1 | 0 | 0 | 0 | 0 |
| 1 | 0 | 0 | 0 | 1 | 1 | 0 | 0 | 0 | 0 | 1 | 0 | 0 | 0 | 0 |
| 1 | 0 | 0 | 0 | -1 | 0 | -1 | 0 | 0 | 1 | 0 | 0 | 0 | 0 | 0 |
| 1 | 0 | 0 | 0 | -1 | 0 | 1 | 0 | 0 | -1 | 0 | 0 | 0 | 0 | 0 |
| 1 | 0 | 0 | 0 | 1 | 0 | -1 | 0 | 0 | -1 | 0 | 0 | 0 | 0 | 0 |
| 1 | 0 | 0 | 0 | 1 | 0 | 1 | 0 | 0 | 1 | 0 | 0 | 0 | 0 | 0 |
| 1 | 0 | 0 | 0 | 0 | -1 | -1 | 0 | 1 | 0 | 0 | 0 | 0 | 0 | 0 |
| 1 | 0 | 0 | 0 | 0 | -1 | 1 | 0 | -1 | 0 | 0 | 0 | 0 | 0 | 0 |
| 1 | 0 | 0 | 0 | 0 | 1 | -1 | 0 | -1 | 0 | 0 | 0 | 0 | 0 | 0 |
| 1 | 0 | 0 | 0 | 0 | 1 | 1 | 0 | 1 | 0 | 0 | 0 | 0 | 0 | 0 |
| 3 | -1 | -1 | -1 | 2 | 2 | 2 | 1 | 1 | 1 | 1 | -1 | -1 | -1 | 1 |
| 3 | -1 | -1 | 1 | 2 | -2 | -2 | -1 | 1 | -1 | -1 | 1 | 1 | 1 | -1 |
| 3 | -1 | 1 | -1 | -2 | 2 | -2 | -1 | -1 | 1 | -1 | 1 | 1 | 1 | -1 |
| 3 | -1 | 1 | 1 | -2 | -2 | 2 | 1 | -1 | -1 | 1 | -1 | -1 | -1 | 1 |
| 3 | 1 | -1 | -1 | -2 | -2 | 2 | -1 | -1 | -1 | 1 | 1 | 1 | 1 | -1 |
| 3 | 1 | -1 | 1 | -2 | 2 | -2 | 1 | -1 | 1 | -1 | -1 | -1 | -1 | 1 |
| 3 | 1 | 1 | -1 | 2 | -2 | -2 | 1 | 1 | -1 | -1 | -1 | -1 | -1 | 1 |
| 3 | 1 | 1 | 1 | 2 | 2 | 2 | -1 | 1 | 1 | 1 | 1 | 1 | 1 | -1 |
| 4 | -2 | 0 | 0 | -3 | -2 | -2 | 1 | 1 | 0 | 2 | 1 | 1 | 0 | -1 |
| 4 | -2 | 0 | 0 | -3 | 2 | 2 | -1 | 1 | 0 | -2 | -1 | -1 | 0 | 1 |
| 4 | -2 | 0 | 0 | 3 | -2 | 2 | -1 | -1 | 0 | -2 | -1 | -1 | 0 | 1 |
| 4 | -2 | 0 | 0 | 3 | 2 | -2 | 1 | -1 | 0 | 2 | 1 | 1 | 0 | -1 |
| 4 | 2 | 0 | 0 | -3 | -2 | -2 | -1 | 1 | 0 | 2 | -1 | -1 | 0 | 1 |
| 4 | 2 | 0 | 0 | -3 | 2 | 2 | 1 | 1 | 0 | -2 | 1 | 1 | 0 | -1 |
| 4 | 2 | 0 | 0 | 3 | -2 | 2 | 1 | -1 | 0 | -2 | 1 | 1 | 0 | -1 |
| 4 | 2 | 0 | 0 | 3 | 2 | -2 | -1 | -1 | 0 | 2 | -1 | -1 | 0 | 1 |
| 4 | 0 | -2 | 0 | -2 | -2 | -3 | 1 | 0 | 2 | 1 | 0 | 1 | 1 | -1 |
| 4 | 0 | -2 | 0 | -2 | 2 | 3 | -1 | 0 | -2 | -1 | 0 | -1 | -1 | 1 |
| 4 | 0 | -2 | 0 | 2 | -2 | 3 | 1 | 0 | 2 | -1 | 0 | 1 | 1 | -1 |
| 4 | 0 | -2 | 0 | 2 | 2 | -3 | -1 | 0 | -2 | 1 | 0 | -1 | -1 | 1 |
| 4 | 0 | 2 | 0 | -2 | -2 | -3 | -1 | 0 | 2 | 1 | 0 | -1 | -1 | 1 |
| 4 | 0 | 2 | 0 | -2 | 2 | 3 | 1 | 0 | -2 | -1 | 0 | 1 | 1 | -1 |
| 4 | 0 | 2 | 0 | 2 | -2 | 3 | -1 | 0 | 2 | -1 | 0 | -1 | -1 | 1 |
| 4 | 0 | 2 | 0 | 2 | 2 | -3 | 1 | 0 | -2 | 1 | 0 | 1 | 1 | -1 |
| 4 | 0 | 0 | -2 | -2 | -3 | -2 | 1 | 2 | 1 | 0 | 1 | 0 | 1 | -1 |
| 4 | 0 | 0 | -2 | -2 | 3 | 2 | 1 | 2 | -1 | 0 | 1 | 0 | 1 | -1 |
| 4 | 0 | 0 | -2 | 2 | -3 | 2 | -1 | -2 | 1 | 0 | -1 | 0 | -1 | 1 |
| 4 | 0 | 0 | -2 | 2 | 3 | -2 | -1 | -2 | -1 | 0 | -1 | 0 | -1 | 1 |
| 4 | 0 | 0 | 2 | -2 | -3 | -2 | -1 | 2 | 1 | 0 | -1 | 0 | -1 | 1 |
| 4 | 0 | 0 | 2 | -2 | 3 | 2 | -1 | 2 | -1 | 0 | -1 | 0 | -1 | 1 |
| 4 | 0 | 0 | 2 | 2 | -3 | 2 | 1 | -2 | 1 | 0 | 1 | 0 | 1 | -1 |
| 4 | 0 | 0 | 2 | 2 | 3 | -2 | 1 | -2 | -1 | 0 | 1 | 0 | 1 | -1 |
| 4 | 0 | 0 | 0 | -2 | -2 | -2 | -1 | 2 | 2 | 2 | -1 | -1 | -1 | 0 |
| 4 | 0 | 0 | 0 | -2 | -2 | -2 | 1 | 2 | 2 | 2 | 1 | 1 | 1 | 0 |
| 4 | 0 | 0 | 0 | -2 | 2 | 2 | -1 | 2 | -2 | -2 | -1 | -1 | -1 | 0 |
| 4 | 0 | 0 | 0 | -2 | 2 | 2 | 1 | 2 | -2 | -2 | 1 | 1 | 1 | 0 |
| 4 | 0 | 0 | 0 | 2 | -2 | 2 | -1 | -2 | 2 | -2 | -1 | -1 | -1 | 0 |
| 4 | 0 | 0 | 0 | 2 | -2 | 2 | 1 | -2 | 2 | -2 | 1 | 1 | 1 | 0 |
| 4 | 0 | 0 | 0 | 2 | 2 | -2 | -1 | -2 | -2 | 2 | -1 | -1 | -1 | 0 |
| 4 | 0 | 0 | 0 | 2 | 2 | -2 | 1 | -2 | -2 | 2 | 1 | 1 | 1 | 0 |

### Appendix G: Recovering the Bell inequalities from the inflation technique

To further illustrate the power of our inflation DAG approach, we now demonstrate how to recover all Bell inequalities [9, 10, 34] via our method. To keep things simple we only discuss the case of a bipartite Bell scenario with two values for both "settings" and "outcome" variables here, but the case of more parties and/or more values per variable is totally analogous.

The causal structure associated to the Bell [8–10, 34] experiment [13 (Fig. E#2), 11 (Fig. 19), 24 (Fig. 1), 14 (Fig. 1), 35 (Fig. 2b), 36 (Fig. 2)] is depicted in Fig. 11. The observed variables are $A, B, X, Y$, and $\Lambda$ is the latent common cause of $A$ and $B$. In a Bell scenario, one traditionally works with the conditional distribution $P_{AB|XY}$, to be understood as an array of distributions indexed by the possible values of $X$ and $Y$, instead of with the original distribution $P_{ABXY}$, which is what we do.

In the inflation DAG of Fig. 12, the maximal pre-injectable sets are

$$\begin{aligned}
&\{A_1B_1X_1X_2Y_1Y_2\},\\
&\{A_1B_2X_1X_2Y_2Y_2\},\\
&\{A_2B_1X_1X_2Y_2Y_2\},\\
&\{A_2B_2X_1X_2Y_2Y_2\},
\end{aligned} \tag{G.1}$$

where notably every maximal pre-injectable set contains all "settings" variables $X_1$ to $Y_2$. The marginal distributions on these pre-injectable sets are then specified by the original observed distribution via

$$\forall abx_1x_2y_1y_2: \begin{cases}
P_{A_1B_1X_1X_2Y_1Y_2}(abx_1x_2y_1y_2) = P_{ABXY}(abx_1y_1)P_X(x_2)P_Y(y_2),\\
P_{A_1B_2X_1X_2Y_1Y_2}(abx_1x_2y_1y_2) = P_{ABXY}(abx_1y_2)P_X(x_2)P_Y(y_1),\\
P_{A_2B_1X_1X_2Y_1Y_2}(abx_1x_2y_1y_2) = P_{ABXY}(abx_2y_1)P_X(x_1)P_Y(y_2),\\
P_{A_2B_2X_1X_2Y_1Y_2}(abx_1x_2y_1y_2) = P_{ABXY}(abx_2y_2)P_X(x_1)P_Y(y_1),\\
\qquad P_{X_1X_2Y_1Y_2}(x_1x_2y_1y_2) = P_X(x_1)P_X(x_2)P_Y(y_1)P_Y(y_2).
\end{cases} \tag{G.2}$$

By dividing each of the first four equations by the fifth, we obtain

$$\forall abx_1x_2y_1y_2: \begin{cases}
P_{A_1B_1|X_1X_2Y_1Y_2}(ab|x_1x_2y_1y_2) = P_{AB|XY}(ab|x_1y_1),\\
P_{A_1B_2|X_1X_2Y_1Y_2}(ab|x_1x_2y_1y_2) = P_{AB|XY}(ab|x_1y_2),\\
P_{A_2B_1|X_1X_2Y_1Y_2}(ab|x_1x_2y_1y_2) = P_{AB|XY}(ab|x_2y_1),\\
P_{A_2B_2|X_1X_2Y_1Y_2}(ab|x_1x_2y_1y_2) = P_{AB|XY}(ab|x_2y_2).
\end{cases} \tag{G.3}$$

The existence of a joint distribution over all six variables—i.e. the existence of a solution to the marginal problem—implies in particular

$$\forall abx_1x_2y_1y_2: \quad P_{A_1B_1|X_1X_2Y_1Y_2}(ab|x_1x_2y_1y_2) = \sum\nolimits_{a',b'} P_{A_1A_2B_1B_2|X_1X_2Y_1Y_2}(aa'bb'|x_1x_2y_1y_2), \tag{G.4}$$

and similarly for the other three conditional distributions under consideration. For compatibility with the Bell scenario, Eq. (G.3) therefore implies that the original distribution must satisfy in particular

$$\forall ab: \begin{cases}
P_{AB|XY}(ab|00) = \sum_{a',b'} P_{A_1A_2B_1B_2|X_1X_2Y_1Y_2}(aa'bb'|0101)\\
P_{AB|XY}(ab|10) = \sum_{a',b'} P_{A_1A_2B_1B_2|X_1X_2Y_1Y_2}(a'abb'|0101)\\
P_{AB|XY}(ab|01) = \sum_{a',b'} P_{A_1A_2B_1B_2|X_1X_2Y_1Y_2}(aa'b'b|0101)\\
P_{AB|XY}(ab|11) = \sum_{a',b'} P_{A_1A_2B_1B_2|X_1X_2Y_1Y_2}(a'ab'b|0101)
\end{cases} \tag{G.5}$$

The possibility to write the conditional probabilities in the Bell scenario in this form is equivalent to the existence of a latent variable model, as noted in Fine's theorem [104]. Thus, the existence of a solution to our marginal problem implies the existence of a latent variable model for the original distribution; the converse follows from our Lemma 3. Hence the inflation DAG of Fig. 12 provides necessary and sufficient conditions for the compatibility of the original distribution with the Bell scenario causal structure.

Moreover, it is possible to describe the marginal polytope over the pre-injectable sets of Eq. (G.1), resulting in a concrete correspondence between tight Bell inequalities and the facets of our marginal polytope. This is based on the observation that the "settings" variables $X_1$ to $Y_2$ occur in all four contexts. The marginal polytope lives in

$\oplus_{i=1}^{4}\mathbb{R}^{2^6} = \oplus_{i=1}^{4}(\mathbb{R}^2)^{\otimes 6}$, where each tensor factor has basis vectors corresponding to the two possible outcomes of each variable, and the direct summands enumerate the four contexts. It is given by the convex hull of the points

$$\begin{aligned}&(e_{A_1}\otimes e_{B_1}\otimes e_{X_1}\otimes e_{X_2}\otimes e_{Y_1}\otimes e_{Y_2})\\ \oplus\,&(e_{A_1}\otimes e_{B_2}\otimes e_{X_1}\otimes e_{X_2}\otimes e_{Y_1}\otimes e_{Y_2})\\ \oplus\,&(e_{A_2}\otimes e_{B_1}\otimes e_{X_1}\otimes e_{X_2}\otimes e_{Y_1}\otimes e_{Y_2})\\ \oplus\,&(e_{A_2}\otimes e_{B_2}\otimes e_{X_1}\otimes e_{X_2}\otimes e_{Y_1}\otimes e_{Y_2}),\end{aligned}$$

where all six variables range over their possible values. Since the last four tensor factors occur in every direct summand in exactly the same way, we can also write the point as

$$[(e_{A_1}\otimes e_{B_1})\oplus(e_{A_1}\otimes e_{B_2})\oplus(e_{A_2}\otimes e_{B_1})\oplus(e_{A_2}\otimes e_{B_2})]\otimes[e_{X_1}\otimes e_{X_2}\otimes e_{Y_1}\otimes e_{Y_2}]$$

in $\left(\oplus_{i=1}^{4}\mathbb{R}^{2^2}\right)\otimes\mathbb{R}^{2^4}$. Now since the first four variables in the first tensor factor vary completely independently of the latter four variables in the second tensor factor, the resulting polytope will be precisely the tensor product [105, 106] of two polytopes: first, the convex hull of all points of the form

$$(e_{A_1}\otimes e_{B_1})\oplus(e_{A_1}\otimes e_{B_2})\oplus(e_{A_2}\otimes e_{B_1})\oplus(e_{A_2}\otimes e_{B_2}),$$

and second the convex hull of all $e_{X_1}\otimes e_{X_2}\otimes e_{Y_1}\otimes e_{Y_2}$. While the latter polytope is just the standard probability simplex in $\mathbb{R}^8$, the former cone is precisely the "local polytope" or "Bell polytope" that is traditionally used in the context of Bell scenarios [10, Sec. II.B]. This implies that the facets of our marginal polytope are precisely the pairs consisting of a facet of the Bell polytope and a facet of the simplex, the latter of which are only the nonnegativity of probability inequalities like $P_{X_1X_2Y_1Y_2}(0101)\geq 0$. For example, in this way we obtain one version of the CHSH inequality as a facet of our marginal polytope,

$$\sum_{a,b,x,y}(-1)^{a+b+xy}P_{A_xB_yX_1X_2Y_1Y_2}(ab0101)\leq 2P_{X_1X_2Y_1Y_2}(0101).$$

This translates into the standard form of the CHSH inequality as follows. Upon using Eq. (G.3), the inequality becomes

$$\begin{aligned}\sum_{a,b}(-1)^{a+b}\big(&P_{ABXY}(ab00)P_X(1)P_Y(1)+P_{ABXY}(ab01)P_X(1)P_Y(0)\\ &+P_{ABXY}(ab10)P_X(0)P_Y(1)-P_{ABXY}(ab11)P_X(0)P_Y(0)\big)\leq P_X(0)P_X(1)P_Y(0)P_Y(1),\end{aligned}$$

so that dividing by the right-hand side results in one of the conventional forms of the CHSH inequality,

$$\sum_{a,b}(-1)^{a+b}\left(P_{AB|XY}(ab|00)+P_{AB|XY}(ab|01)+P_{AB|XY}(ab|10)-P_{AB|XY}(ab|11)\right)\leq 2.$$

In conclusion, the inflation technique is powerful enough to get a precise characterization of all distributions compatible with the Bell causal structure, and our technique for generating polynomial inequalities through solving the marginal constraint problem recovers all Bell inequalities.

Some Bell inequalities may also be derived using the hypergraph transversals technique discussed in Sec. IV D. For example, the inequality

$$\begin{aligned}&P_{A_1B_1X_1Y_1}(0000)P_{X_2}(1)P_{Y_2}(1)\\ &\leq P_{A_1B_2X_1Y_2}(0001)P_{X_2}(1)P_{Y_1}(0)+P_{A_2B_1X_2Y_1}(0010)P_{X_1}(0)P_{Y_2}(1)+P_{A_2B_2X_2Y_2}(1111)P_{X_1}(0)P_{Y_1}(0)\end{aligned}\tag{G.6}$$

is the inflationary precursor of the Bell inequality

$$P_{AB|XY}(00|00)\leq P_{AB|XY}(00|01)+P_{AB|XY}(00|10)+P_{AB|XY}(11|11),\tag{G.7}$$

as Eq. (G.7) is obtained from Eq. (G.6) by dividing both sides by $P_{X_1Y_1X_2Y_2}(0011)=P_{X_1}(0)P_{Y_2}(0)P_{X_2}(1)P_{Y_2}(1)$ and then dropping copy indices. On the other hand, Eq. (G.6) follows directly from factorization relations on pre-injectable sets and the tautology

$$\begin{aligned}&[\mathbf{A_1{=}0},\mathbf{B_1{=}0},\mathbf{X_1{=}0},\mathbf{Y_1{=}0},\mathbf{X_2{=}1},\mathbf{Y_2{=}1}]\\ &\quad\implies[\mathbf{A_1{=}0},B_2{=}0,\mathbf{X_1{=}0},\mathbf{Y_1{=}0},\mathbf{X_2{=}1},\mathbf{Y_2{=}1}]\\ &\qquad\vee[A_2{=}0,\mathbf{B_1{=}0},\mathbf{X_1{=}0},\mathbf{Y_1{=}0},\mathbf{X_2{=}1},\mathbf{Y_2{=}1}]\\ &\qquad\vee[A_2{=}1,B_2{=}1,\mathbf{X_1{=}0},\mathbf{Y_1{=}0},\mathbf{X_2{=}1},\mathbf{Y_2{=}1}].\end{aligned}\tag{G.8}$$

which corresponds to the original "Hardy paradox" [32] in our notation.

---


[1] J. Pearl, *Causality: Models, Reasoning, and Inference* (Cambridge University Press, 2009).

[2] P. Spirtes, C. Glymour, and R. Scheines, *Causation, Prediction, and Search*, Lecture Notes in Statistics (Springer New York, 2011).

[3] M. Studený, *Probabilistic Conditional Independence Structures*, Information Science and Statistics (Springer London, 2005).

[4] D. Koller, *Probabilistic Graphical Models: Principles and Techniques* (MIT Press, Cambridge, MA, 2009).

[5] C. M. Lee and R. W. Spekkens, "Causal inference via algebraic geometry: necessary and sufficient conditions for the feasibility of discrete causal models," arXiv:1506.03880 (2015).

[6] R. Chaves, "Polynomial Bell inequalities," Phys. Rev. Lett. **116**, 010402 (2016).

[7] D. Rosset and N. Gisin, "Finite local models for all finite correlation scenarios," unpublished (2016).

[8] J. S. Bell, "On the Einstein-Podolsky-Rosen paradox," Physics **1**, 195 (1964).

[9] J. F. Clauser, M. A. Horne, A. Shimony, and R. A. Holt, "Proposed experiment to test local hidden-variable theories," Phys. Rev. Lett. **23**, 880 (1969).

[10] N. Brunner, D. Cavalcanti, S. Pironio, V. Scarani, and S. Wehner, "Bell nonlocality," Rev. Mod. Phys. **86**, 419 (2014).

[11] C. J. Wood and R. W. Spekkens, "The lesson of causal discovery algorithms for quantum correlations: causal explanations of Bell-inequality violations require fine-tuning," New J. Phys. **17**, 033002 (2015).

[12] T. Fritz, "Beyond Bell's theorem: correlation scenarios," New J. Phys. **14**, 103001 (2012).

[13] J. Henson, R. Lal, and M. F. Pusey, "Theory-independent limits on correlations from generalized Bayesian networks," New J. Phys. **16**, 113043 (2014).

[14] T. Fritz, "Beyond Bell's theorem II: Scenarios with arbitrary causal structure," Comm. Math. Phys. **341**, 391 (2015).

[15] R. Chaves and C. Budroni, "Entropic nonsignalling correlations," arXiv:1601.07555 (2015).

[16] R. Chaves, L. Luft, T. O. Maciel, D. Gross, D. Janzing, and B. Schölkopf, "Inferring latent structures via information inequalities," in *Proc. of the 30th Conference on Uncertainty in Artificial Intelligence* (AUAI, 2014) pp. 112–121.

[17] M. Weilenmann and R. Colbeck, "Non-Shannon inequalities in the entropy vector approach to causal structures," arXiv:1605.02078 (2016).

[18] J. Åberg, R. Chaves, D. Gross, A. Kela, and K. U. von Prillwitz, "Inferring causal structures with covariance information," poster session, Quantum Networks conference (2016).

[19] A. Tavakoli, P. Skrzypczyk, D. Cavalcanti, and A. Acín, "Nonlocal correlations in the star-network configuration," Phys. Rev. A **90**, 062109 (2014).

[20] D. Rosset, C. Branciard, T. J. Barnea, G. Pütz, N. Brunner, and N. Gisin, "Nonlinear Bell inequalities tailored for quantum networks," Phys. Rev. Lett. **116**, 010403 (2016).

[21] A. Tavakoli, "Bell-type inequalities for arbitrary noncyclic networks," Phys. Rev. A **93**, 030101 (2016).

[22] J. Pearl, "On the testability of causal models with latent and instrumental variables," in *Proc. 11th Conference on Uncertainty in Artificial Intelligence*, AUAI (Morgan Kaufmann, San Francisco, CA, 1995) pp. 435–443.

[23] B. Steudel and N. Ay, "Information-theoretic inference of common ancestors," Entropy **17**, 2304 (2015).

[24] R. Chaves, L. Luft, and D. Gross, "Causal structures from entropic information: geometry and novel scenarios," New J. Phys. **16**, 043001 (2014).

[25] T. Fritz and R. Chaves, "Entropic inequalities and marginal problems," IEEE Trans. Info. Theo. **59**, 803 (2013).

[26] J. Pienaar, "Which causal scenarios are interesting?" arXiv:1606.07798 (2016).

[27] S. L. Braunstein and C. M. Caves, "Information-theoretic Bell inequalities," Phys. Rev. Lett. **61**, 662 (1988).

[28] B. W. Schumacher, "Information and quantum nonseparability," Phys. Rev. A **44**, 7047 (1991).

[29] R. Chaves, C. Majenz, and D. Gross, "Information–theoretic implications of quantum causal structures," Nat. Comm. **6**, 5766 (2015).

[30] C. Branciard, D. Rosset, N. Gisin, and S. Pironio, "Bilocal versus nonbilocal correlations in entanglement-swapping experiments," Phys. Rev. A **85**, 032119 (2012).

[31] W. Dür, G. Vidal, and J. I. Cirac, "Three qubits can be entangled in two inequivalent ways," Phys. Rev. A **62**, 062314 (2000).

[32] L. Hardy, "Nonlocality for two particles without inequalities for almost all entangled states," Phys. Rev. Lett. **71**, 1665 (1993).

[33] S. Mansfield and T. Fritz, "Hardy's non-locality paradox and possibilistic conditions for non-locality," Found. Phys. **42**, 709 (2012).

[34] J. S. Bell, "On the problem of hidden variables in quantum mechanics," Rev. Mod. Phys. **38**, 447 (1966).

[35] J. M. Donohue and E. Wolfe, "Identifying nonconvexity in the sets of limited-dimension quantum correlations," Phys. Rev. A **92**, 062120 (2015).

[36] G. V. Steeg and A. Galstyan, "A sequence of relaxations constraining hidden variable models," in *Proc. 27th Conference on Uncertainty in Artificial Intelligence* (AUAI, 2011) pp. 717–726.

[37] B. S. Cirel'son, "Quantum generalizations of Bell's inequality," Lett. Math. Phys. **4**, 93 (1980).

[38] S. Popescu and D. Rohrlich, "Quantum nonlocality as an axiom," Found. Phys. **24**, 379 (1994).

[39] J. Barrett and S. Pironio, "Popescu-rohrlich correlations as a unit of nonlocality," Phys. Rev. Lett. **95**, 140401 (2005).

[40] Y.-C. Liang, R. W. Spekkens, and H. M. Wiseman, "Speckers parable of the overprotective seer: A road to contextuality, nonlocality and complementarity," Phys. Rep. **506**, 1 (2011).

[41] D. Roberts, *Aspects of Quantum Non-Locality*, Ph.D. thesis, University of Bristol (2004).

[42] I. Pitowsky, "George Boole's conditions of possible experience and the quantum puzzle," Br. J. Philos. Sci. **45**, 95 (1994).

[43] I. Pitowsky, *Quantum Probability - Quantum Logic*, Lecture Notes in Physics, Berlin Springer Verlag, Vol. 321 (Springer Berlin Heidelberg, 1989).

[44] H. G. Kellerer, "Verteilungsfunktionen mit gegebenen Marginalverteilungen," Z. Wahrscheinlichkeitstheorie **3**, 247 (1964).

[45] A. J. Leggett and A. Garg, "Quantum mechanics versus macroscopic realism: is the flux there when nobody looks?" Phys. Rev. Lett. **54**, 857 (1985).

[46] M. Araújo, M. Túlio Quintino, C. Budroni, M. Terra Cunha, and A. Cabello, "All noncontextuality inequalities for the $n$-cycle scenario," Phys. Rev. A **88**, 022118 (2013), arXiv:1206.3212.

[47] R. Horodecki, P. Horodecki, M. Horodecki, and K. Horodecki, "Quantum entanglement," Rev. Mod. Phys. **81**, 865 (2009).

[48] S. Abramsky and A. Brandenburger, "The sheaf-theoretic structure of non-locality and contextuality," New J. Phys. **13**, 113036 (2011).

[49] N. N. Vorob'ev, "Consistent families of measures and their extensions," Theory Probab. Appl. **7**, 147 (1960).

[50] T. Kahle, "Neighborliness of marginal polytopes," Beiträge Algebra Geom. **51**, 45 (2010).

[51] E. D. Andersen, "Certificates of primal or dual infeasibility in linear programming," Comp. Optim. Applic. **20**, 171 (2001).

[52] A. Garuccio, "Hardy's approach, Eberhard's inequality, and supplementary assumptions," Phys. Rev. A **52**, 2535 (1995).

[53] A. Cabello, "Bell's theorem with and without inequalities for the three-qubit Greenberger-Horne-Zeilinger and $W$ states," Phys. Rev. A **65**, 032108 (2002).

[54] D. Braun and M.-S. Choi, "Hardy's test versus the Clauser-Horne-Shimony-Holt test of quantum nonlocality: Fundamental and practical aspects," Phys. Rev. A **78**, 032114 (2008).

[55] L. Maninska and S. Wehner, "A unified view on Hardy's paradox and the ClauserHorneShimonyHolt inequality," J. Phys. A **47**, 424027 (2014).

[56] G. Ghirardi and L. Marinatto, "Proofs of nonlocality without inequalities revisited," Phys. Lett. A **372**, 1982 (2008).

[57] T. Eiter, K. Makino, and G. Gottlob, "Computational aspects of monotone dualization: A brief survey," Discrete Appl. Math. **156**, 2035 (2008).

[58] L. D. Garcia, M. Stillman, and B. Sturmfels, "Algebraic geometry of Bayesian networks," J. Symbol. Comp. **39**, 331 (2003), arXiv:math/0301255.

[59] C. Barrett, P. Fontaine, and C. Tinelli, "The Satisfiability Modulo Theories Library (SMT-LIB)," `www.SMT-LIB.org` (2016).

[60] M. S. Leifer and R. W. Spekkens, "Towards a formulation of quantum theory as a causally neutral theory of Bayesian inference," Phys. Rev. A **88**, 052130 (2013).

[61] K. Ried, M. Agnew, L. Vermeyden, D. Janzing, R. W. Spekkens, and K. J. Resch, "A quantum advantage for inferring causal structure," Nature Physics **11**, 414 (2015).

[62] R. W. Spekkens, "The paradigm of kinematics and dynamics must yield to causal structure," *Questioning the Foundations of Physics: Which of Our Fundamental Assumptions Are Wrong?*, Questioning the Foundations of Physics , 5 (2015).

[63] J. Henson, "Causality, Bell's theorem, and Ontic Definiteness," arXiv:1102.2855 (2011).

[64] J. Barrett, N. Linden, S. Massar, S. Pironio, S. Popescu, and D. Roberts, "Nonlocal correlations as an information-theoretic resource," Phys. Rev. A **71**, 022101 (2005).

[65] V. Scarani, "The device-independent outlook on quantum physics," Acta Physica Slovaca **62**, 347 (2012).

[66] J.-D. Bancal, *On the Device-Independent Approach to Quantum Physics* (Springer International Publishing, 2014).

[67] R. Chaves and T. Fritz, "Entropic approach to local realism and noncontextuality," Phys. Rev. A **85**, 032113 (2012).

[68] H. Barnum and A. Wilce, "Post-classical probability theory," arXiv:1205.3833 (2012).

[69] P. Janotta and H. Hinrichsen, "Generalized probability theories: what determines the structure of quantum theory?" J. Phys. A **47**, 323001 (2014).

[70] T. C. Fraser and E. Wolfe, "Witnessing uniquely quantum correlations in the triangle scenario," unpublished (2016).

[71] H. Barnum, C. M. Caves, C. A. Fuchs, R. Jozsa, and B. Schumacher, "Noncommuting mixed states cannot be broadcast," Phys. Rev. Lett. **76**, 2818 (1996).

[72] H. Barnum, J. Barrett, M. Leifer, and A. Wilce, "Cloning and broadcasting in generic probabilistic theories," quant-ph/0611295 (2006).

[73] S. Popescu, "Nonlocality beyond quantum mechanics," Nat. Phys. **10**, 264 (2014).

[74] T. H. Yang, M. Navascus, L. Sheridan, and V. Scarani, "Quantum Bell inequalities from macroscopic locality," Phys. Rev. A **83**, 022105 (2011).

[75] D. Rohrlich, "Pr-box correlations have no classical limit," *Quantum Theory: A Two-Time Success Story: Yakir Aharonov Festschrift*, Yakir Aharonov Festschrift , 205 (2014).

[76] M. Pawlowski and V. Scarani, "Information Causality," arXiv:1112.1142 (2011).

[77] T. Fritz, A. B. Sainz, R. Augusiak, J. B. Brask, R. Chaves, A. Leverrier, and A. Acin, "Local Orthogonality as a Multipartite Principle for Quantum Correlations," Nat. Comm. **4**, 2263 (2013).

[78] A. B. Sainz, T. Fritz, R. Augusiak, J. B. Brask, R. Chaves, A. Leverrier, and A. Acn, "Exploring the Local Orthogonality Principle," Phys. Rev. A **89**, 032117 (2014).

[79] A. Cabello, "Simple explanation of the quantum limits of genuine $n$-body nonlocality," Phys. Rev. Lett. **114**, 220402 (2015).

[80] H. Barnum, M. P. Mller, and C. Ududec, "Higher-order interference and single-system postulates characterizing quantum theory," New Journal of Physics **16**, 123029 (2014).

[81] M. Navascus, Y. Guryanova, M. J. Hoban, and A. Acn, "Almost quantum correlations," Nat. Commun. **6**, 6288 (2015).

[82] A. Fordan, *Projection in Constraint Logic Programming* (Ios Press, 1999).

[83] G. B. Dantzig and B. C. Eaves, "Fourier-Motzkin elimination and its dual," J. Combin. Th. A **14**, 288 (1973).

[84] S. I. Bastrakov and N. Y. Zolotykh, "Fast method for verifying Chernikov rules in Fourier-Motzkin elimination," Comp. Mat. & Math. Phys. **55**, 160 (2015).

[85] E. Balas, "Projection with a minimal system of inequalities," Comp. Optimiz. Applic. **10**, 189 (1998).

[86] C. N. Jones, E. C. Kerrigan, and J. M. Maciejowski, "On polyhedral projection and parametric programming," J. Optimiz. Theo. Applic. **138**, 207 (2008).

[87] C. Jones, *Polyhedral Tools for Control*, Ph.D. thesis, University of Cambridge (2005).

[88] C. Jones, E. C. Kerrigan, and J. Maciejowski, *Equality set projection: A new algorithm for the projection of polytopes in halfspace representation*, Tech. Rep. (Cambridge University Engineering Dept, 2004).

[89] C. Kang and J. Tian, "Polynomial constraints in causal bayesian networks," in *Proc. of the 23rd Conference on Uncertainty in Artificial Intelligence* (AUAI, 2007) pp. 200–208.

[90] M. Navascus, S. Pironio, and A. Acn, "A convergent hierarchy of semidefinite programs characterizing the set of quantum correlations," New J. Phys. **10**, 073013 (2008).

[91] K. F. Pl and T. Vrtesi, "Quantum bounds on bell inequalities," Phys. Rev. A **79**, 022120 (2009).

[92] D. Avis, D. Bremner, and R. Seidel, "How good are convex hull algorithms?" Computational Geometry **7**, 265 (1997).

[93] K. Fukuda and A. Prodon, "Double description method revisited," Combinatorics and Computer Science: 8th Franco-Japanese and 4th Franco-Chinese Conference , 91 (1996).

[94] D. V. Shapot and A. M. Lukatskii, "Solution building for arbitrary system of linear inequalities in an explicit form," Am. J. Comp. Math. **02**, 1 (2012).

[95] D. Avis, "A revised implementation of the reverse search vertex enumeration algorithm," in *Polytopes — Combinatorics and Computation*, DMV Seminar, Vol. 29, edited by G. Kalai and G. M. Ziegler (Birkhäuser Basel, 2000) pp. 177–198.

[96] D. Bremner, M. Dutour Sikiric, and A. Schürmann, "Polyhedral representation conversion up to symmetries," in *Polyhedral computation*, CRM Proc. Lecture Notes, Vol. 48 (Amer. Math. Soc., 2009) pp. 45–71, arXiv:math/0702239.

[97] A. Schrmann, "Exploiting symmetries in polyhedral computations," Disc. Geom. Optim. , 265 (2013).

[98] V. Kaibel, L. Liberti, A. Schürmann, and R. Sotirov, "Mini-workshop: Exploiting symmetry in optimization," Oberwolfach Rep. , 2245 (2010).

[99] T. Rehn and A. Schürmann, "C++ tools for exploiting polyhedral symmetries," in *Proceedings of the Third International Congress Conference on Mathematical Software*, ICMS'10 (Springer-Verlag, Berlin, Heidelberg, 2010) pp. 295–298.

[100] S. Lörwald and G. Reinelt, "Panda: a software for polyhedral transformations," EURO Journal on Computational Optimization , 1 (2015).

[101] R. W. Yeung, *Information Theory and Network Coding* (Springer US, Boston, MA, 2008) Chap. Beyond Shannon-Type Inequalities, pp. 361–386.

[102] T. Kaced, "Equivalence of two proof techniques for non-Shannon-type inequalities," in *Information Theory Proceedings (ISIT)* (IEEE, 2013) pp. 236–240, arXiv:1302.2994.

[103] R. Dougherty, C. F. Freiling, and K. Zeger, "Non-Shannon information inequalities in four random variables," arXiv:1104.3602 (2011).

[104] A. Fine, "Hidden variables, joint probability, and the Bell inequalities," Phys. Rev. Lett. **48**, 291 (1982).

[105] I. Namioka and R. Phelps, "Tensor products of compact convex sets," Pacific J. Math. **31**, 469 (1969).

[106] T. Bogart, M. Contois, and J. Gubeladze, "Hom-polytopes," Math. Z. **273**, 1267 (2013).